

MAGNETIC FIELD VARIATIONS IN THE POLAR REGION DURING MAGNETICALLY QUIET PERIODS AND INTERPLANETARY MAGNETIC FIELDS

YA. I. FELDSTEIN

IZMIRAN, Akademgorodok, Moscow, U.S.S.R.

(To my friend Neil Brice prematurely killed in an air crash)

Abstract. The concepts of near-pole magnetic field variations during magnetically quiet periods are explored, with special emphasis on the relationships of these variations to interplanetary magnetic field components. Methods are proposed for relating the variations which have been observed to the fields from the various sources, based on a thorough selection of reference levels. We assume that the field variations in the summer polar cap during magnetically quiet periods consist of the following components: (i) the middle-latitude S_q variation extended to the polar region; (ii) the DPC(B_Y) single-cell current system with a polar electrojet in day-side cusp latitudes; (iii) the DMC(B_Z) two-cell current system of magnetospheric convection, in the form of a homogeneous current sheet in the polar cap towards the sun, with return currents through lower latitudes; (iv) the DPC(B_Z) single-cell counterclockwise current system with a focus in the day-side cusp region. Quantitative relations between the near-pole variation intensities and the value and sign of the IMF azimuthal component, with a 1 hr time resolution, have been obtained and used to suggest ways of diagnosing the interplanetary magnetic field on the basis of ground observations.

1. Introduction

When studying magnetic disturbances, most attention has for decades been paid to magnetic storms and their components with certain physical meaning, i.e.: DCF – magnetospheric surface currents; DR – the ring current in the radiation zone; and DP – polar magnetic disturbances. The DP fields are the main contributors to the high-latitude magnetic disturbances. These fields are most intense at the auroral oval latitudes in the night sector (westward electrojet) and at the auroral zone latitudes in the evening sector (eastward electrojet). Throughout this paper these electrojets will be called auroral electrojets, while the variations in the current system field will be denoted as DP1. Recent studies have revealed the great importance of interplanetary magnetic fields (IMF) for the development of intense polar magnetic disturbances, which constitute a part of global magnetospheric substorms. It has become possible to understand why the earlier measurements of cosmic plasma parameters (density, velocity and temperature) failed to reveal noticeable variations that could be considered responsible for the generation of intense magnetic disturbances and auroras (Gosling *et al.*, 1967). In fact, the measurements revealed variations in solar wind density and velocity prior to and during disturbances, within several tens of percent (Foster *et al.*, 1971); whereas the intensity of auroras and magnetic disturbances and the total energy release in the upper atmosphere varied by several orders. This apparent disagreement could be explained on the basis of measurements of the interplanetary magnetic field components in the undisturbed solar wind before the bow shock.

The near-pole magnetic field variations, which are often closely connected with the development of auroral electrojets but are much less intense, were considered to be the effect of DP1 current systems observed in both ionosphere and magnetosphere. The studies of magnetic activity, however, revealed the existence of intense magnetic disturbances during daylight hours in the near-pole region (Mayaud, 1955; Nikolsky, 1956). Such disturbances can be observed during summer season even in extremely quiet periods at $K_p=0_0$ (Bobrov, 1961; Fukushima, 1962). During these intervals, the auroral latitude magnetic field is quiet and, therefore, the near-pole disturbances cannot be associated with auroral electrojets.

The current system of magnetic field variations, S_q^P , which are not associated with auroral electrojets, was first obtained by Nagata and Kokubun (1962) for the international magnetically quiet days of the IGY period. In their studies Feldstein and Zaitzev (1967, 1968a, b), and Kawasaki and Akasofu (1967) substantially modified this current system and revealed the main feature of such disturbances: the highest intensity on the day side. According to Feldstein and Zaitzev (1968c), the intensity of the day-side disturbances which are not associated with auroral electrojets and can be described by the counterclockwise single cell current (DPC), increases with K_p . The results obtained are reviewed in Akasofu and Chapman (1972); Akasofu *et al.* (1973); Afonina *et al.* (1975).

Nishida *et al.* (1966) described the world-wide magnetic field variations which are not directly associated with auroral electrojet enhancement. These variations, called subsequently DP2, were studied in detail by Nishida (1968a, b; 1971a, b) and correlate closely with the change of orientation of the North-South (Z_{SE}) component of interplanetary magnetic field. The quasiperiodic field fluctuations of DP2 type which occur in phase over the entire planet exist before, during, and after the substorm. DP2 can be most clearly seen in the variations of the horizontal field component in the polar region, and during daylight hours on the equator. The equivalent DP2 current system is composed of two cell currents located in the morning and evening sectors; the polar cap current flows from the night to the day side. Kawasaki and Akasofu (1972) showed that the DP2 variations often accompanied the auroral electrojet development and concluded from this fact that DP2 was not a new type of magnetic field variation but one of magnetosphere substorm display. Iijima (1973) also noted the substorm-time enhancement of S_q^P variations. The existence of the westward current at the auroral oval latitudes during the DP2 periods and, in connection with this, the necessity to substantially modify the two cell current system DP2 for these periods is also noted by Afonina *et al.* (1975) and Feldstein (1974). However, in the case of more quiet magnetic field and short-term Z_{SE} fluctuations, the DP2 type variations cophased with them exist undoubtedly in the polar region, and are not associated with auroral electrojet development (Troshichev *et al.*, 1974; Akasofu *et al.*, 1973; see also the discussion in Nishida, 1973a, Kawasaki and Akasofu, 1973). The difficulties encountered when distinguishing the DP2 variations at the equator were also examined by Matsushita and Balsley (1972, 1973), Nishida (1973), and Onwumechilli *et al.* (1973). The similarity of the S_q^P and DP2 current

systems makes one believe that they are probably of common nature and that DP2 is due to the rapid increase of S_q^p when IMF turns southwards.

Recently, a close connection between the near-pole variations and the direction and intensity of the azimuthal (Y_{SE}) IMF component has been found and the main spatio-temporal regularities of these variations have been established. There is every reason, therefore, to isolate them as a special type of magnetic field variation which will be denoted below as DPC (Y_{SE}). The study of DPC (Y_{SE}) variations is of great diagnostic importance since it permits the magnitude and direction of Y_{SE} to be fairly safely determined from the ground observation data. The main regularities in DPC (Y_{SE}) obtained before 1973 are briefly set out in reviews (Wilcox, 1972; Feldstein, 1973). Subsequently in the present review the solar-ecliptic coordinate system with X-axis along the Earth-Sun line, Z-axis vertically upward, and Y-axis to the evening side in the ecliptic plane will be used to describe the IMP components.

2. Variations in the Polar Region and the Sector IMF Structure

Svalgaard (1968) was the first to indicate the existence of two characteristic types of variations in the polar region, with disturbances occurring simultaneously in the north and south polar caps. Figure 1 presents, following Svalgaard (1968), the magnetograms characterizing these types of variations in the northern hemisphere. At $\Phi' \sim 86^\circ$ (Thule) during the daytime the Z-component is larger or smaller than the field values in non-disturbed periods; at $\Phi' \sim 78^\circ$ (Godhavn) the antiphase change of the H-component is observed. A certain type of disturbance usually persists for several successive days and constitute a group. The groups exhibit the tendency to recur at 27–29 day intervals, which indicates the solar origin of the disturbance source. The variation type with $\Delta Z > 0$, $\Delta H < 0$ is characteristic of days with predominant sunward direction of the IMF sector in the ecliptic plane, according to Ness and Wilcox (1967), Wilcox (1967); while that with $\Delta Z < 0$, $\Delta H > 0$ is characteristic of days with the IMF sector directed from the Sun. The fairly good agreement between the types of ground near-pole variations in the geomagnetic field and sector structure has enabled Svalgaard to use the ground observation data for determining the interplanetary sector polarity; and this was extended by Friis-Christensen (1971), Friis-Christensen *et al.* (1971), Mansurov and Mansurova (1973a), and Svalgaard (1972).

The dependence of the absolute values of Z in the polar region on the IMF sector polarity at day-time hours was independently obtained by Mansurov (1969) from the data of Vostok ($\Phi' = -88^\circ$) and Resolute Bay ($\Phi' \sim 84^\circ$) stations. The change of IMF polarity (from away to towards the Sun) is accompanied by the transition from low to high values of Z at Resolute Bay and from high to low values of $|Z|$ at Vostok. The variations in Z value are substantially in excess of IMF intensity; their amplitude is a function of season, and was $\sim 150 \gamma$ in the summer and $\sim 15 \gamma$ in the winter of 1964. The studies of near-pole variations relative to sector polarity were continued by Mansurov and Mansurova (1970), and Friis-Christensen (1971).

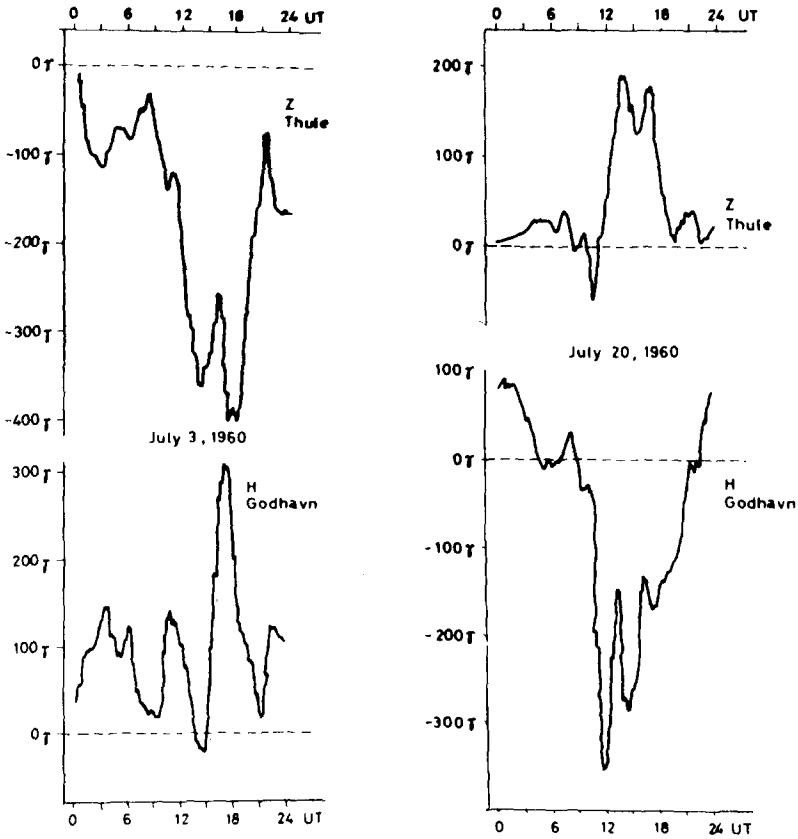


Fig. 1. Two types of magnetic field variation in the northern polar cap according to Svalgaard (1968). The undisturbed level is indicated by broken lines. Shown in the left and right parts of the figure are the variations characteristic of IMF toward sector (+B) and away sector (-B) respectively.

It has been established while summarizing the results of near-pole variation analysis relative to the IMF sector structure in the above mentioned works that:

(a) The effect can be most clearly seen in the vertical component at $\Phi > 80^\circ$. In the case of the *away sector* the Z-variations in both hemispheres are directed *away from the Earth*; in the case of the *toward sector* the Z-variations are directed *earthwards*.

(b) At lower latitudes ($\Phi \sim 78^\circ$) the sector structure effect can be most clearly seen in the horizontal component which *increases in the case of the away sector and decreases in the case of the toward sector*.

(c) The field variations associated with the change of the IMF sector polarity were not found in the Y' component.

(d) At $\Phi \leq 75^\circ$ the field variations due to sector structure decrease markedly and are practically absent.

(e) The magnitude of the effect depends substantially on season and is at maximum in summer and at minimum in winter.

(f) The field variations due to sector structure can be clearly seen only in the day sector. At night the field values are close to the undisturbed level.

Friis-Christensen (1971) drew attention to a considerable difference between the field variations in the polar region expected on the basis of sector polarity and those actually observed on individual days in 1968. The causes of such discrepancies for 1968 were analysed by Friis-Christensen *et al.* (1972); while Sumaruk and Feldstein (1973) examined similar discrepancies for individual time intervals in 1965. It has been shown in these independent and simultaneous works – the works of Friis-Christensen *et al.* and Sumaruk and Feldstein were accepted for publication in the corresponding editions of 23 March 1972 and 3 April 1972 respectively – that the above mentioned disagreement can be eliminated on the assumption that the mode of magnetic field variations in the polar region is controlled not by the interplanetary sector polarity but by the direction of the azimuthal (east-west) IMF component.

The results of Friis-Christensen *et al.* (1972) are well known and often referred to in the literature. The conclusions of the second work will therefore be discussed in greater detail below. Figure 2 presents the variations of mean-hourly Z values from 1–6 June 1965 at Thule (T) and Resolute Bay (R) stations. The interplanetary sector polarity, according to Wilcox (1968), corresponds to the sunward IMF ($+B$) or IMF directed away from the Sun ($-B$). Only for two out of five days – the sector polarity on 3 June could not be determined – did the Z variations correspond to the

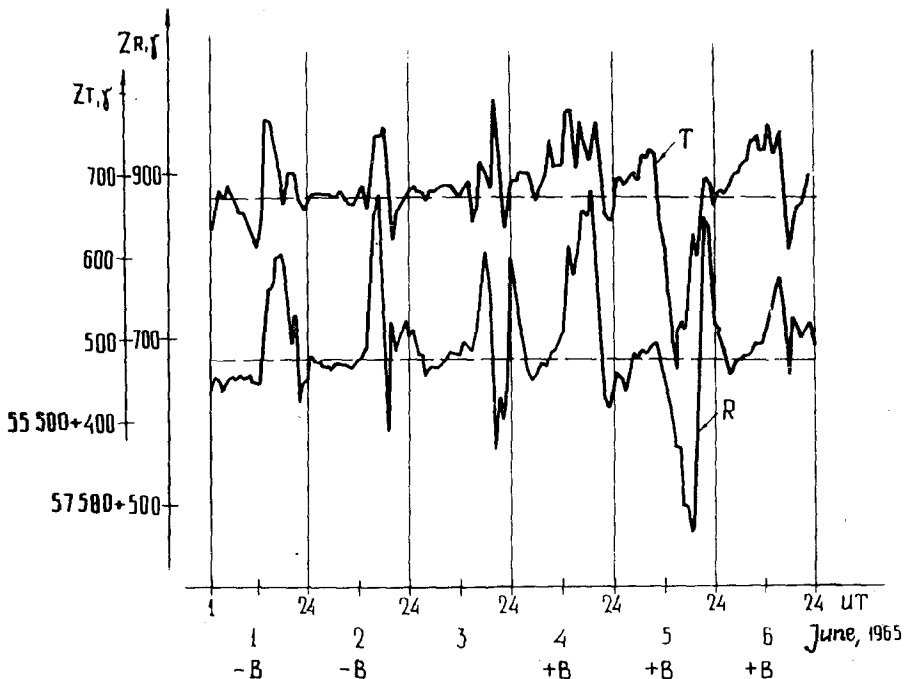


Fig. 2. Variations in mean-hourly values of Z at Thule and Resolute Bay for 1–6 June 1965 and the IMF sector polarity according to Sumaruk and Feldstein (1973). The undisturbed level is indicated by broken lines. IMF toward sector ($+B$) or away sector ($-B$).

regularities obtained in Svalgaard (1968), Mansurov (1969), Friis-Christensen (1971). The disagreements could be observed not only when the sector boundaries were crossed but also inside the sectors. To elucidate the causes of such disagreements, it is necessary to compare the mode of the ground polar variations with direct IMF measurements. Only such a comparison will make it possible to find out if the observed disagreements can be associated with IMF features in the ecliptic plane and, if possible, to determine which of IMF components (X_{SE} or Y_{SE}) is responsible for the ground variation mode. IMF within a sector is predominantly directed along Archimedes' spiral, i.e. at 135° and 315° toward the Earth-Sun direction at the Earth's orbit (Svalgaard and Wilcox, 1974). Therefore the change of sector polarity accompanied by the change of types of ground variation produces the change in the sign of both X_{SF} and Y_{SF} components of IMF. Hence, it is necessary to study the field variations in the polar region during those intervals when IMF in the ecliptic plane is substantially different from Archimedes' spiral.

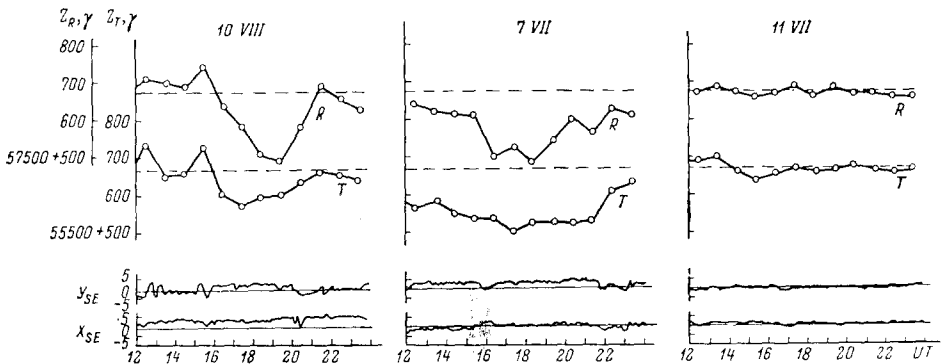


Fig. 3. Variations in mean-hourly values of Z at Resolute Bay (R) and Thule (T) and in Y_{SE} and X_{SE} components of IMF according to Sumaruk and Feldstein (1973). The undisturbed level is indicated by broken lines. Shown in the left, center, and right parts of the figure are the data for 10 August 1965, 7 July 1965, and 11 July 1965 respectively.

Figure 3 presents such cases according to Sumaruk and Feldstein (1973). On 10 August 1965 from 12^h to 16^h UT $X_{SE} > 0$, $Y_{SE} < 0$: i.e. IMF was sunward and the corresponding $\Delta Z > 0$ at near-pole observatories. From 16^h to 20^h UT ΔZ decreased by 100–200 γ with the same sector polarity ($X_{SE} > 0$). The change of near-pole variation types and the disagreement of the sign of the observed changes of Z with those established in Svalgaard (1968) and other regularities, can be naturally associated with the change of the Y_{SE} component direction. In this case the IMF direction was substantially different from Archimedes' spiral. Another example was on 7 July when IMF was directed away from the Sun and $\Delta Z < 0$ at the near-pole observatories from 12^h to 15^h UT. After that the X_{SE} sign changed, IMF deflected from Archimedes' spiral while the near-pole variation mode was conserved. The steady decrease in Z can be naturally associated not with radial component X_{SE} of IMF or sector polarity

but with the positive values of Y_{SE} from 12^h to 22^h UT. On 11 July 1965 the field variations in the polar region were unusually small. The IMF components $X_{SE} \sim 1-2 \gamma$ and $Y_{SE} \sim 0 \gamma$. Disappearance of the characteristic variations in Z was associated with the low strength of the IMF azimuthal component, which was additionally indicative of a close connection between the near-pole variations and Y_{SE} . The mean daily values of Z for 11 July 1965 are taken as the reference level in Figures 2 and 3. Comparison between IMF component variations in the ecliptic plane and the changes of Z at Thule and Resolute Bay stations for a 50-day period from June to August, 1965, when the IMP 3 satellite was in interplanetary space, enabled Sumaruk and Feldstein (1973) to conclude that:

(1) The mode of field variations in the polar region is determined by the Y_{SE} component of IMF. At $Y_{SE} > 0$ (the field directed from the morning to the evening side), Z decreases relative to the non-disturbed level; at $Y_{SE} < 0$, Z increases.

(2) The dependence of Z variation mode on sector polarity (or X_{SE} component) is but indirect and due to a high correlation between the Y_{SE} and X_{SE} directions because of the IMF spiral structure at the Earth's orbit.

(3) The change of the magnetic field variation mode in the polar region is due to the change of the Y_{SE} component sign. At $Y_{SE} \sim 0$, the ground variations practically disappear.

These conclusions coincide completely with the results of Friis-Christensen *et al.* (1972), where it was shown that during long (~ 1 day) periods of disagreements between the IMF polarity inferred from the results of near-pole Z variations and that observed actually in interplanetary space, IMF deflected considerably from the mean Archimedes' spiral. In this case the IMF azimuthal component was opposite to what was expected for the spiral and, hence, the mode of the ground magnetic field variations in the polar region is determined not by the IMF sector polarity (toward or away from the Sun) but by the direction of the IMF azimuthal component. The absolute value of Z at Thule (Z_T) at times close to midday was shown to correlate closely with the intensity of Y_{SM} (azimuthal component in the solar-magnetospheric coordinate system), and it appeared that the linear relation between Z_T and Y_{SM} of the form

$$Z_T = -KY_{SM} + Z_0$$

was valid.

The correlation of Z_T with X_{SM} is much worse, but the tendency for Z_T to increase with X_{SM} can be seen. This tendency may be an indirect result of the IMF spiral structure because of which the increase in the field modulus results in a simultaneous increase in Y_{SM} and X_{SM} .

The determinant effect of Y_{SE} on near-pole magnetic field variations is now beyond doubt. To reveal the possible effect of X_{SE} which was indicated in Mishin *et al.* (1972), and Bassolo *et al.* (1972), it is necessary to subtract the part associated with Y_{SE} from the observed variations and to study the remainder for possible association with X_{SE} intensity. To this end, Sumaruk *et al.* (1974) used hourly values of Z_T in August 1965 for six daylight hours. Figure 4 presents the corresponding hourly Z_T as functions of

Y_{SE} intensity at the preceding hour. The correlation factor $r = -0.91 \pm 0.06$. The regression straight line gives the linear dependence of Z_T on Y_{SE} for which the standard deviation of individual points from the straight line is minimum. The deviation of individual values of Z_T from the regression straight line (ΔZ_T) characterizes the field variation part which is not associated with Y_{SE} . Figure 5 presents the values of ΔZ_T as functions of X_{SE} values. The cloud of points and correlation factor $r = -0.01$ are

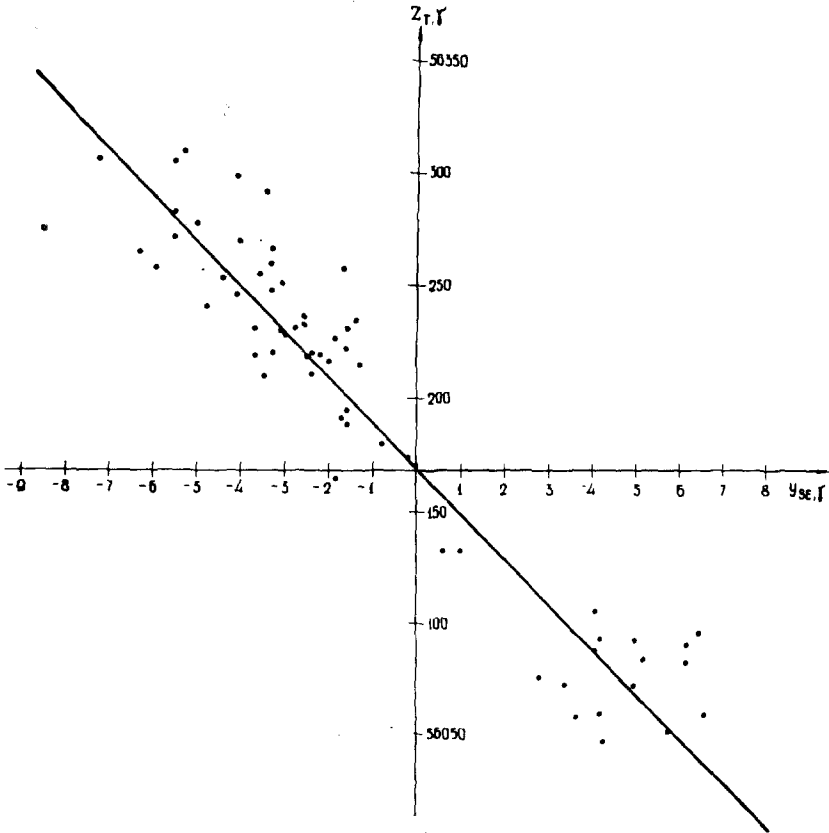


Fig. 4. Hourly-mean values of Z during the day-time in August, 1965 versus Y_{SE} intensity with 1 hr delay of ground variations according to Sumaruk *et al.* (1974).

indicative of the absence of an explicit connection between X_{SE} and Z variations at Thule. This conclusion agrees with the thorough analysis by Shelomentsev (1974), made on the basis of the data from the near-pole observatories of the northern and southern hemispheres.

The number of cases of anomalous IMF direction within a long time interval is relatively small; and it is this fact that results in a fairly good agreement between the IMF sector polarity and the mode of geomagnetic variations in the polar cap, when the interplanetary sector polarity characterizes a day as a whole. Within shorter time

intervals, however, the deflections from Archimedes' spiral are observed much more frequently. Figure 6, following Ness *et al.* (1966), presents the histogram of IMF directions in the ecliptic plane plotted on the basis of IMP-1 observations in 1963-1964. The dashed line denotes the isotropic distribution. Attention is drawn to the fairly frequent deviations of IMF direction from the mean spiral. The number of these deviations decreases with the increase in the average interval. This means that the data on the IMF sector polarity characterizing a day as a whole should be used

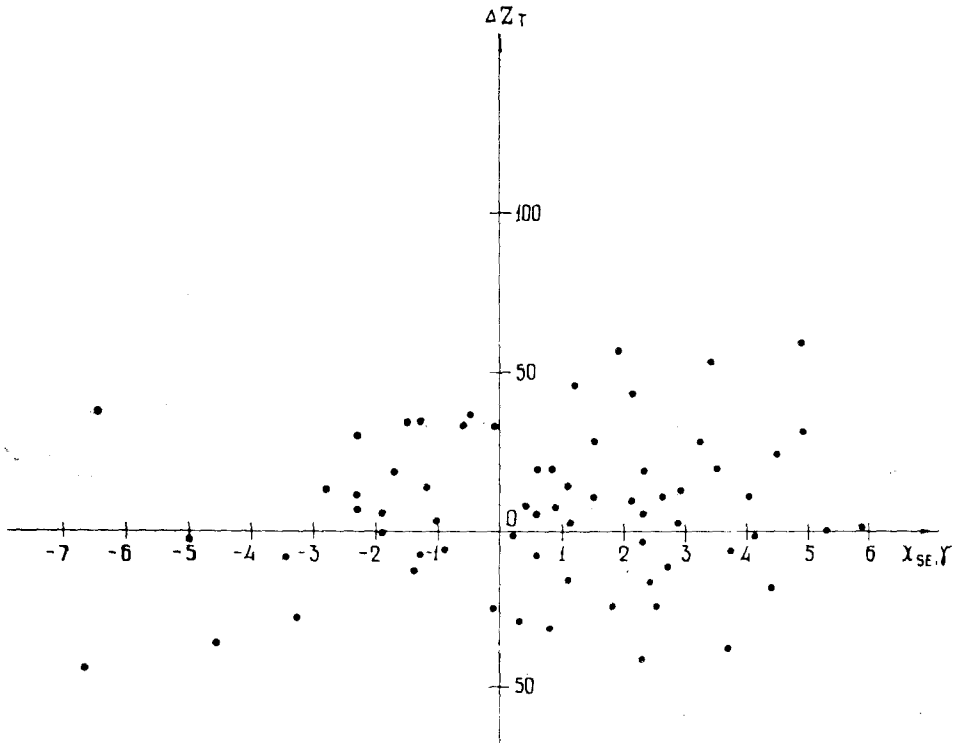


Fig. 5. Deviations of individual hourly-mean values of Z_T from the regression line at the various values of X_{SE} according to Sumaruk *et al.* (1974).

cautiously when studying in detail the mode of field variations on the Earth's surface - for example, daily variations. These data fail to include the IMF direction changes during the day; and, besides that, they fail to characterize the IMF radial component. It is this circumstance that explains the significant disagreement between the modes of daily near-pole variations in Z shown in Figure 1 and those obtained by Mansurov and Mansurova (1973a), which are shown in Figure 7.

According to Figure 7, in the case of the toward sector, the near-pole Z variations in the northern hemisphere (N_p^-) in the summer season are of the form of a simple wave with its maximum at 8^h and its minimum at 16^h of local geomagnetic time and

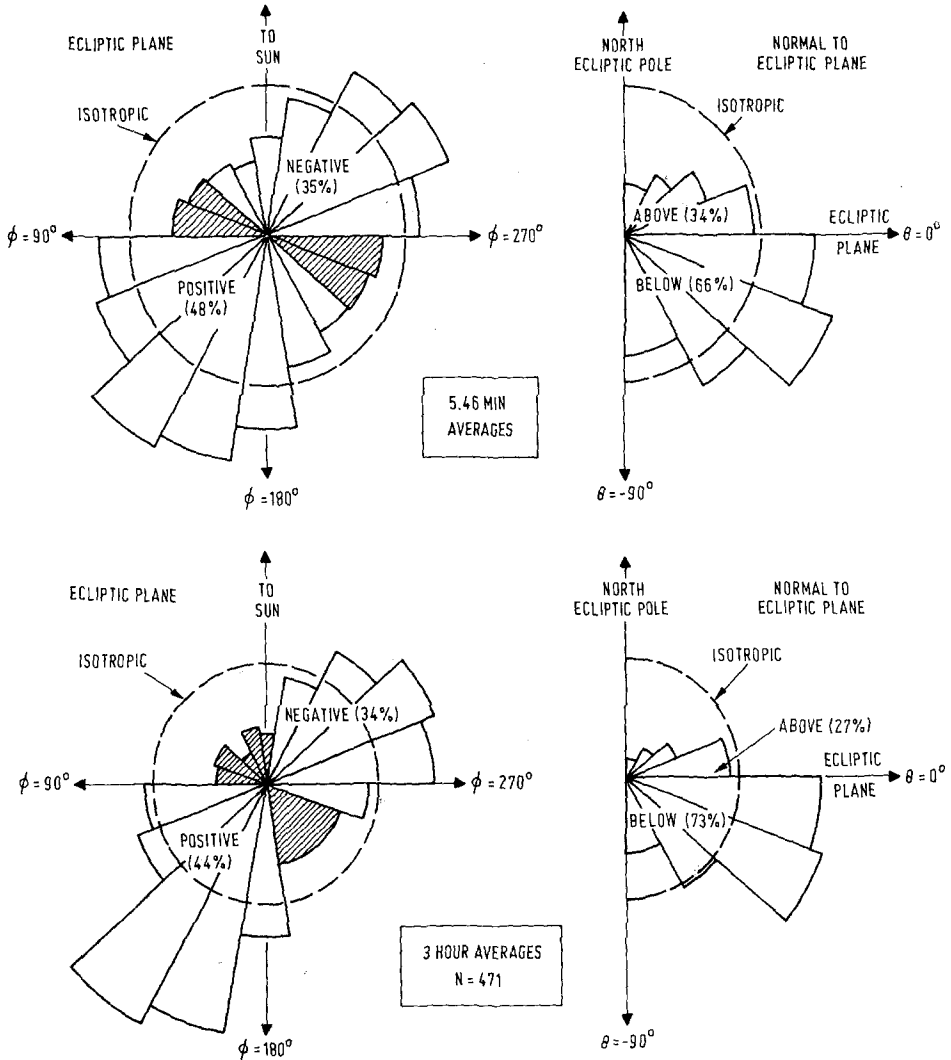


Fig. 6. Histograms of IMF direction in the ecliptic plane plotted on the basis of IMP-1 observations for averaging intervals of 5.46 min (top) and 3 hr (bottom) according to Ness *et al.* (1966).

with about the same values near noon and near midnight. However, such field variations are considerably different from those described in Svalgaard (1968), Friis-Christensen (1971), and in other works according to which Z is maximum near noon, and the greatest deviation of Z from its midnight values is observed very close to noon. The equality of the noon and midnight values of Z is probably responsible for the constancy of the mean-daily level of Z throughout the year in the toward sector. Mansurov and Mansurova (1973a, b) attach great importance to this constancy.

Besides this, the regularities represented in Figure 7 are not free of variations determined by other field sources unconnected with \mathcal{X}_{SE} .

The close relation of the near-pole Z variations with Y_{SE} was shown by Kawasaki *et al.* (1973), where the short-term Y_{SE} variations were compared to the magnetograms from ground observatories. They note the similarity of not only long-term but also short-term (shorter than 30 min) day-time Y_{SE} fluctuations to Z variations at Thule. Such similarity occurs every day during the summer months and is not suppressed by magnetic disturbances from other sources, in particular those associated with DP1. The similarity to Y_{SE} variations in the horizontal component on the Earth's surface can be traced only during magnetically quiet periods.

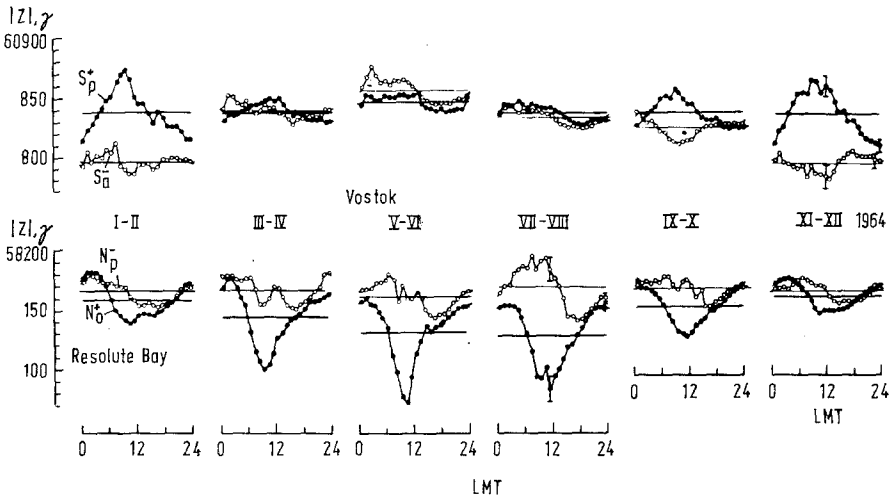


Fig. 7. Variations in Z averaged for each 2 months of 1964 at Vostok (top) and Resolute Bay (bottom) stations according to Mansurov and Mansurova (1973a). Variations in N_p^- and S_p^- are observed at the IMF toward sector, variations in N_p^+ and S_p^+ are observed at the IMF away sector. Local geomagnetic time.

Figure 8 presents the changes of the 5 min averages of X at Mould Bay station during the day-time, and the variations in three IMF components and in the AE index. Close correlation of X with Y_{SE} from 23^h to 04^h UT persists during the magnetically quiet interval and becomes worse at $AE \geq 200 \gamma$. The time necessary for the satellite-observed IMF structure to be transferred to the Earth's vicinity at the solar wind velocity has been included by shifting the time scales by 12 min. Of all three IMF components, the clear visual correlation of ground variations exists only with Y_{SE} . This example is indicative of the existence of short-term polar cap variations with $T < 1$ hr closely following the Y_{SE} variations and existing not only in vertical but also in horizontal components. However, the latitudes where this association is most clear are different: $\Phi' \geq 83^\circ$ for Z and $\Phi' \sim 81^\circ$ for X component on the Earth's day side. Thus, the interrelated variations in the vertical and horizontal components can be observed in the polar cap during magnetically quiet periods, which suggests the existence of a common current system associated with the Y_{SE} component of IMF. However, other near-pole sources of field variations may exist, which can be seen,

particularly, in the close association of the changes in horizontal components with the Z_{SE} component of IMF (Nishida, 1968b, 1971b; Kawasaki *et al.*, 1973). In this case the near-pole current system is characterized either by the current distributed from the night to the day side (S_q^P or DP2), or by the closing of the auroral westward electrojet through the polar region and the field-aligned currents to and from the auroral oval (DP1). Quiet solar-diurnal variations (S_q^0) exist undoubtedly in the polar region, similarly to medium and low latitudes. Besides that, as was mentioned in the Introduction, there can exist a DPC current system which is a single cell counterclockwise current on the Earth's day side focused at $\Phi' \sim 78-80^\circ$ during very quiet periods (Feldstein, 1969).

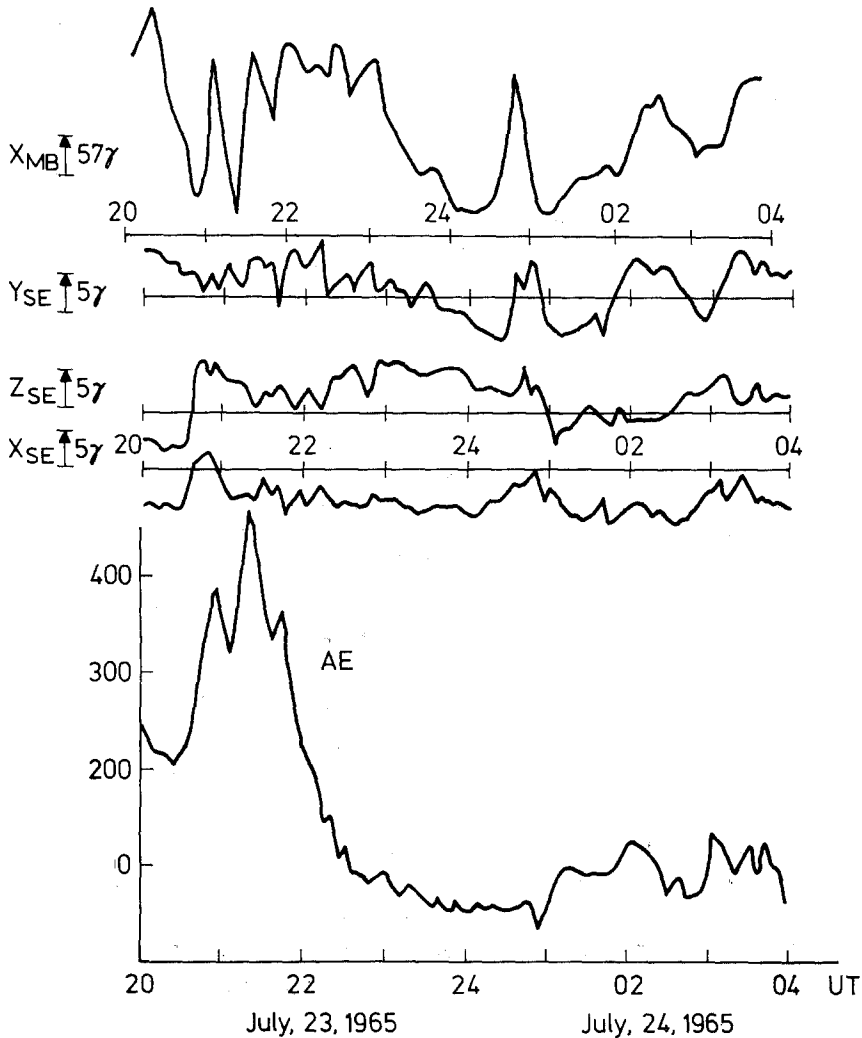


Fig. 8. Variations in the 5 min averages of the north (X) component at Mould Bay and in three components of IMF for 23-24 July 1965. Shown at the bottom are the variations of the 2.5 min AE -index. The IMF magnetogram is shifted by 12 min relative to ground field variations.

Such a diversity of variations is responsible for the complicated mode of the near-pole field variations and requires a thorough analysis when separating and studying the specific types of variations.

3. Separation of the High-latitude DPC (Y_{SE}) Variations

The published data on the current system responsible for the near-pole variations relative to the Y_{SE} component of IMF are extremely diverse. Such a diversity of the results is partly due to the fact that in some pioneer studies, the conclusions about the nature of current systems were drawn from the sector structure sign, not the Y_{SE} component. However, the differences in the reference level employed for the variation field will probably prove to be most significant.

Figure 9 presents the variations in the magnetic field horizontal components during the summer season of 1965 for two observatories on $80^\circ \leq \Phi' \leq 84^\circ$ where these variations are largest. The variations were not actually observed but have been calculated for three values of Y_{SE} on the basis of relations which will be presented in Section 3 of the present review and correspond to the Y_{SE} intensities of 3γ , 0γ , and -3γ con-

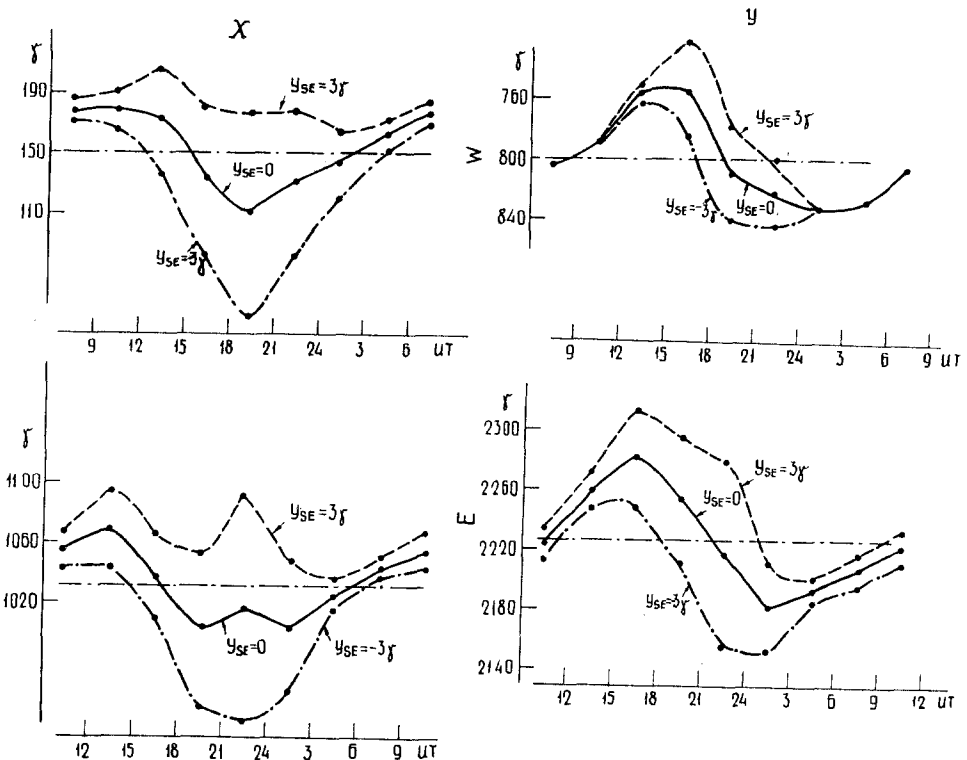


Fig. 9. Variations in the north (X) and east (Y) components of magnetic field at Resolute Bay (top) and Mould Bay (bottom) calculated for Y_{SE} values of 3γ , 0γ , and -3γ in July–August, 1965. The dash-dot line shows the mean daily value of X or Y at $Y_{SE}=0$.

served at the steady level throughout a day. To isolate the DPC (Y_{SE}) variation, the field reference level should be a curve corresponding to $Y_{SE}=0 \gamma$ which reflects the field variations from the sources other than those associated with the azimuthal component of the interplanetary magnetic field.

This reference level for separating DPC (Y_{SE}) differs from the following reference levels used in the literature.

(1) The daily mean values of the corresponding components for the time interval studied, irrespective of sector polarity (Bassolo *et al.*, 1972; Matsushita *et al.*, 1973; Mansurov and Mansurova, 1973a), or the daily mean values of quiet days in winter extrapolated to any period of the year including secular variations (Langel, 1973; Sumaruk and Feldstein, 1973b). Such methods of separating the variations fail to exclude the diurnal variations that are not associated with the Y_{SE} component and may reach $\sim 100 \gamma$ (see Figure 9). The methods for excluding the near-pole S_q^o variations used by Matsushita *et al.* (1973) may be considered to be the first approximation.

(2) The near-midnight field values (Sumaruk and Feldstein, 1973b; Rostoker *et al.*, 1974). In this case also, the diurnal variations not associated with Y_{SE} cannot be excluded. Besides that, it follows from Figure 9 that the midnight field level at some observatories may be a function, though fairly weak, of Y_{SE} strength.

(3) Diurnal field variations at $Y_{SE} < 0$ for northern and at $Y_{SE} > 0$ for southern polar caps (Mansurov and Mansurova, 1970b; Bassolo *et al.*, 1972; Mansurov and Mansurova, 1973c). Such methods assume in advance that at $Y_{SE} < 0$ in the northern hemisphere, the variations associated with the IMF azimuthal component are absent and that all the field variations (for example, $\sim 120 \gamma$ in X -component at Resolute Bay in Figure 9) are due to the fields arising from other sources. With such choice of reference level, the near-pole zonal currents will be always eastward and exist in the northern polar cap at $Y_{SE} > 0$ and in southern polar cap at $Y_{SE} < 0$.

(4) The diurnal field variations obtained by averaging the corresponding dependences for two polarities of Y_{SE} (Svalgaard, 1973). Such methods of separating the variations should, in principle, exclude all field variations which are not associated with Y_{SE} . When used, they automatically give the same absolute values but different sign for variations in opposite directions of Y_{SE} , which are responsible for the appearance of the near-pole eastward or westward currents depending on Y_{SE} sign.

Application of such methods, however, presumes identical dependence of the ground variation intensities on Y_{SE} at $Y_{SE} > 0$ and $Y_{SE} < 0$. We have thoroughly analyzed a vast volume of observation data and found out that such a condition is frequently, but not always, satisfied. In particular, when the observations for all days, embracing disturbed and quiet periods, are used, somewhat different dependences at different Y_{SE} signs are possible. This circumstance is illustrated by Figure 10 which presents the mean hourly values of the northern component at Resolute Bay (X_R) relative to Y_{SE} intensity. The dots and crosses denote the quiet and disturbed ($AE > 150 \gamma$) periods. The dashed line shows the regression equations calculated by the least square method for all periods separately where $Y_{SE} > 0$ and $Y_{SE} < 0$; while the solid line represents those for magnetically quiet periods irrespective of Y_{SE} sign. The methods of separat-

ing the field variations independently of Y_{SE} , proposed by Svalgaard (1973), may be successfully used for quiet or disturbed periods separately, when the field component intensity varies linearly with Y_{SE} or is independent of Y_{SE} . In the example presented in Figure 10, the values of X_R for magnetically quiet periods are linearly related to Y_{SE} (correlation factor 0.92), while those for disturbed periods are independent of Y_{SE} ,

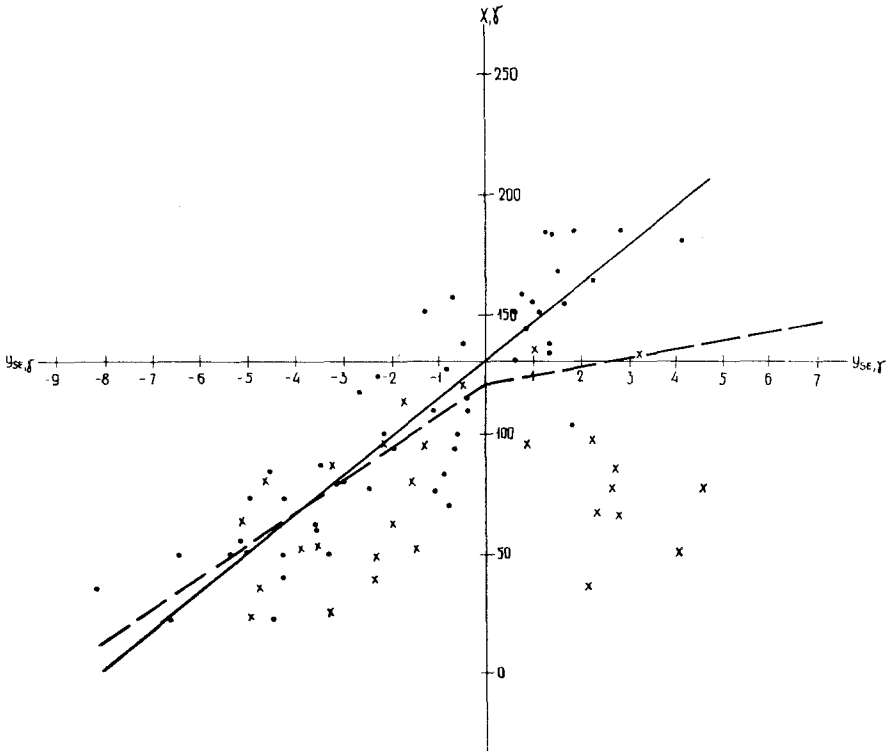


Fig. 10. Hourly mean values of X_R at Resolute Bay during day-time hours (21^h–24^h UT) versus Y_{SE} intensity in July–August, 1965. The black circles show the magnetically quiet periods, the crosses denote the hours with $AE > 150 \gamma$. The solid line is the regression equation for magnetically quiet intervals, the dashed line is the regression equation for all intervals, separately for $Y_{SE} > 0$ and $Y_{SE} < 0$.

and at $Y_{SE} = 0 \gamma$, are decreased by 60γ as compared to X_R for quiet periods. The different kinds of relations between X_R and Y_{SE} are due to the shift of the polar electrojet of DPC (Y_{SE}) current system from latitude $\Phi' \sim 82^\circ$ in magnetically quiet periods to lower latitudes during disturbances. The shift amounts to several degrees of latitude and is responsible for a closer correlation of the horizontal component at Godhavn station ($\Phi' \sim 78^\circ$), and a more considerable response of its variations, with Y_{SE} , in disturbed than in magnetically quiet periods.

(5) Diurnal variations of field values at $|Y_{SE}| < 1 \gamma$ (Berthelie, 1972; Berthelie *et al.*, 1974), $|Y_{SE}| < 1.5 \gamma$ (Shelomentsev, 1974) or on individual extremely quiet days when Y_{SE} is several tenths of a gamma (Sumaruk and Feldstein, 1973c, d). With such

a method for separating the variations, the variations independent of Y_{SE} are excluded. The drawbacks of the method are the absence of intervals with $Y_{SE} \sim 0 \gamma$, and an extremely small number of cases where $|Y_{SE}| \leq 1 \gamma$. Therefore, the statistical substantiation of the variation field reference levels is very small.

It is not surprising that such a diversity of field reference levels has resulted in different concepts of near-pole DPC (Y_{SE}) current systems. Iijima and Kokubun (1973), Troshichev *et al.* (1974) also indicate that the resulting current systems are functions of the accepted reference level.

It is beyond doubt that the DPI field variations associated with the appearance of electrojets along the auroral oval, and the increase in the oval dimension, result in near-pole field variations. For example, in Figure 10 such changes in X -component, on $\Phi' \sim 84^\circ$ are $\sim 60 \gamma$ at $AE > 150 \gamma$. To separate the near-pole field variations which are not associated with auroral electrojets, it is necessary to estimate the threshold

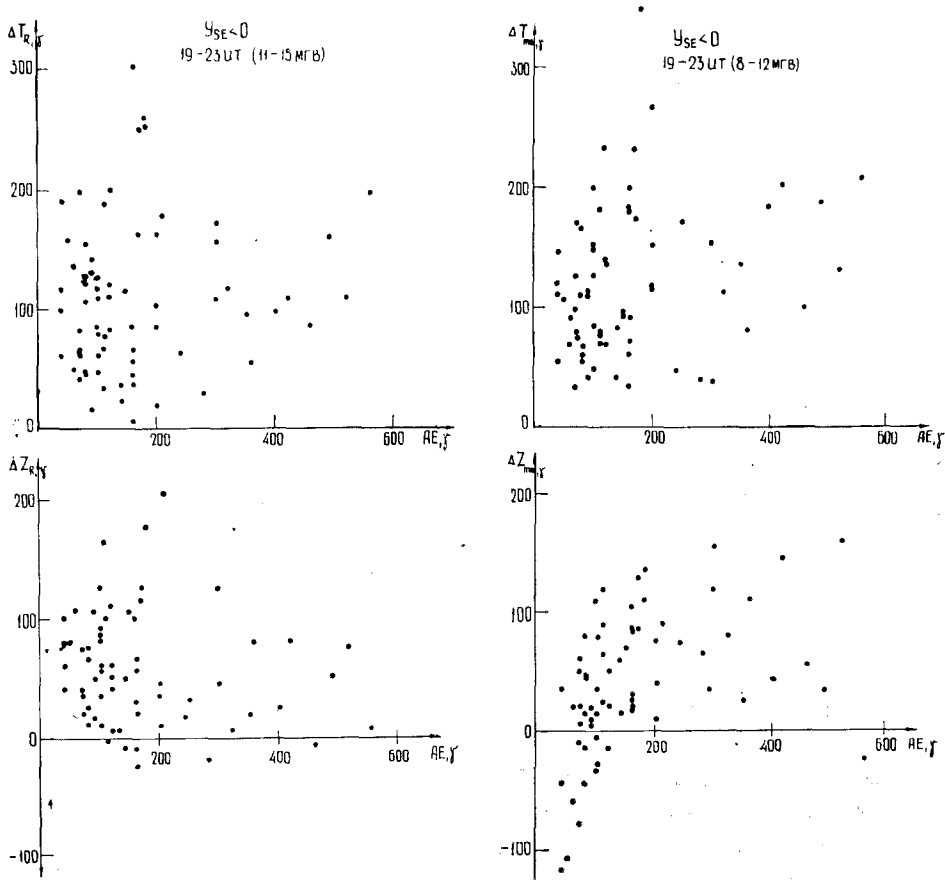


Fig. 11. The values of ΔT (top) and ΔZ (bottom) during the day-time at $80^\circ \leq \Phi' \leq 84^\circ$ at different AE in July–August, 1965 for $Y_{SE} < 0$ according to Sumaruk and Feldstein (1973d). Shown in the left and right of the figure are the data from Resolute Bay (11^h–15^h LGT) and Mould Bay (8^h–12^h LGT) respectively.

below which the electrojet intensity fails to appreciably affect the near-pole variation intensity. Figure 11 presents the day sector values of $\Delta T = \sqrt{[(\Delta X)^2 + (\Delta Y)^2]}$ and ΔZ as functions of AE at $Y_{SE} < 0$ at Resolute Bay and Mould Bay stations. The hourly values of ΔT and ΔZ were calculated for every day in July and August, 1965 with a stable Y_{SE} direction in the deviations from the field value of 11 July 1965. The AE index at the corresponding hour represents the maximum value of 24 AE values in each 2.5 min as calculated on the basis of the data from the chain of 10 magnetic observations in WDCA (1969). The large scatter of points for ΔT at $AE \leq 200 \gamma$ is indicative of the relative independence of the day sector near-pole variations on auroral electrojets. At $AE > 200 \gamma$ ΔT tends to increase with AE . At night time on the same latitudes this boundary also corresponds to $AE \sim 150\text{--}200 \gamma$ with a fairly good correlation between ΔT and AE for high AE . Thus, the DP1 contribution to the near-pole variations of horizontal components may be excluded by selecting the periods with $AE \leq 150 \gamma$. This result does not contradict the conclusions arrived at by Kokubun (1971), who studied the relations between near-pole disturbances (PC index) and auroral electrojet intensities on 23–24 August 1966.

The example of Z_T variations at Thule is used below to describe the method for separating the field variations associated with Y_{SE} proposed in Sumaruk *et al.* (1974). The method is based on the close linear relationship between the mean-hourly Z_T and the value of Y_{SE} , which was described for daylight hours by Friis-Christensen *et al.* (1972). Figures 12a–b illustrate the variations in the mean hourly values Z_T as functions of Y_{SE} intensity during July 1965 at near-noon and near-midnight hours respectively. A 3 hr interval is used to increase the statistics. All mean-hourly Z for the above time intervals, for which Y_{SE} was known from IMP-3 measurements, have been plotted. According to the mean 5 min data, the Y_{SE} sign was not changed during these intervals. Intervals with $AE > 150 \gamma$ are excluded. The delay of ground Z variations relative to Y_{SE} is included. Since the near-pole values of Z_T are affected by the magnetospheric ring current, the hourly intervals with $D_{st} < -10 \gamma$ are excluded. The straight lines shown in the figures were obtained by the least square method, and characterize the relation of near-pole Z_T to the value and direction of Y_{SE} on the assumption of the linear relationship between the two parameters. Similar dependences have been obtained for all 3 hr intervals of universal time in each month from the July to the December of 1965 and 1966. Analysis of the dependences has shown:

- (a) The presence of a fairly close relationship between Z_T value and Y_{SE} intensity.
- (b) In the summer months this relationship can be traced both during the day and during the night, but at the equinox, only during the day. In the winter months the relationship between Z_T and Y_{SE} is practically absent during the day.
- (c) The response of Z_T to Y_{SE} variations is greater during the day than at night.

Table I lists the coefficients of linear correlation Z_T – Y_{SE} ; and their dispersion confirms the fairly close relation of Z_T to Y_{SE} throughout the day (though closest at daytime) in the summer season. Table II contains the regression equations permitting the Y_{SE} values to be used for calculating the Z_T intensity. It can be seen from Table II that these relations vary throughout both the day and the season. The interval

within a day then there is a dependence of Z_T on Y_{SE} decreases from 24 hrs in July-August to practically 0 hrs in December.

The regression equations permit Z_T to be determined for each 3 hr interval at $Y_{SE}=0$. This value has been obtained using all intervals of interplanetary magnetic

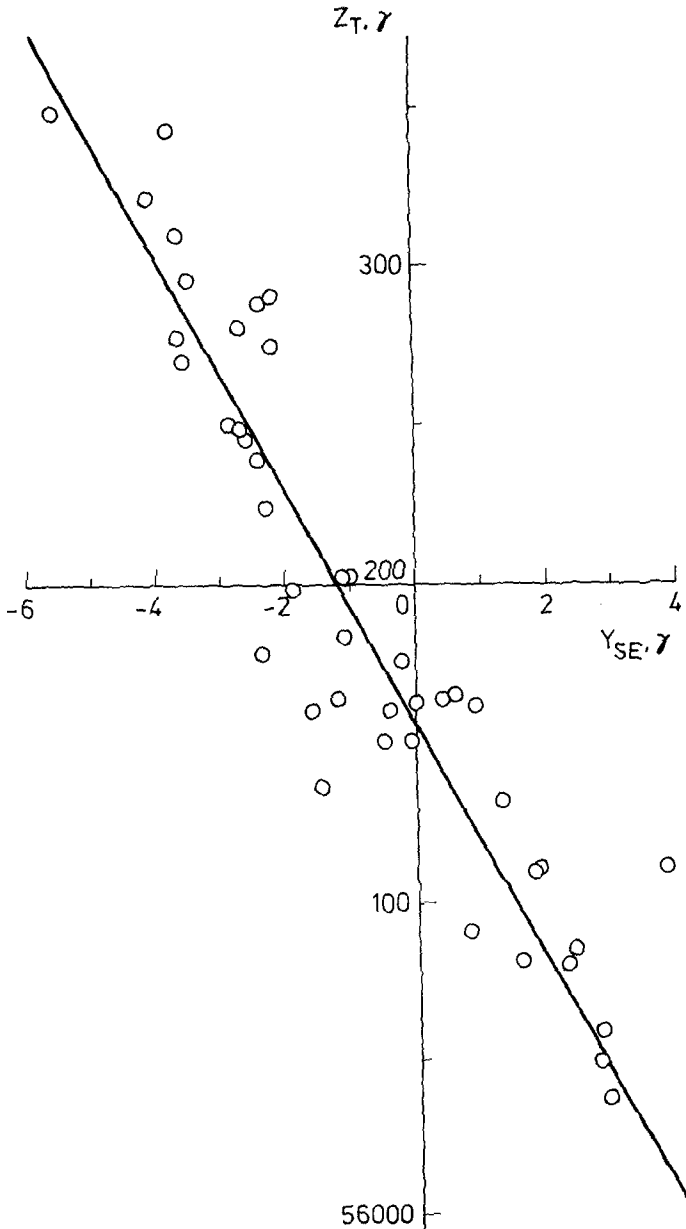


Fig. 12a.

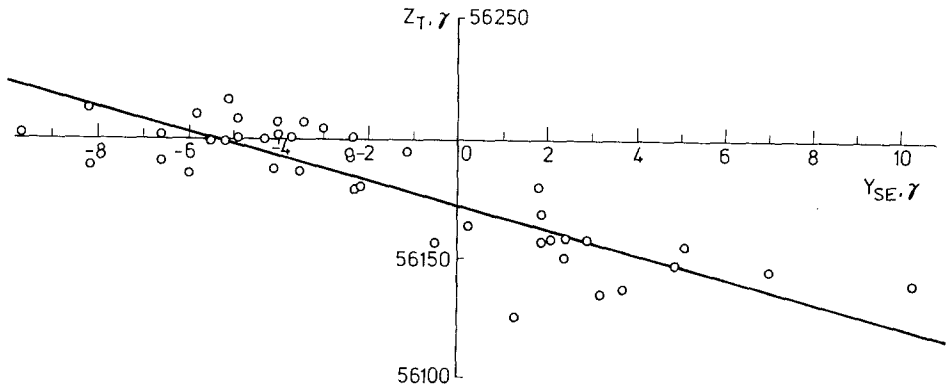


Fig. 12b.

Fig. 12a-b. Hourly averages of Z_T at Thule in July, 1965 versus Y_{SE} intensity and direction according to Sumaruk *et al.* (1974). The ground variations are delayed by 1 hr relative to interplanetary variations. The straight lines have been obtained using the least square method. Fig. 12a: near-noon hours. Fig. 12b: near-midnight hours.

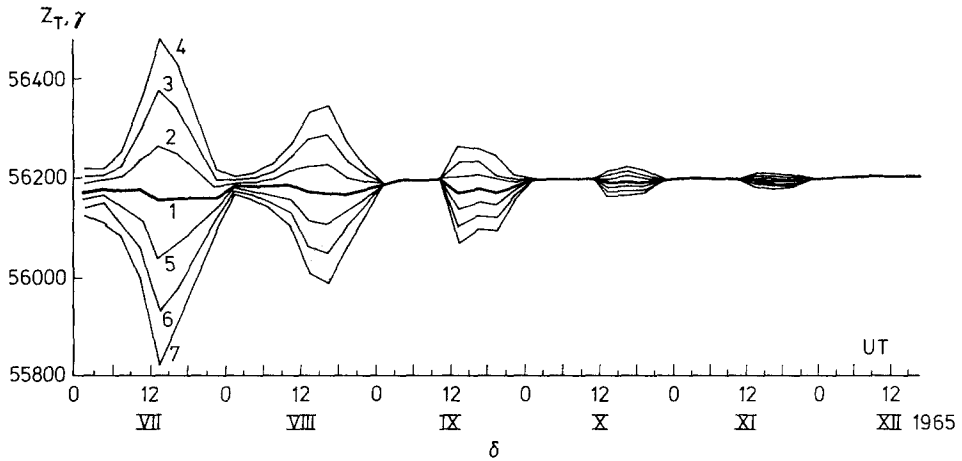


Fig. 13. Variations in Z_T throughout a day in the second half-year of 1965 at the various values of Y_{SE} according to Sumaruk *et al.* (1974). 1: $Y_{SE}=0 \gamma$; 2: $Y_{SE}=-3 \gamma$; 3: $Y_{SE}=-6 \gamma$; 4: $Y_{SE}=-9 \gamma$; 5: $Y_{SE}=3 \gamma$; 6: $Y_{SE}=6 \gamma$, 7: $Y_{SE}=9 \gamma$.

field measurements; and is therefore much better founded statistically than that obtained when selecting only the intervals with $Y_{SE} \sim 0 \gamma$. The values of Z_T at $Y_{SE}=0 \gamma$ are determined by the external sources independent of Y_{SE} . The Z_T variation due to Y_{SE} may be determined as the difference between the Z_T value in a given 1 hr interval and the Z_T value at $Y_{SE}=0 \gamma$.

The close relationship between Z_T and Y_{SE} permits the relations listed in Table II to be used for calculating Z_T at arbitrary values of Y_{SE} . Figure 13 presents the corresponding values of Z_T from July to December, 1965, at $Y_{SE} = \pm 3 \gamma$ (lines 5 and 2),

TABLE I
 Correlation factors between the values of the azimuthal component of the interplanetary field (Y_{SE}) and the vertical component of the geomagnetic field at Thule. Time UT

	0 ^h -3 ^h	3 ^h -6 ^h	6 ^h -9 ^h	9 ^h -12 ^h	12 ^h -15 ^h	15 ^h -18 ^h	18 ^h -21 ^h	21 ^h -24 ^h
July 1965								
-0.80±0.05	-0.72±0.08	-0.77±0.08	-0.72±0.1	-0.95±0.02	-0.93±0.02	-0.89±0.03	-0.82±0.06	
August 1965								
-0.41±0.16	-0.45±0.12	-0.74±0.07	-0.63±0.1	-0.88±0.05	-0.96±0.01	-0.82±0.06	-0.73±0.08	
July 1966								
-0.82±0.06	-0.60±0.12	-0.56±0.13	-0.77±0.07	-0.81±0.06	-0.67±0.09	-0.75±0.09	-0.72±0.1	
August 1966								
-0.80±0.06	-0.75±0.07	-0.85±0.04	-0.74±0.08	-0.84±0.04	-0.80±0.05	-0.83±0.05	-0.83±0.04	

TABLE II

Linear regression equations between the values of Z at Thule and Y_{SE} . $Z=56,000 \gamma +$ tabulated value

1965				
Hours	July	August	September	October
0-3	- 5.1 $Y_{SE}+171$	- 1.3 $Y_{SE}+187$		
3-6	- 4.1 $Y_{SE}+180$	- 2.4 $Y_{SE}+185$		
6-9	- 9.6 $Y_{SE}+171$	- 5.0 $Y_{SE}+184$		
9-12	-15.3 $Y_{SE}+178$	- 9.0 $Y_{SE}+189$		
12-15	-36.0 $Y_{SE}+154$	-18.4 $Y_{SE}+172$	-10.7 $Y_{SE}+171$	-2.8 $Y_{SE}+193$
15-18	-30.4 $Y_{SE}+158$	-20.5 $Y_{SE}+170$	- 8.9 $Y_{SE}+181$	-3.2 $Y_{SE}+198$
18-21	-18.0 $Y_{SE}+162$	-11.7 $Y_{SE}+168$	- 8.0 $Y_{SE}+173$	
21-24	- 8.0 $Y_{SE}+164$	- 6.4 $Y_{SE}+175$	- 1.7 $Y_{SE}+183$	
1966				
Hours	July	August	September	October
0-3	- 6.4 $Y_{SE}+208$	- 5.6 $Y_{SE}+212$		
3-6	- 4.6 $Y_{SE}+217$	- 4.0 $Y_{SE}+217$	- 3.8 $Y_{SE}+243$	
6-9	- 6.3 $Y_{SE}+219$	- 6.4 $Y_{SE}+211$	- 3.0 $Y_{SE}+248$	
9-12	-25.5 $Y_{SE}+208$	-14.9 $Y_{SE}+200$	- 6.5 $Y_{SE}+243$	-1.4 $Y_{SE}+239$
12-15	-19.1 $Y_{SE}+208$	-23.2 $Y_{SE}+186$	-14.5 $Y_{SE}+235$	-6.3 $Y_{SE}+229$
15-18	-16.9 $Y_{SE}+198$	-18.3 $Y_{SE}+185$	-10.4 $Y_{SE}+222$	-3.7 $Y_{SE}+230$
18-21	-15.6 $Y_{SE}+191$	-17.9 $Y_{SE}+185$	- 8.5 $Y_{SE}+220$	
21-24	- 7.3 $Y_{SE}+205$	-10.3 $Y_{SE}+193$	- 1.8 $Y_{SE}+231$	

$\pm 6 \gamma$ (lines 6 and 3) and $\pm 9 \gamma$ (lines 7 and 4). Thick line 1 shows variations in $Z_T(Y_{SE}=0 \gamma)$. The difference $\Delta Z_T = Z_T(Y_{SE} \neq 0) - Z_T(Y_{SE}=0)$ gives the pure form of the vertical component variation associated with the azimuthal component of the interplanetary magnetic field. The data presented above, together with the known fact of variation intensity decrease from summer to winter, indicate the following features:

(a) The night-time field values are functions of Y_{SE} values in July and August even during sunspot minimum, as in 1965. Hence, the midnight field values in summer season may be used as a field variation reference level, but only approximately. This is possible at the equinox, but the duration of the night-time interval unaffected by Y_{SE} is a function of solar activity.

(b) The Z variations at Thule during the winter of 1965 cannot be used to determine the Y_{SE} polarity. However, already at the equinox and during the winter of 1966, the Z_T values are more sensitive to Y_{SE} variations. This effect is probably due to the density increase of the high-latitude ionosphere ionization which is determined by solar activity level. It is not impossible that at even higher solar activity level the Y_{SE} polarity may be determined on the basis of Z_T data throughout the year, including the winter. Such a possibility has been demonstrated by Mansurov *et al.* (1973d) for the period from October 1972 to March 1973.

(c) At $Y_{SE} < 0$ the diurnal Z_T variation is of the form of a simple wave with maximum at day and minimum at night time (see Figure 7).

(d) Seasonal variations in ΔZ_T associated with Y_{SE} exist at both $Y_{SE} > 0$ and $Y_{SE} < 0$. Such seasonal variations indicate the existence of near-pole zonal currents at any polarity of Y_{SE} . A similar conclusion was also drawn when analyzing the observational material from other stations (Sumaruk and Feldstein, 1973c; Shelomentsev, 1974).

The special attention paid to the Z component variation and the ΔZ reference level is due to the fact that it is the variations in this geomagnetic field component on the Earth's surface that respond in the purest form to the IMF azimuthal component variations. This problem was discussed by Feldstein *et al.* (1974). It has been shown that within $\pm 10 \gamma$ the Z values near midnight in the summer season coincide with the mean-daily Z values in winter season (including secular variations). Within the same limits, the near-midnight values of Z in the summer season coincide with mean-diurnal Z values in periods of extremely quiet days when $|Y_{SE}| \ll 1 \gamma$. Therefore, within an accuracy of $\pm 10 \gamma$, the mean-daily values of the field component on extremely quiet days (for example, 11 July 1965), the mean-daily values of magnetically quiet days in the winter season (including secular variations), and the field values at near-midnight hours may be used for calculating the value and sign of near-pole Z in the summer season of years close to sunspot minimum. This conclusion is also confirmed by a more accurate analysis, the results of which are presented in Figure 13 (see Z_T variations at $Y_{SE} = 0 \gamma$).

4. Near-pole DPC (Y_{SE}) Variations in the Summer Season

The correlation method described above was used to separate DPC (Y_{SE}) into the three components of the field variations at near-pole stations of the northern hemisphere in the summer seasons of 1965 and 1966 (Sumaruk and Feldstein, 1975; Feldstein *et al.*, 1975). The hourly intervals when $AE \geq 150 \gamma$, $D_{st} < -10 \gamma$, and the Y_{SE} sign was changed during an interval, were excluded. In the remaining intervals Z_{SE} was $+1 \gamma$ on the average. It appeared that if these conditions are satisfied, the correlation of X , Y , Z with the IMF Y_{SE} intensity, if any, is practically always close to a linear one. Plotting of the correlation relationships has shown that a closer relationship of Y_{SE} with the $X(H)$ and $Y(D)$ components can be obtained by comparing coinciding hourly intervals without an hour shift. The small delay due to the magnetic field transfer from the satellite to the magnetosphere does not exceed ~ 10 min for IMP-3 satellite. A similar delay in the horizontal component relative to IMF variation can be traced in specific cases (see Figure 8). For this reason the correlation relationships of horizontal component intensities with Y_{SE} were plotted for coinciding hourly intervals. The Z component delay relative to Y_{SE} variation and its possible causes will be discussed at greater length below.

Tables III–V present, for each 3 hr interval of UT, the correlation factors (r) and their dispersion (σ_r) for the $X(H)$, $Y(D)$, and Z variations at near-pole stations

relative to Y_{SE} in July-August 1965. The intervals with $r \leq 0.4$ when $r \leq 3\sigma_r$ are not presented in the Table. A fairly high correlation in Z persists for all hours of the day on $\Phi' \sim 86^\circ$ (Alert and Thule stations); and an appreciable diurnal dependence of r with its minimum at near-midnight and maximum at near-noon can be observed at $\Phi' \sim 84^\circ$ (Resolute Bay station). Already at $\Phi' \sim 81^\circ$ (Mould Bay station) the correlation exists for but a small interval of the day, with r sign changing within a single 3 hr interval. At $\Phi' > 81^\circ$, Z decreases with increasing Y_{SE} while at $\Phi' < 81^\circ$ the inverse dependence holds. Positive correlation is observed in the day sector up to $\Phi' \sim 75^\circ$ (Baker Lake station). At $\Phi' \sim 70^\circ$ (Churchill) no significant correlation was found. In $X(H)$, a fairly close correlation persists practically throughout the day on $81^\circ \leq \Phi' \leq 84^\circ$; its value and duration decreases beyond this latitude range. Near noon at magnetically quiet periods the values of r indicate a nearly functional relationship between the X -component intensity and Y_{SE} , which is not worse than that described earlier for Z at $\Phi' \geq 84^\circ$. However, r decreases significantly if the disturbed periods are also used, because of a considerable response of the X -component at $\Phi' \sim 81-84$ to the fields of the DP1 current system. It is this circumstance that gives rise to the extensive use of the near-pole variations in Z , but not in $X(H)$, for the determination of the IMF azimuthal component. In the magnetically quiet periods near sunspot minimum, the relation between $X(H)$ and Y_{SE} can still be traced at $\Phi' \sim 78^\circ$ but is already absent at $\Phi' \sim 75^\circ$. Correlation of a single sign ($r > 0$) is characteristic of the entire polar region at $78^\circ \leq \Phi \leq 86^\circ$. The day-time difference between r signs at Alert and Thule stations, located on about the same latitude, may probably tell in favour of a more significant control of variation mode by geomagnetic than local time. Relationship with Y_{SE} in the $Y(D)$ component has been fixed only at $\Phi' > 80^\circ$ and is probably due to the fact that the horizontal plane disturbance vector is oriented at an angle to both geographic and magnetic meridians. The general regularities of r behaviour in July-August 1966 are similar to those described for 1965. There exist, however, some differences:

(1) An increase in the interval with $r \geq 0.4$ within a day for the vertical component at Resolute-Bay and Godhavn stations.

(2) This interval is also increased for the horizontal component at $\Phi' \sim 75-78^\circ$. At Godhavn station, the correlation persists throughout the day excluding the near-noon 3 hr interval (12^h-15^h UT). At Baker Lake station the correlation covers the morning sector.

(3) The correlation in the eastward component can be found at Godhavn and Baker Lake stations during individual intervals.

These differences can be naturally explained by the enhancement of the DPC (Y_{SE}) field variations due to solar activity increase and the subsequent increase of ionospheric conductivity from 1965 to 1966.

Tables VI-VIII present the equations of linear regression of Z , $X(H)$, $Y(D)$ to Y_{SE} obtained by the least square method, and the possible errors in the corresponding terms. The angular coefficients at Y_{SE} characterize the response of the ground magnetic field values at the various stations to the variation in the IMF azimuthal component, while the free term and its variations describe the field variations which are not

TABLE VI

Equations of linear regression between the values of the vertical component of the geomagnetic field at near-pole stations and Y_{SE} of the interplanetary magnetic field in July–August, 1965. Time UT

Station	Alert 55000 $\gamma+$	Thule 56000 $\gamma+$	Resolute Bay 57500 $\gamma+$
0 ^h –3 ^h	$-7.2 \pm 1.4 Y_{SE} + 450 \pm 2$	$-3.2 \pm 0.5 Y_{SE} + 179 \pm 1$	–
3 ^h –6 ^h	$-7.3 \pm 0.6 Y_{SE} + 461 \pm 1$	$-3.3 \pm 0.4 Y_{SE} + 182 \pm 1$	–
6 ^h –9 ^h	$-9.0 \pm 0.8 Y_{SE} + 465 \pm 1$	$-7.3 \pm 0.6 Y_{SE} + 178 \pm 1$	$-2.4 \pm 2.4 Y_{SE} + 679 \pm 1$
9 ^h –12 ^h	$-16.5 \pm 0.4 Y_{SE} + 464 \pm 1$	$-12.2 \pm 1.3 Y_{SE} + 183 \pm 1$	$-5.6 \pm 0.9 Y_{SE} + 682 \pm 2$
12 ^h –15 ^h	$-17.3 \pm 1.1 Y_{SE} + 440 \pm 1$	$-27.2 \pm 0.8 Y_{SE} + 163 \pm 1$	$-15.0 \pm 1.5 Y_{SE} + 674 \pm 2$
15 ^h –18 ^h	$-15.0 \pm 0.5 Y_{SE} + 437 \pm 1$	$-25.4 \pm 0.3 Y_{SE} + 164 \pm 1$	$-21.6 \pm 1.1 Y_{SE} + 662 \pm 1$
18 ^h –21 ^h	$-12.8 \pm 0.3 Y_{SE} + 442 \pm 2$	$-14.0 \pm 0.4 Y_{SE} + 165 \pm 1$	$-25.3 \pm 1.6 Y_{SE} + 662 \pm 3$
21 ^h –24 ^h	$-10.0 \pm 1.3 Y_{SE} + 442 \pm 2$	$-7.2 \pm 0.4 Y_{SE} + 170 \pm 1$	$-9.7 \pm 1.0 Y_{SE} + 678 \pm 2$

Station	Mould Bay 57500 $\gamma+$	Godhavn 55000 $\gamma+$	Baker Lake 60000 $\gamma+$
0 ^h –3 ^h	–	–	–
3 ^h –6 ^h	–	–	–
6 ^h –9 ^h	–	–	$4.7 \pm 0.7 Y_{SE} + 403 \pm 1$
9 ^h –12 ^h	–	–	–
12 ^h –15 ^h	$-8.6 \pm 1.0 Y_{SE} + 455 \pm 2$	$8.2 \pm 1.7 Y_{SE} + 553 \pm 2$	$9.5 \pm 1.2 Y_{SE} + 412 \pm 2$
15 ^h –18 ^h	$-6.1 \pm 1.4 Y_{SE} + 481 \pm 3$	–	$5.2 \pm 0.6 Y_{SE} + 373 \pm 1$
18 ^h –21 ^h	–	–	–
21 ^h –24 ^h	$6.1 \pm 1.7 Y_{SE} + 425 \pm 3$	–	–

associated with Y_{SE} . The field values corresponding to the free term are the reference level of the field variations that are functions of Y_{SE} (zero level). This level corresponds to the curve $Y_{SE} = 0 \gamma$ in Figure 9, while the curves for $Y_{SE} = \pm 3 \gamma$ in Figure 9 have been calculated on the basis of regression equations from Tables VII and VIII.

In the Z component (Table VI), the amplitude of the response changes within a day increases from Alert to Resolute Bay, and the responsiveness peaks in the period between the local and the local geomagnetic noons. At Alert station (a 7 hr 5 min difference between the local, 16^h UT, and local geomagnetic, 8^h05^m UT, noons) the maximum values of response are closer to the local noon. These features of Z response to Y_{SE} are due to the close relationship between the magnetic field variation values and the ionospheric conductivity and, hence, to a more strict control of variation intensity by local than geomagnetic time (Langel and Svalgaard, 1974).

The maximum responsiveness in the $X(H)$ and $Y(D)$ components to Y_{SE} is observed near noon. Its value in the horizontal plane at $\Phi' \sim 81$ – 84° is ~ 25 – 35γ , which even somewhat exceeds the responsiveness for Z at $\Phi' > 84^\circ$, which is $\sim 25 \gamma$ per 1γ of change in Y_{SE} . The relations presented in Tables 6–8 may be used to calculate the field variation values on the Earth's surface at fixed values of Y_{SE} . Presented in polar coordinates in Figure 14 is the distribution of magnetic variation vectors in horizontal (arrows) and vertical (numerals) planes for $Y_{SE} = \pm 6 \gamma$. The solid lines show the equivalent current system. On the day-side $\Phi' \sim 81^\circ$, the horizontal vectors are more

TABLE VII

Equations of linear regression between the values of the northward (horizontal) component of the geomagnetic field at near-pole stations and Y_{SE} of the interplanetary magnetic field in July–August, 1965. Time UT

Station	Alert X	Thule H (3 500 γ +)	Resolute Bay X	Mould Bay X (500 γ +)	Godhavn H (7 500 γ +)
0 ^h –3 ^h	–	–	7.0 \pm 0.7 Y_{SE} + 141 \pm 1	14.3 \pm 0.3 Y_{SE} + 503 \pm 1	3.0 \pm 0.6 Y_{SE} + 791 \pm 1
3 ^h –6 ^h	2.9 \pm 0.8 Y_{SE} + 783 \pm 1	–	3.8 \pm 0.7 Y_{SE} + 163 \pm 1	3.5 \pm 0.5 Y_{SE} + 526 \pm 1	–
6 ^h –9 ^h	7.2 \pm 0.6 Y_{SE} + 774 \pm 1	–	–	2.4 \pm 0.7 Y_{SE} + 545 \pm 1	–
9 ^h –12 ^h	–	–	4.4 \pm 1.1 Y_{SE} + 179 \pm 2	4.4 \pm 0.8 Y_{SE} + 555 \pm 1	–
12 ^h –15 ^h	–3.7 \pm 1.0 Y_{SE} + 754 \pm 1	–	12.0 \pm 1.2 Y_{SE} + 172 \pm 2	8.6 \pm 0.7 Y_{SE} + 569 \pm 1	–
15 ^h –18 ^h	–4.5 \pm 1.0 Y_{SE} + 717 \pm 2	9.2 \pm 1.9 Y_{SE} + 479 \pm 3	16.3 \pm 1.6 Y_{SE} + 132 \pm 3	10.3 \pm 0.9 Y_{SE} + 537 \pm 2	6.0 \pm 0.9 Y_{SE} + 804 \pm 1
18 ^h –21 ^h	–	10.0 \pm 0.8 Y_{SE} + 504 \pm 1	22.6 \pm 1.1 Y_{SE} + 110 \pm 2	17.7 \pm 2.0 Y_{SE} + 503 \pm 3	5.0 \pm 1.7 Y_{SE} + 786 \pm 3
21 ^h –24 ^h	–	8.0 \pm 0.2 Y_{SE} + 526 \pm 1	16.0 \pm 0.3 Y_{SE} + 131 \pm 1	25.5 \pm 1.2 Y_{SE} + 516 \pm 4	6.1 \pm 0.9 Y_{SE} + 791 \pm 2

TABLE VIII

Equations of linear regression between the values of the eastward (declination) component of the geomagnetic field at near-pole stations and Y_{SE} of the interplanetary magnetic field in July–August, 1965. Time UT

Station	Alert – 3 500 γ +	Thule – 72° +	Resolute Bay	Mould Bay 2 000 γ +
0 ^h –3 ^h	–	+1'.8 \pm 0.6 Y_{SE} – 374' \pm 1	–	9.6 \pm 0.5 Y_{SE} + 183 \pm 1
3 ^h –6 ^h	–	+2'.4 \pm 0.2 Y_{SE} – 359' \pm 2	–	2.5 \pm 0.5 Y_{SE} + 193 \pm 1
6 ^h –9 ^h	–	+3'.4 \pm 0.3 Y_{SE} – 355' \pm 2	–	3.6 \pm 0.4 Y_{SE} + 207 \pm 1
9 ^h –12 ^h	–	–	–	3.7 \pm 0.6 Y_{SE} + 223 \pm 1
12 ^h –15 ^h	–	–	1.9 \pm 0.5 Y_{SE} – 755 \pm 1	4.4 \pm 0.8 Y_{SE} + 259 \pm 1
15 ^h –18 ^h	– 7.8 \pm 1.4 Y_{SE} – 198 \pm 2	–	10.5 \pm 1.0 Y_{SE} – 754 \pm 2	10.9 \pm 0.9 Y_{SE} + 282 \pm 2
18 ^h –21 ^h	–10.0 \pm 1.4 Y_{SE} – 237 \pm 3	+3'.1 \pm 0.9 Y_{SE} – 401' \pm 2	10.5 \pm 2.8 Y_{SE} – 809 \pm 5	14.1 \pm 1.7 Y_{SE} + 253 \pm 3
21 ^h –24 ^h	– 6.8 \pm 0.8 Y_{SE} + 263 \pm 1	+3'.6 \pm 0.8 Y_{SE} – 396' \pm 1	7.2 \pm 0.8 Y_{SE} – 820 \pm 1	20.3 \pm 0.7 Y_{SE} + 217 \pm 1

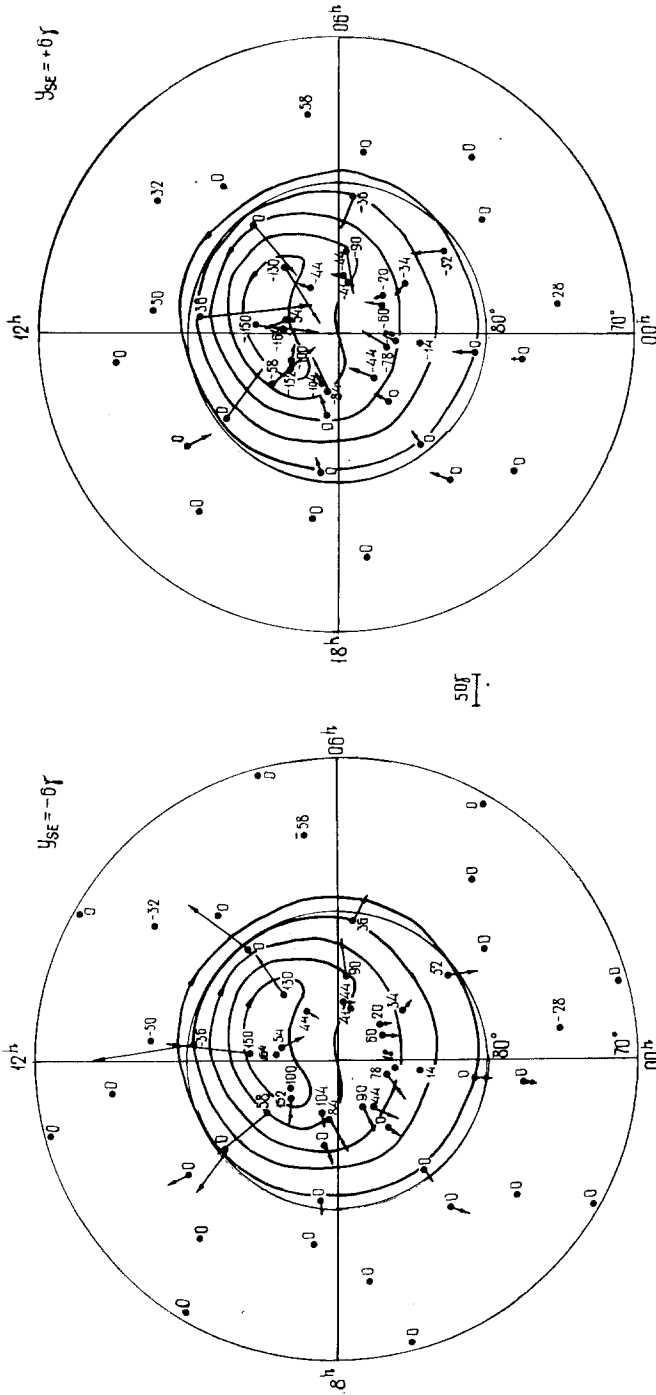


Fig. 14. Spatio-temporal distribution of magnetic variation vectors in horizontal (arrows) and vertical (numerals) planes at $Y_{SE} = -6 \gamma$ (to the left) and $Y_{SE} = +6 \gamma$ (to the right) for July-August, 1965 according to Feldstein *et al.* (1975). The solid lines with arrows show the current lines of the equivalent current system, the current between which is $45,000 \text{ A}$. The total current intensity is $1.8 \times 10^8 \text{ A}$. The coordinates are the corrected geomagnetic latitude - local geomagnetic time.

intensive, which is described by the convergence of the current lines. This convergence may be interpreted as a polar electrojet in which the current direction and intensity are determined by Y_{SE} sign and value respectively. The current in the electrojet is westward at $Y_{SE} < 0$ and eastward at $Y_{SE} > 0$. The current system with a 18×10^4 A total current covers the polar region ($\Phi' > 80^\circ$) with a focus on the day-side $\Phi' \sim 86^\circ$; the values of Z are maximum in the same region. The DPC(Y_{SE}) current system in July–August, 1966 (Figure 15) is roughly the same as that presented in Figure 14, except that the total current is 24×10^4 A, the current system covers the region with $\phi' > 75^\circ$, and its focus (maximum values of Z) on the day side is shifted to $\Phi' \sim 84\text{--}85^\circ$.

It is of interest to compare the DPC(Y_{SE}) field variation in Figure 14 to the results obtained when using other reference levels. Presented in Figure 16 according to Sumaruk and Feldstein (1973d) is the distribution of magnetic variation vectors in July–August, 1965. The field variations were determined separately for $Y_{SE} > 0$ or $Y_{SE} < 0$, only in those hour intervals when $Z_{SE} > 0$. The values of the components were calculated from the diurnal variations of the corresponding elements at each station for the extremely quiet day of 11 July 1965. The method is based on the assumption that the field variations independent of Y_{SE} do not alter much in the selected hour intervals or on 11 July. In the hour intervals with $Y_{SE} < 0$ the mean value of $Z_{SE} = 1.6 \gamma$ (the maximum and minimum values are within $0\text{--}4 \gamma$); at $Y_{SE} > 0$ the mean $Z_{SE} = 1.4 \gamma$ (the maximum and minimum values are within $0\text{--}3 \gamma$). The use of the intervals with $Z_{SE} > 0$ substantially diminishes the effect of magnetospheric substorm fields. The D_{st} variation is $2\text{--}4 \gamma$ and, therefore, the effect of the ring current field may be neglected. The field vector distribution and the features of the equivalent currents at $\phi' \geq 80^\circ$ are mainly similar to these shown in Figure 14. The most characteristic features are the day-side westward (at $Y_{SE} < 0$) or eastward (at $Y_{SE} > 0$) currents and the day-side convergence of currents. The absence of the equatorward-directed vectors on the night-sector $\Phi' \sim 70^\circ$ indicates a sufficiently complete exclusion of DP1 fields. The difference in magnetic variations shown in Figures 14 and 16 mainly concerns $\Phi' < 80^\circ$: the polar electrojets in Figure 16 are closed not only through the night side of the polar region, as in Figure 14, but also through lower latitudes on the day side. This results in the asymmetric distribution of field vectors in Figure 16 at $75^\circ \leq \Phi \leq 80^\circ$, i.e. in the descent to these latitudes of the westward and eastward electrojets in the morning and afternoon sectors respectively.

When the daily mean field values are used as the reference level, a substantial contribution to the resulting value of the field vector is from the fields of quasi-stationary magnetospheric convection (of S_q^p or DP2 type), convection around a neutral point (of DPC type: see, for example, Shabansky, 1971), associated with the middle- and low-latitude S_q solar-diurnal variations S_q^o , and (when the data for all days are considered) also from the fields of magnetospheric substorms (DP1) and ring current (DR). Figure 17 presents according to Sumaruk and Feldstein (1973b) the variation vector distribution for all days of July–August, 1965 at $Y_{SE} < 0$ and $Y_{SE} > 0$. The daily mean values for 11 July 1965 and the daily mean values of the quiet days of the winter season corrected for secular variations were taken as the reference

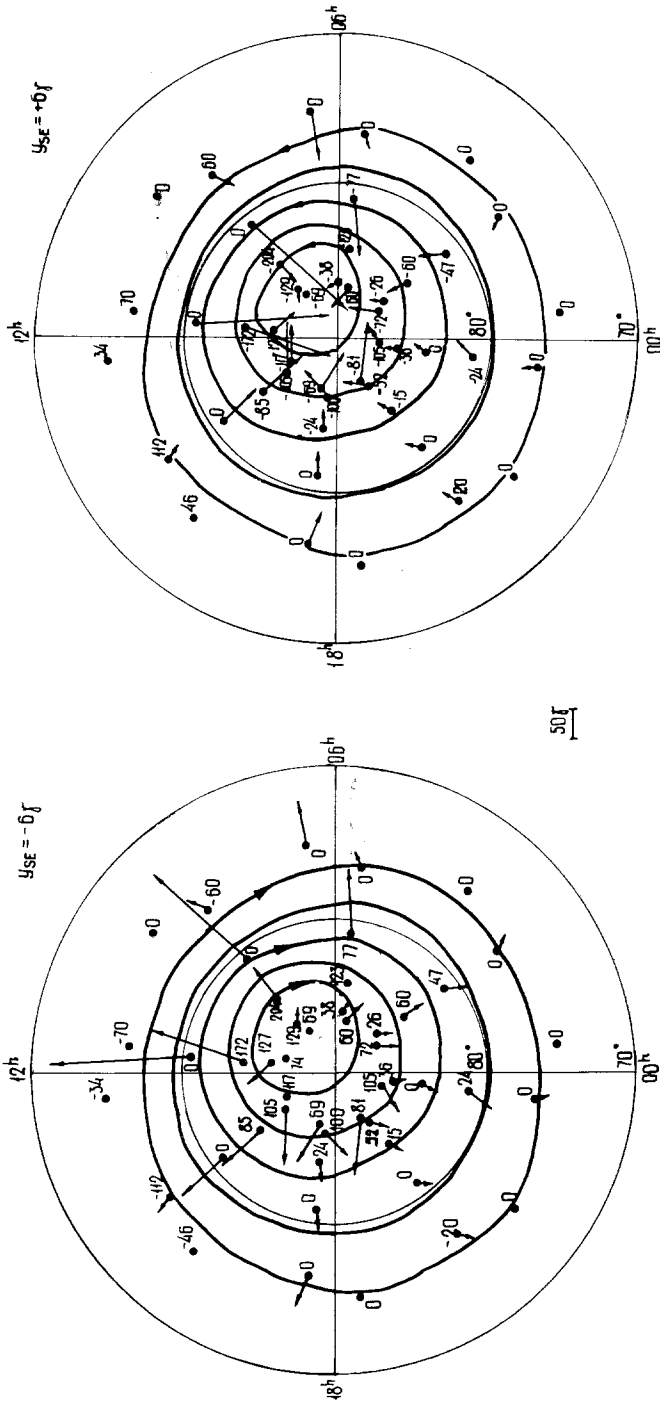


Fig. 15. The same as in Figure 14 for July-August, 1966 according to Sumaruk and Feldstein (1975). The total current intensity is 2.4×10^5 A.

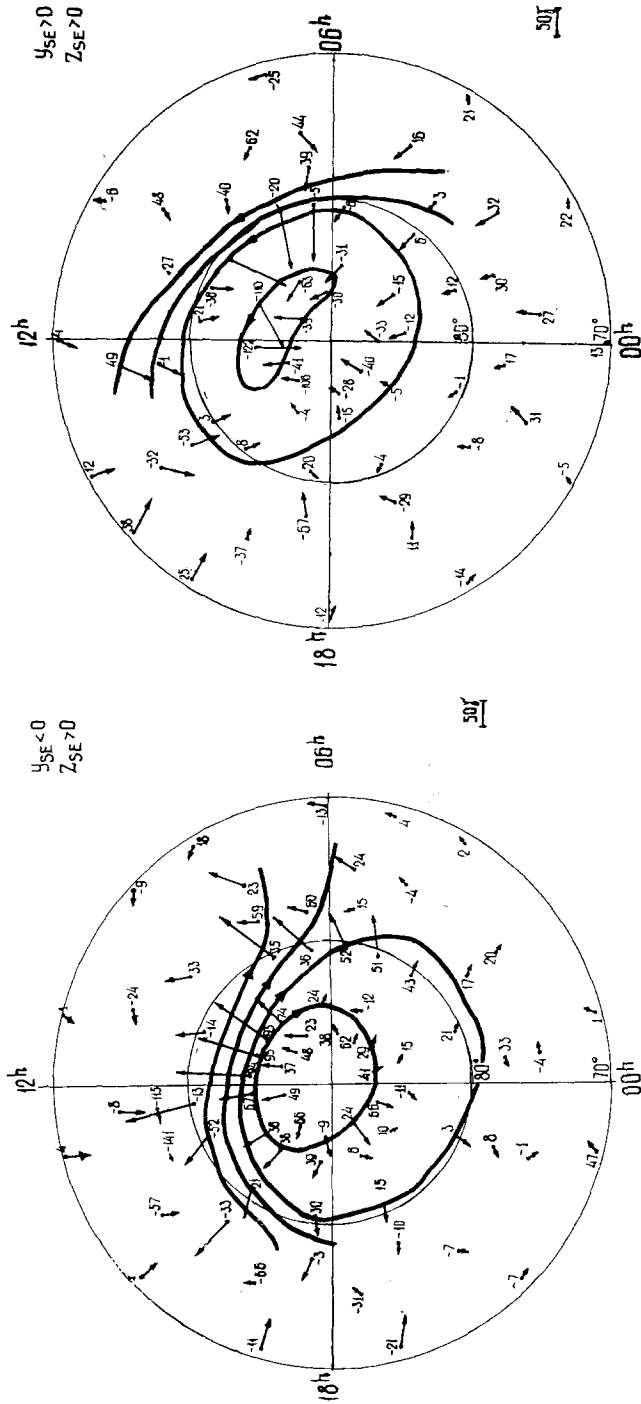


Fig. 16. Spatio-temporal distribution of magnetic variation vectors in July-August, 1965 in horizontal (arrows) and vertical (numerals) planes according to Sumaruk and Feldstein (1973d). The solid lines with arrows show the current directions. The variations are calculated from the diurnal dependence of the corresponding elements at each observatory on 11 July 1965. To the left: $Y_{SE} < 0, Z_{SE} > 0$. To the right: $Y_{SE} > 0, Z_{SE} > 0$. The coordinates are the corrected geomagnetic latitude - local geomagnetic time.

level. The distributions for all days and in magnetically quiet periods (when $AE < 150 \gamma$ and D_{st} variations were on the average $2-4 \gamma$) were analysed separately.

The main features of the current systems for the various Y_{SE} directions may be reduced to the following.

At $Y_{SE} < 0$ there exists an intense westward polar electrojet in the day sector, in the form of a spiral located at $\Phi' \sim 83^\circ$ at 18^h , 82° at 12^h , and 75° at 9^h of local geomagnetic time. The electrojet can be clearly seen in the quiet periods and in observations for all days. It is closed through lower latitudes on the evening and night sides. The day-evening sector contains a vortex with a counter-clockwise current and focus at latitudes $75^\circ \leq \Phi' \leq 78^\circ$ at 16^h LGT. The latitude of the focus is conserved for the periods with different disturbance levels.

At $Y_{SE} > 0$ an eastward polar electrojet in the form of a spiral can be observed in the morning sector at $\Phi' \sim 85^\circ$ at 03^h and $\Phi' \sim 80^\circ$ at 09^h LGT. The electrojet forms a vortex with a counter-clockwise current covering the entire polar cap and with a current convergence at $\phi' \sim 74^\circ$ at 16^h LGT. The current focus is located on the 15^h meridian at $78^\circ \leq \Phi' \leq 80^\circ$. A portion of the polar electrojet current is closed through the night sector on the auroral oval latitudes. Weak distributed currents flow during the magnetically quiet period on the night-side $\Phi' < 80^\circ$. The latitude cross-sections of three components of the variation fields in the various time sectors have shown that at 15^h-17^h LGT the focus of the evening current cell is shifted from $\Phi' \sim 77^\circ$ at $Y_{SE} < 0$ to $\Phi' \sim 79^\circ$ at $Y_{SE} > 0$. This shift is responsible for the sign change of the horizontal component variation at Godhavn station ($\Phi' \sim 78^\circ$) relative to the sector polarity of the interplanetary magnetic field when the daily mean values are used as the reference level (Svalgaard, 1968). Such a small latitude shift of the evening current cell focus cannot explain the observed near-pole Z variations when the Y_{SE} sign is changed. The change of the ΔZ sign from positive at $Y_{SE} < 0$ to negative at $Y_{SE} > 0$ is due to the replacement of the westward current band in the evening-day sector of the polar cap at $Y_{SE} < 0$ by the eastward current band in the night-morning sector at $Y_{SE} > 0$. In Figure 17 the DP1 effect can be traced as negative vectors in the horizontal plane at $\Phi' \sim 70^\circ$ in the early morning.

The field variations calculated from the daily mean values of winter days in Figure 17 characterize the variations caused by the effect of several sources. However, the most characteristic features of the DPC(Y_{SE}) variations (the westward and eastward electrojets at $\Phi' > 80^\circ$) are conserved in the summer seasons of minimum sunspot activity. Additional features (the cell currents in the evening sector with focuses at $77^\circ \leq \Phi' \leq 79^\circ$) are from those field sources which are supplementary to DPC (Y_{SE}). Besides that, the polar electrojets themselves vary somewhat. The most perceptible difference – that the eastward electrojet fails to cover the day-time – is due to the field decrease in the day sector as compared with the daily mean level, resulting from the DPC and S_q^o currents.

The variation vector distributions at $\Phi' > 70^\circ$ during the equinox at the various Y_{SE} orientations are described in Sumaruk and Feldstein (1973e). The daily values of the winter season quiet days including secular variations, and the daily mean values for

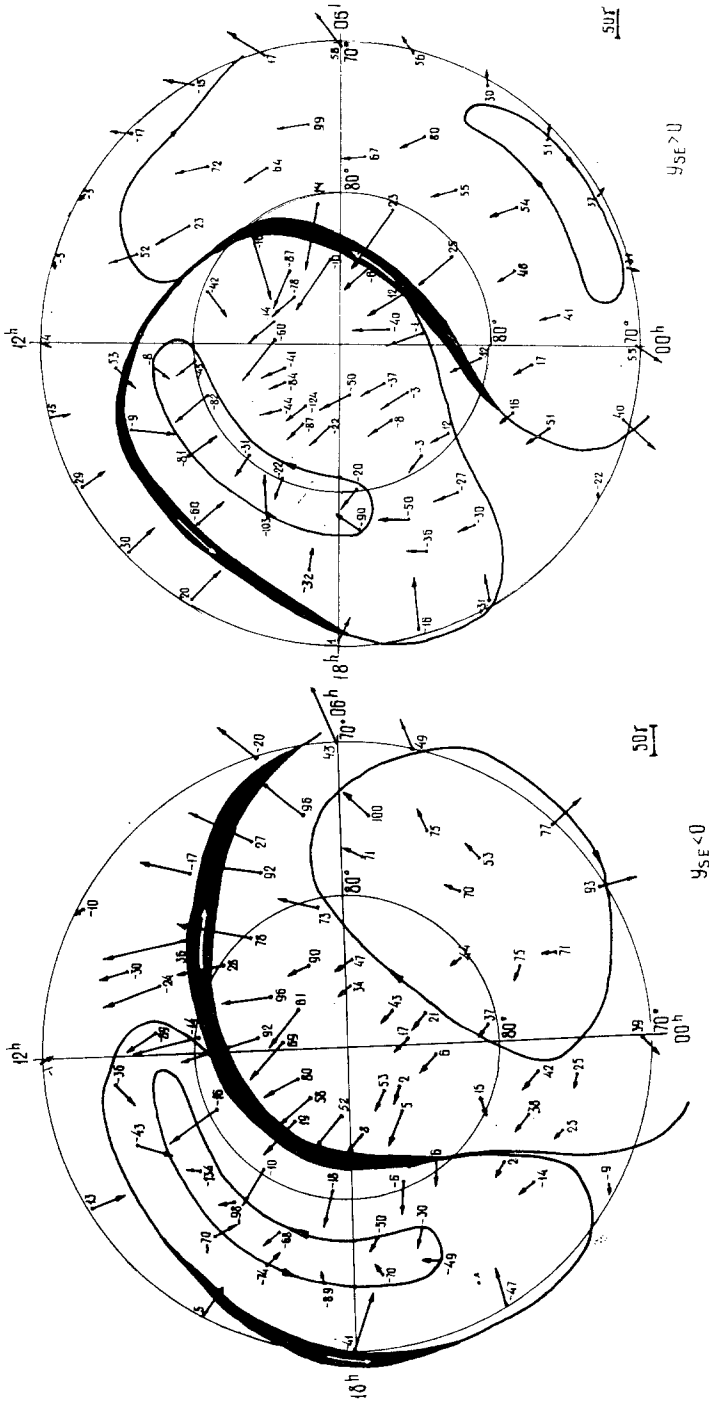


Fig. 17. Variation vector distribution at $\phi^m > 70^\circ$ in July-August, 1965 in horizontal (arrows) and vertical (numerals) planes according to Sumaruk and Feldstein (1973b). The variations are calculated from the mean-daily values. The thick lines denote the current convergence of an electrojet nature. The arrows indicate the current directions. Observations for all days have been used. The coordinates are the corrected geomagnetic latitude and the local geomagnetic time. Intervals with $Y_{SE} < 0$ and $Y_{SE} > 0$ are at the left and right respectively.

30 October 1965, when $|Y_{SE}| < 1 \gamma$, were taken as the field reference level. The D_{st} variation was 1–3 γ .

The equinox current systems at different Y_{SE} orientations are similar to the summer current systems. At $Y_{SE} < 0$, the current is enhanced during the day-sector at $\Phi' \sim 82^\circ$. The current is closed through lower latitudes in the evening and morning sectors. The evening cell with counter-clockwise current has its focus at $\Phi' \sim 79^\circ$, 13–14^h LGT. During the equinox, the variation intensity decreases by a factor of ~ 3 as compared to summer, the polar current convergence exists only near noon, and the evening cell focus shifts to noon.

At $Y_{SE} > 0$ the day-evening cell current focus is on the $\sim 13^h$ LGT meridian at $\Phi' \sim 80^\circ$. Thus, the variation intensity decrease and the shift of the evening cell current focus to noon at $\Phi' \sim 80^\circ$ from summer to equinox, are the characteristic features of this type of variation.

5. Models of the DPC(Y_{SE}) Field Variation Source

The first model representations of DPC(Y_{SE}) generation as a result of interaction between the interplanetary magnetic field and the periphery portion of the geomagnetic field, whose force lines are projected on the polar cap, emphasized the role of radial component (Bassolo *et al.*, 1972) or assumed the alternating reconnection of force lines from northern or southern polar caps with the interplanetary field depending on IMF polarity (Forbes and Speiser, 1971). At present, however, the main role in DPC(Y_{SE}) generation is ascribed to the IMF azimuthal component, while the variation itself exists independently of IMF polarity. The convective motion of geomagnetic force lines across the polar cap or the shifts of the polar cap-auroral belt boundary (Heppner, 1972) are hardly responsible for the DPC(Y_{SE}) variation. This variation exists during magnetically quiet periods and there is no confirmation of its relationship with polar magnetic substorms or the near-pole variations of S_q^p or DP2 type (Kawasaki and Akasofu, 1972) which are in close correlation with the IMF Z_{SE} component fluctuations (Nishida and Kokubun, 1971).

At present, the mechanism of reconnection of interplanetary and geomagnetic fields has been proposed to explain the DPC(Y_{SE}) variations relative to the IMF Y_{SE} component (Wilhelm and Friis-Christensen, 1972; Jørgensen *et al.*, 1972; Russel, 1972). This mechanism has been developed by Leontyev and Lyatsky (1974), and Matveev (1974) up to the construction of three-dimensional and equivalent current systems describing the DPC(Y_{SE}) variation. Interesting representations explaining the appearance of the polar cap electric field relative to the Y_{SE} component may be found in Stern (1973), and Ivanov (1973, 1974).

Leontyev and Lyatsky (1974) postulate penetration of the electric field, $E_Z = -(1/c) \times V_X \times Y_{SE}$, from the solar wind to the magnetosphere, which will cause a potential difference between the northern and southern boundaries of the magnetotail. On the assumption of a high conductivity along the magnetic field lines, the electric field E_Z can exist only in the region of open field lines rooted at the polar caps, and will be

short-circuited along the closed field lines. Thus, the boundary between closed and open field lines will be the line of zero potential for the field E_Z , and $\phi|_{r=r_2}=0$ at this boundary in the ionosphere (a circle of radius r_2). At the polar cap boundary (a circle of radius r_1) the potential in the ionosphere is set in the form

$$\phi|_{r=r_1} = \phi_0(1 + \sin \lambda)$$

where ϕ_0 is the electric potential proportional to the Y_{SE} component of interplanetary magnetic field, and the angle λ is measured from the morning meridian counterclockwise. By inserting the analytical functions and turning to complex variables, the electric potential and the function of ionospheric current can be found. Magnetic field on the Earth's surface is produced by both ionospheric and field-aligned currents. The summary function of equivalent ionospheric currents Ψ^{eq} determining the resulting magnetic disturbances on the Earth's surface is of the form

$$\Psi_1^{eq} = \frac{1}{2}\phi_0\sqrt{(\sigma_P^2 + \sigma_H^2)}(r/r_1)\cos(\lambda - \lambda_1); \quad (1)$$

$$\Psi_2^{eq} = \sigma_H\phi_0\left(\frac{\ln(r/r_2)}{\ln(r_1/r_2)} + \frac{r_2^2}{r_2^2 - r_1^2}\frac{r_1}{r}\sin\lambda - \frac{r_1^2}{r_2^2 - r_1^2}\frac{r}{r_1}\sin\lambda\right) + \Psi_3^{eq}; \quad (2)$$

$$\Psi_3^{eq} = \frac{1}{2}\phi_0(-2\sigma_H + (r_1/r))\sqrt{(\sigma_P^2 + \sigma_H^2)}\cos(\lambda + \lambda_1). \quad (3)$$

where Ψ_1^{eq} , Ψ_2^{eq} , Ψ_3^{eq} are respectively the current functions in the polar cap (zone 1), at the broad boundary between the polar cap and the closed magnetosphere including the day-side cusp (zone 2), and in the region of closed force lines (zone 3); σ_H and σ_P respectively are the height-integrated Hall and Pedersen ionospheric conductivities in the day-side cusp region. The ionospheric conductivity in the polar cap is assumed to be zero, and the angle λ_1 is determined from the relation $\tan \lambda_1 = \sigma_H/\sigma_P$.

Figure 18 presents the equivalent ionospheric current systems calculated from the above relations for the northern hemisphere at $Y_{SE} < 0$ (left) and $Y_{SE} > 0$ (right). It was assumed that the boundary radius ratios $r_1/r_2 = 3/4$, that $\sigma_H = \sigma_P$ in the zone confined by radii r_1 and r_2 , and that the polar cap conductivity was zero. The current systems in Figure 18 are very similar to those described above for the DPC(Y_{SE}) variation (Figures 14 and 15). This suggests that the initial postulates for the model calculations in Leontyev and Lyatsky (1974) correctly represent the essence of the phenomenon. Relations (1–3) comprise parameters r_1 , r_2 , ϕ_0 , which may be estimated from experimental data. On the assumption that the day-side field variations are due to a flat current jet in the ionosphere, the jet boundaries were determined on the basis of observation data from Resolute Bay and Mould Bay stations. The method for determining the electrojet parameters on the basis of observation data from a pair of stations is similar to that described by Loginov and Starkov (1972). The polar electrojet width is $\sim 6^\circ$ of latitude and confined within $\Phi' = 78.4^\circ$ and 84.4° . On the assumption that the day-side polar electrojet coincides with the region of effective influence of electric field, the values of r_1 and r_2 are respectively $5.6 R_E/57.3$ km and $11.6 R_E/57.3$ km, where R_E is the Earth radius. The total equivalent current inter-

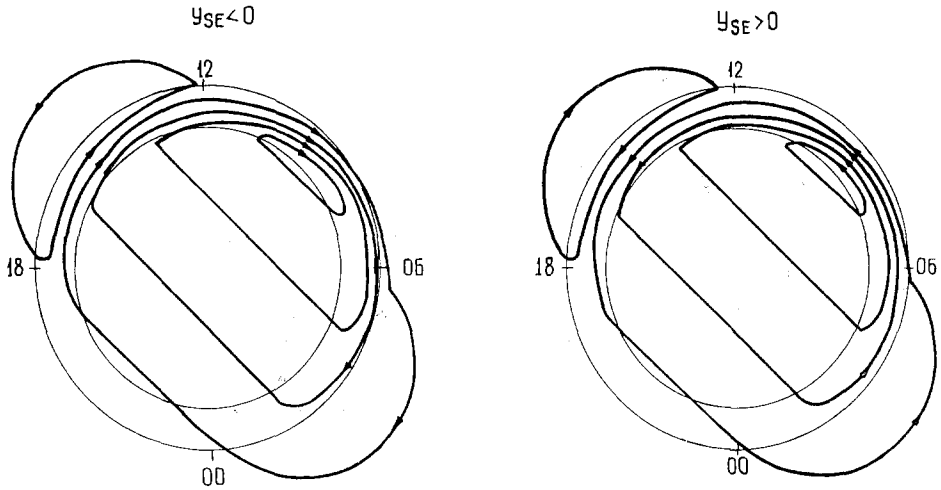


Fig. 18. Calculated equivalent ionospheric currents in the northern polar cap for $Y_{SE} < 0$ (at the left) and $Y_{SE} > 0$ (at the right) according to Leontyev and Lyatsky (1974).

secting the noon meridian in the polar electrojet is

$$I = \Psi_2^{eq}(r_2, \pi/2) - \Psi_2^{eq}(r_1, \pi/2) = \\ = \varphi_0 \left[-2\sigma_H - \frac{1}{2}(r_1/r_2 - 1) \sqrt{(\sigma_H^2 + \sigma_P^2)} \sin \lambda_1 \right].$$

Substituting the values of parameters r_1 and r_2 and replacing $\sin \lambda_1$ by $\tan \lambda_1 = \sigma_H / \sigma_P$ we get

$$I = 1.74 \sigma_H \varphi_0 \quad (4)$$

In July–August 1965 at $\Phi' \sim 81^\circ$, 18–24^h UT (near-noon hours at Resolute Bay and Mould Bay stations) $\sigma_H \approx \sigma_P \approx 7$ mhos (Feldstein *et al.*, 1975b). It follows from (4) at $I = 1.8 \times 10^5$ A that $\varphi_0 = 1.5 \times 10^4$ V, $E \sim 45 \times 10^{-5}$ V cm⁻¹. The potential difference between the northern and southern boundaries of the magnetotail can be determined from the relation

$$\varphi = E_Z D_M = - (1/c) V_X Y_{SE} D_M$$

where V_X is the solar wind velocity, D_M is the size of the magnetosphere. At $V_X \sim 400$ km sec⁻¹, $Y_{SE} = 6 \gamma$, $D_M \sim 2.5 \times 10^{10}$ cm, we get for the potential difference

$$\varphi = 6 \times 10^5 \text{ V}$$

Thus, the effectiveness of electric field penetration from the solar wind to the polar ionosphere in the summer hemisphere is $\sim 10\%$ if the voltage drop is the same in the northern and southern hemispheres. If the more considerable voltage drop in the dark hemisphere due to a lower ionospheric conductivity is included, the effectiveness of

electric field penetration will increase up to 25%. Disagreement between the voltage drops in the polar cap actually observed and those calculated was discussed by Stern (1973).

If the ionospheric conductivity in the polar cap is not zero, the pattern of currents shown in Figure 18 will be somewhat different. According to Leontyev (1974), the current system symmetry axis will turn towards the noon meridian but the current jet in the polar cusp region will be conserved. As a result, the current system will be even more like the DPC(Y_{SE}) shown in Figures 14 and 15.

Electric field in zone 2 is oppositely directed in the morning and the evening. In conjunction with the electric field of quasistationary convection (Heppner, 1972b;

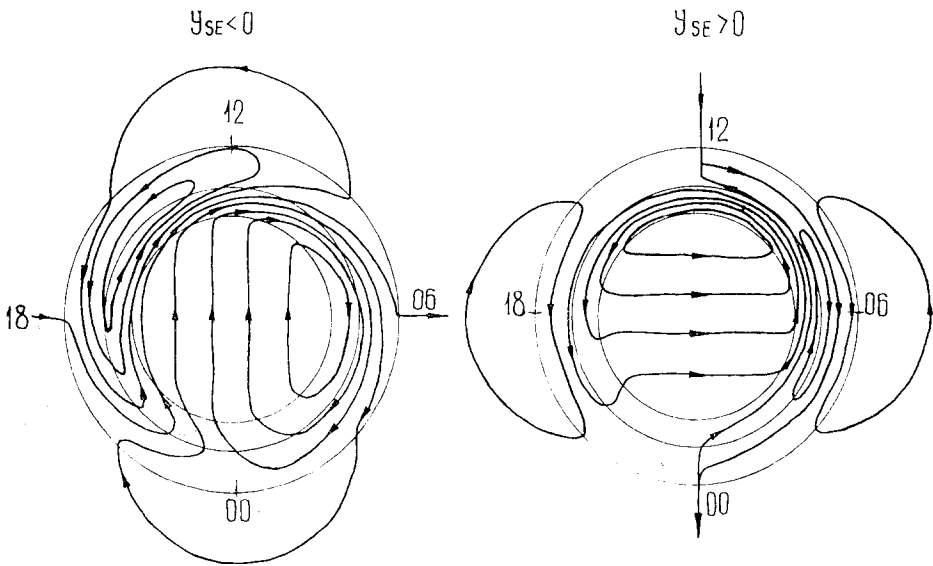


Fig. 19. Calculated resulting (including the electric field of quasistationary convection) equivalent ionospheric current systems in the northern polar cap at $Y_{SE} < 0$ (at the left) and $Y_{SE} > 0$ (at the right) according to Leontyev and Lyatsky (1974).

Cauffman and Gurnett, 1972) directed from the morning to the evening side, the zone 2 field results in an increase of antisolar convection at one of the polar cap boundaries (morning or evening) and a decrease at the other boundary. The resulting current system is presented in Figure 19 according to Leontyev and Lyatsky (1974), on the assumption of equality between the electric field of quasistationary magnetospheric convection and that caused by the IMF Y_{SE} component. The calculated equivalent current systems are very similar to those shown in Figure 17. This similarity will be even more pronounced, especially for $Y_{SE} > 0$, if the S_q^o and DPC variations resulting in a horizontal component decrease at $\Phi' \sim 80-82^\circ$ during day hours

are included. This will confine the eastward current in Figure 19 mainly to the morning sector, as in Figure 17.

Thus, the current systems describing the DPC(Y_{SE}) field variation, shown in Figures 14 and 15, are very similar to the theoretically calculated model equivalent current systems including both ionospheric and field-aligned currents.

According to Matveev (1974), the Y_{SE} component produces a uniform electric field in the geomagnetospheric cavity which, under the condition of IMF-geomagnetic field reconnection, generates currents within a thin sheet near the magnetopause penetrating into the ionosphere along the polar cusp. The resulting current system (field-aligned currents at the near-pole and equatorial cusp boundaries closed by Pedersen currents in the ionosphere across the cusp; Hall current along the cusp) is similar to that considered by Leontyev and Lyatsky (1974). However, the Hall currents in the morning and evening sectors are closed from one hemisphere to another along magnetic force lines, thereby causing the field variations associated with the Y_{SE} component on medium latitudes.

Stern (1973) has qualitatively described the properties of the polar cap electric field in terms of the open-magnetosphere model in connection with the IMF Y_{SE} component. In his model, the electric field in the central polar cap is directed from the morning to the evening side irrespective of Y_{SE} sign. However, inclusion of the deformation of the solar wind magnetic field near the magnetosphere results in a change of electric equipotentials which take the form of crescents in the polar-cap ionosphere. Stern's model explains the appearance of intense currents in the morning or evening sectors within a narrow region at the polar cap boundary, the change of direction of these currents in connection with the IMF Y_{SE} component sign, and the morning-evening asymmetry of the electric field observed in the polar cap. The existing models will probably be further improved in the direction of more accurate representation of the electric field distribution in the polar caps, including the complex structure of the interplanetary magnetic field and its dynamics near the magnetosphere and the actual distribution of conductivity in the high-latitude ionosphere.

Ivanov (1973, 1974) has shown that the observed properties of the polar cap electric field and, in particular, the relationships with the IMF azimuthal component, result from the conditions at the boundary magnetosphere discontinuity, if one proceeds from the concepts of an open magnetosphere with a non-zero normal component of the magnetic field at the boundary, and a flow of plasma into the magnetospheric inside. The tangential component E_t at the boundary is continuous and is transferred along geomagnetic field lines into the polar ionosphere. Its value increases due to field line convergence towards the Earth's surface. The calculations based on observations give a 4-fold increase in the electric field in the morning, as compared to the evening, at $Y_{SE} > 0$, and the reverse relation at $Y_{SE} < 0$. The potential difference across the polar cap in the morning-evening direction is ~ 50 kV. The main contribution to the electric field component in the day-night direction is from the E_n component normal to magnetopause. Ivanov (1974) discusses the possibility of E_n transfer to the polar ionosphere, the resulting difficulties, and the possible ways to overcome them. As a result,

it is possible to outline the construction of a physical model of the electric field transfer from the solar wind to the polar ionosphere, which makes it realistic to hope that the very near future will see a consistent theory of DPC (Y_{SE}) generation of the polar cap current system closely associated with the orientation of interplanetary magnetic field.

6. The Conductivity of the High-latitude Ionosphere

According to relations (1–3), the intensity of the DPC (Y_{SE}) current system and, in particular, its most characteristic feature, the day-sector polar electrojet, bears a direct relation with the height-integrated conductivities of the ionosphere (σ_H and σ_P) at polar cusp latitudes. The DPC (Y_{SE}) intensity is known to decrease substantially from summer to winter. A possible cause of the seasonal variations is the decrease in conductivity of the polar ionosphere which is sunlit throughout the day in summer and completely dark in winter. Ionospheric conductivity in the day-cusp region (at $\Phi' \sim 80\text{--}82^\circ$) exhibits diurnal variations associated with magnetic pole rotation around the geographic pole and with the change in the geographic latitude of the polar electrojet. These diurnal conductivity variations controlled by universal time (UT) may be sufficiently intense, since the geographical latitude (in Φ') of the polar region changes by $\sim 23^\circ$ during a day. As a result, the variations in magnetic disturbance intensities controlled by UT should appear.

Compare the magnitude of the observed variations in intensity of near-pole magnetic disturbances and those expected from conductivity variations. This is possible on the basis of quantitative relations between the field variation intensity and Y_{SE} intensity presented in Section 2. It is assumed in the discussion below that the currents are generated at the day-cusp latitudes in the region of the polar electrojet, and that their intensity is determined by the values of σ_H and σ_P at a fixed value of the electric field which is itself determined by the value and direction of Y_{SE} .

The total ionospheric conductivity in the day cusp is composed of conductivities caused by the ionization of atmospheric components when affected by corpuscular and wave emissions. In this case the conductivity in the ionospheric E -region comprising the currents responsible for magnetic disturbances is proportional to n_e , the electron concentration at an altitude of $\sim 100\text{--}120$ km. It has been shown by Osipova (1973) that the height-integrated ionospheric conductivities from both corpuscular and wave emissions may be assumed, to a sufficiently good approximation, to be proportional to n_e^m , the maximum ionization density in the ionospheric E -layer. Figure 20 presents σ_H and σ_P as functions of n_e^m according to Osipova (1973). Relationships can be clearly seen between the values of integral conductivities calculated from the real $N(h)$ profiles, obtained as a result of various kinds of ionospheric soundings including rocket experiments, and the electron concentration in the E -layer maximum. There exists a clearly pronounced linear dependence of $\lg \sigma_{H,P}$ on $\lg n_e^m$.

It is possible to estimate the relative contribution of corpuscular and wave sources of ionization at day-cusp latitudes to ionization in the E -region. The calculations of Kennel and Rees (1972) have shown that within a $100 < h < 120$ km interval n_e varies

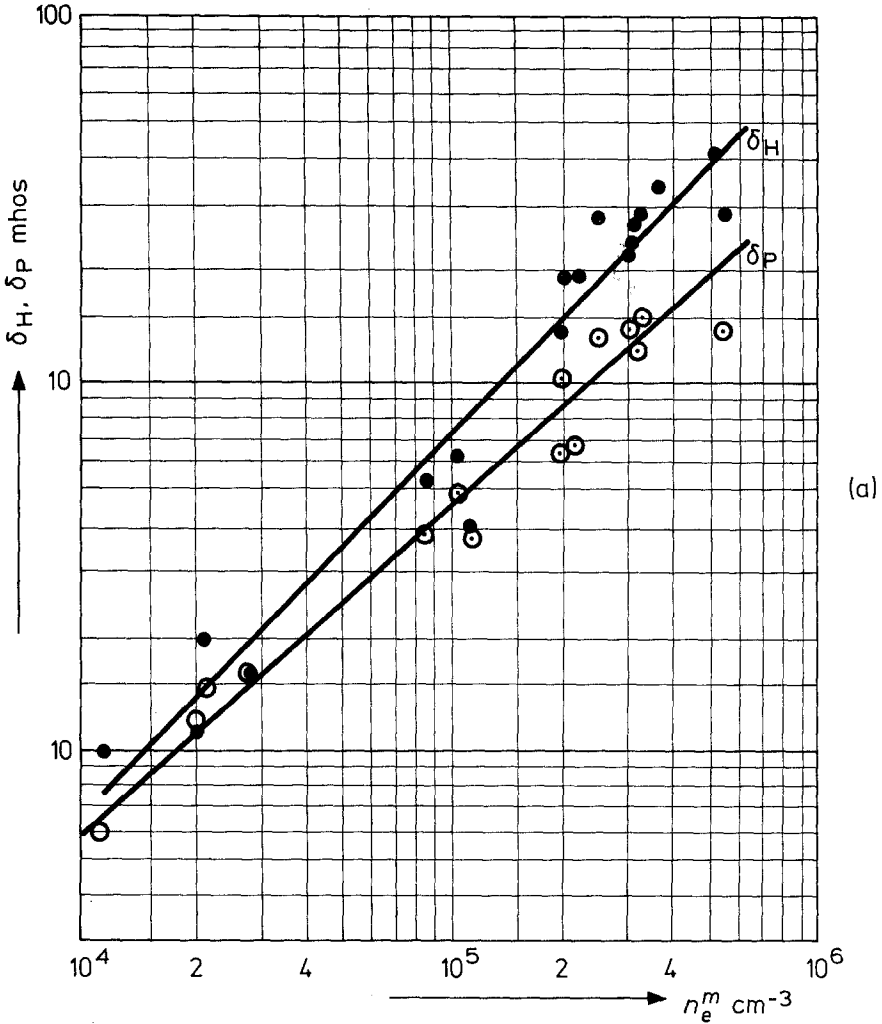


Fig. 20a-b Height-integrated Hall (σ_H) and Pedersen (σ_P) conductivities versus maximum concentration of n_e^m in E -layer according to Osipova (1973). Fig. 12a. Plots are for the dark polar ionosphere (corpuscular emission).

from 9.5×10^3 to $4.1 \times 10^4 \text{ cm}^{-3}$ at a particle flux of $\sim 10 \text{ erg cm}^{-2} \text{ s}^{-1}$. Since the particle inflow into the cusp during magnetically quiet periods is $\sim 0.1 \text{ erg cm}^{-2} \text{ s}^{-1}$ (see, for example, Heikkila and Winningham, 1971, 1974, and other works), n_e will decrease respectively down to $(0.4 - 1.6) \times 10^3 \text{ cm}^{-3}$. The calculations of the day-cusp ionization (Banks *et al.*, 1974) carried out with the effective recombination coefficient $\alpha_{\text{eff}} \sim 2 \times 10^{-7} \text{ cm}^{-3} \text{ s}^{-1}$ have given $n_e \sim 2 \times 10^4 \text{ cm}^{-3}$ at altitudes of 100–120 km. This value should be considered to be substantially overestimated since the conventional spectrum used in the calculations comprised a fairly high number of electrons with $E \geq 10 \text{ keV}$. Thus, the corpuscular stream induces ionization $n_e < 10^4 \text{ cm}^{-3}$ in

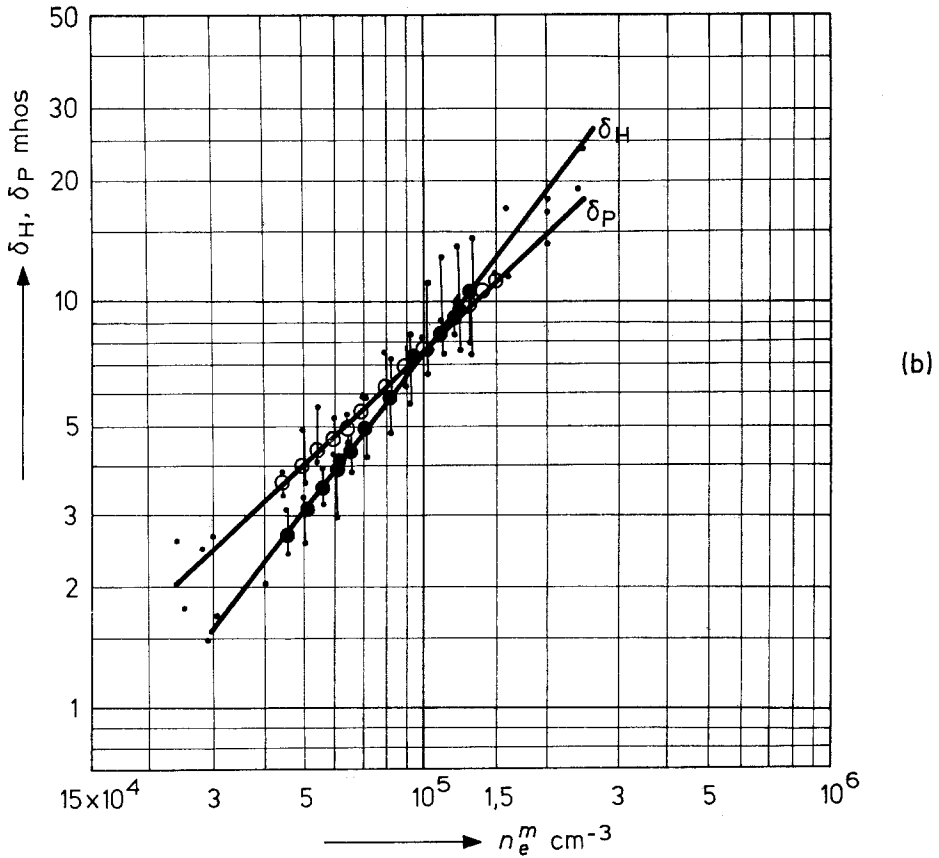


Fig. 20b. Plots are for sunlit polar ionosphere under quiet conditions (wave emission).

the *E*-layer which is sufficiently lower than that observed in the summer at day-cusp latitudes. For example, sounding of the ionosphere at Resolute Bay gives $n_e^m \sim (8-16) \times 10^4 \text{ cm}^{-3}$ during the day-time in July, depending on solar activity phase. Hence, during the summer season, n_e^m of corpuscular origin is a small addition to the wave ionization, while the integral conductivity of the day-cusp ionosphere of corpuscular origin does not exceed 1 mho (see Figures 20a-b). The intensity of the day-cusp corpuscular stream fails to vary with season and universal time (Heikkila, 1974). Therefore, in turning from summer to winter, when the wave emission attenuates, the ionization intensity from the two sources becomes compatible, and near the winter solstice the corpuscular radiation may even become predominant, though it is maintained at a $\lesssim 10^4 \text{ cm}^{-3}$ level. Such a low ionization level of corpuscular origin in the *E*-region on polar-cusp latitudes has also been confirmed experimentally. During the day-time in winter at $78^\circ \leq \varphi' \leq 84^\circ$, the vertical ionospheric sounding at Godhavn and Resolute Bay stations gives $f_o E \leq 1 \text{ MHz}$, which means that $n_e^m \lesssim 10^4 \text{ cm}^{-3}$.

The above considerations show that the ionospheric conductivity in summer in

polar latitudes is mainly determined by the ionization from the wave source. It is well known that at E -layer altitudes the intensity of this type of ionization can be sufficiently well approximated by the expression

$$n_e^m = K (\cos Z)^l. \quad (5)$$

where Z is the zenith angle of the Sun, K and l are the parameters determined by the selected atmospheric model, solar activity phase, etc. Parameters K and l are known from the regularities of E -layer ionization variations in middle latitudes. However, since the model of the polar atmosphere may substantially differ from the middle latitude model, the values of the parameters were determined (Feldstein *et al.*, 1975b)

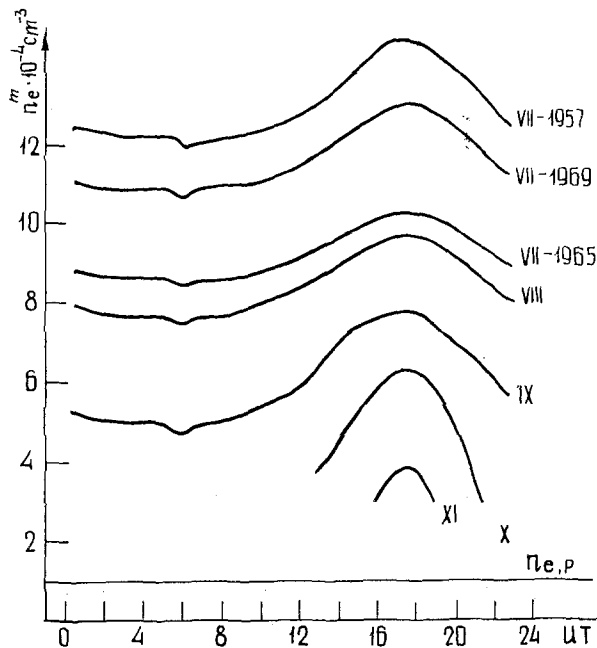


Fig. 21. Variations in the maximum electron concentration n_e^m in ionospheric E -region in the day cusp from July to November, 1965 and in July, 1957 and 1959 at the various hours of UT. The cusp is located at $\Phi' = 78^\circ$.

on the basis of the n_e^m values observed at Resolute Bay and Scott Base stations. Use was made of observation periods when $n_e^m \geq 2.5 \times 10^4 \text{ cm}^{-3}$, i.e. all hours of the day in summer months, the day-time interval at the equinox, and the period near noon in February and November. The values of K and l have been obtained using the least square method by comparing the experimental n_e^m with that calculated from relation (5) so that the rms error was minimum. These values were used when calculating the density of ionization n_e^m for each month of 1965–1966 of polar cusp locations at corrected geomagnetic latitudes $\Phi' = 81^\circ$ and $\Phi' = 78^\circ$. Depending on universal time, the

geographic latitude of the day cusp varies during the day, which results in solar zenith angle variations in the day cusp, Z_k .

Figure 21 presents the calculated n_e^m values for the various hours of universal time of cusp location at $\Phi' = 78^\circ$ in July–November, 1965 and in periods of high solar activity in July 1957 and 1959. The horizontal line denotes the upper limit of corpuscular ionization density $\sim 10^4 \text{ cm}^{-3}$. The maximum values of n_e^m were observed at 17–18^h UT when the day cusp located at the minimum geographic latitude, the broad flat minimum of n_e^m is at 02^h–07^h UT. The ratios of maximum to minimum values of n_e^m increase from 1.2 in June–July to 1.65–2.4 in September and March. The largest variations of n_e^m with UT are in February and October when at 17^h–18^h UT the day cusp is sunlit, whereas during the major part of the remainder interval $Z_k > 90^\circ$ and the corresponding ratios of $n_e^m \sim 5$ –6. Near the winter solstice, when corpuscular ionization is predominant throughout the period, the variations with universal time may be assumed to be absent. The day-cusp location on higher latitudes (at $\Phi' = 81^\circ$) somewhat changes the above presented values. During summer months n_e^m decreases by $\sim 0.5 \times 10^4 \text{ cm}^{-3}$ and the ratio of maximum to minimum values of n_e^m increases somewhat (~ 1.25). In September, n_e^m decreases by $\sim 0.8 \times 10^{-4} \text{ cm}^{-3}$ – the decrease in minimum near 06^h UT and in maximum at 17^h–18^h UT being respectively $1.2 \times 10^{-4} \text{ cm}^{-3}$ and only $0.4 \times 10^{-4} \text{ cm}^{-3}$. Thus, the day-side cusp shift from 78° to 81° latitude results in but a small change of ionization density at altitudes of ionospheric *E*-layer. Such latitude shift of the day cusp may actually take place and is associated with both seasonal and diurnal variations of the angle between the Sun–Earth direction and geomagnetic dipole axis (Feldstein and Starkov, 1970; Burch, 1972).

The seasonal variations in n_e^m are very considerable. In 1965 the decrease from July to December is ~ 10 -fold with slight deviations at various hours of UT. This decrease is several times greater than that presented by Nagata and Kokubun (1962) where a value of ~ 3 is given to explain the seasonal variations in S_q^P intensity for integral conductivity changes from the summer to the winter (averaged for three months).

The cyclic variations of n_e^m in Figure 21 vary by a factor of 1.4 from 1965 (near solar minimum) to 1957 (very high solar activity level). Calculations of the values of parameter K for the period from 1957 to 1972 have shown that the minimum values of K were in 1963 and 1964 ($K = 1.1 \times 10^4 \text{ cm}^{-3}$), and the maximum values were in 1957 and 1958 ($K = 1.7 \times 10^4 \text{ cm}^{-3}$), i.e. ~ 1.6 times the cyclic changes in ionization density.

One-order seasonal changes of ionization density in *E*-region and, hence, of integral conductivity, may be responsible for a pronounced decrease from summer to winter in the intensity of the various types of near-pole magnetic variations. Figure 22 presents the results of a qualitative comparison of the seasonal ionization variations in day cusp with the intensity of magnetic disturbances associated with the Y_{SE} component of the interplanetary magnetic field. Intensity of magnetic disturbance ΔT may be assumed to be proportional to the day-cusp conductivity σ , the electric field E transferred from solar wind to day cusp, and the geometric factor R which is a

function of the location of a station relative to the current system responsible at a given moment for the magnetic field variations:

$$\Delta T \sim \sigma ER.$$

To quantitatively estimate the cause of seasonal variations in ΔT , i.e. if they are due to changes in $\sigma \sim n_e^m$ only, it is necessary to fix R and E . The values of E is mainly determined by the value of Y_{SE} . Therefore, in the 17^h-19^h UT interval the correlations were determined between the magnetic field intensity in Z -component at Resolute Bay and in X -component at Mould Bay and the value and sign of Y_{SE} for each month

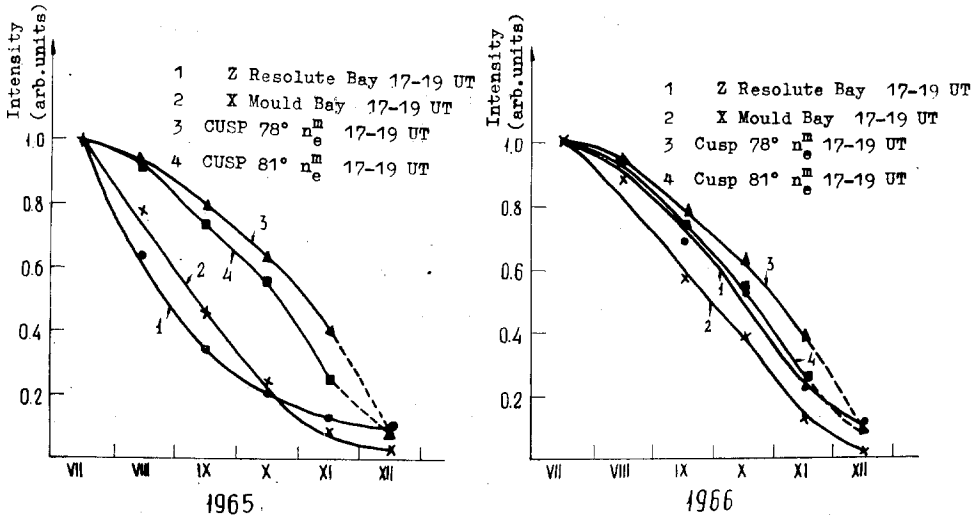


Fig. 22. Seasonal intensity variations of near-pole magnetic disturbances generated by the azimuthal component of the interplanetary magnetic field and the corresponding variations of ionization density in E -region for the various latitudes of the day cusp at 17^h-19^h UT. 1: Z -component at Resolute Bay, 2: X -component at Mould Bay, 3: n_e^m at cusp on $\Phi' = 78^\circ$, 4: n_e^m at cusp on $\Phi' = 81^\circ$.

from July to December of 1965 and 1966. These components were chosen because at the above stations they are most closely associated with Y_{SE} . Variations in Z and X , as functions of Y_{SE} , were found, and ΔZ and ΔX were determined at $\Delta Y_{SE} = \text{const}$ for each month, which permitted the seasonal variations of E and the corresponding changes of ΔZ and ΔX to be excluded to the first approximation. The fixed UT ensures an invariable location of the observation point relative to the current system, i.e. the constancy of R unless, of course, the geometric parameters of the current system vary with the season. The 17^h-19^h UT intervals were chosen just because during these intervals n_e^m is maximum, the stations are on the Earth's day side, and, therefore, ΔZ and ΔX are sufficiently large in the summer season and their seasonal variations can be easily traced. During other intervals of UT the near-pole field variations associated with Y_{SE} are already impossible to isolate by September-

October. Together with relative changes in ΔZ and ΔX , Figure 22 presents the respective changes in n_e^m when the polar cusp is located at $\Phi' = 78^\circ$ and $\Phi' = 81^\circ$. The December value of n_e^m was taken to be $1 \times 10^4 \text{ cm}^{-3}$ – i.e. only corpuscular ionization exists irrespective of cusp latitude – and the corresponding sections of the curves are drawn as dashed lines. Through the difference between curves 3 and 4, representing the different cusp latitudes, is small, n_e^m decreases more abruptly with season when the polar cusp is at $\Phi' = 81^\circ$.

Comparison between the July and December values of ΔZ , ΔX , and n_e^m confirms the assumption that the difference between the summer and winter near-pole variation intensities may be quantitatively explained by variations of ionization density in the ionospheric *E*-region. In this case, in 1966 the ΔZ and ΔX variations throughout the examined period are qualitatively in fairly good correspondence with n_e^m variations in polar cusp. The difference between the relative values of n_e^m (cusp at $\Phi' = 81^\circ$) and ΔZ , is within several hundredths of unity. In 1965 the seasonal magnetic variation intensity changes are steeper than n_e^m changes. Such a discrepancy may be associated with simultaneous changes in *R* and is due, for example, to the shift of the polar electrojet located on polar-cusp latitudes to lower latitudes. In this case the seasonal variations in ΔZ and ΔX will be due not only to the n_e^m decrease from summer to winter but also to the fact that the observation point moved away from the field source. The variations in wave emission were probably the predominant factor in 1966 when the level of solar wave emission was ~ 1.5 times as high as in 1965. Thus, the qualitative estimates of seasonal changes in near-pole intensity variations are indicative of their close relationships with ionization level in the ionospheric *E*-region.

The diurnal variations of polar cusp conductivity during the summer season are only $\sim 20\%$. Moreover, the largest disturbances are observed in the 15^h–21^h UT interval, whereas the amplitude decreases down to zero in the 3^h–9^h UT interval (Svalgaard, 1973). Such abrupt diurnal variations in magnetic disturbance intensities can be interpreted as follows. The 17^h–19^h UT interval is the time of local noon over the magnetic pole in the northern hemisphere. When the magnetic pole is on the Earth's night side, the polar cusp currents are absent or very weak. When the Earth's rotation brings the magnetic pole to the day side, the polar cap current system develops. It is possible that the conditions at 17^h–19^h UT are most favourable for direct interactions between the solar wind and the polar cap geomagnetic field lines (Svalgaard, 1974).

However, the substantial decrease in disturbance amplitudes from 17^h–19^h UT to 5^h–7^h UT may be due to the effect of other factors, such as the decrease in polar ionospheric conductivity and the fact that the western hemisphere stations move away from the day-side polar electrojet.

The decrease in polar ionospheric conductivity from 17^h–19^h UT to 5^h–7^h UT should naturally affect the disturbance level decrease. However, the conductivity changes alone can hardly explain the observed decrease in disturbance amplitudes. This is illustrated in Figure 23 which presents the changes throughout the day in ΔZ

at fixed Y_{SE} relative to the maximum ΔZ , and similar variations in n_e^m , at Resolute Bay in July–August, 1965. At 0^h–9^h UT the magnetic disturbance intensity decreases by more than an order, while the conductivity exhibits only a ~ 2 -fold decrease. A similar result has been obtained for ΔX changes at Mould Bay: the variation of the intensity changes by an order during the day, while the conductivity change is less than two-fold, since Mould Bay is closer to the geographic pole than Resolute Bay.

The disappearance of DPC (Y_{SE}) disturbances at 5^h–7^h UT, when the magnetic pole is turned towards the night side, could be convincingly verified on the basis of obser-

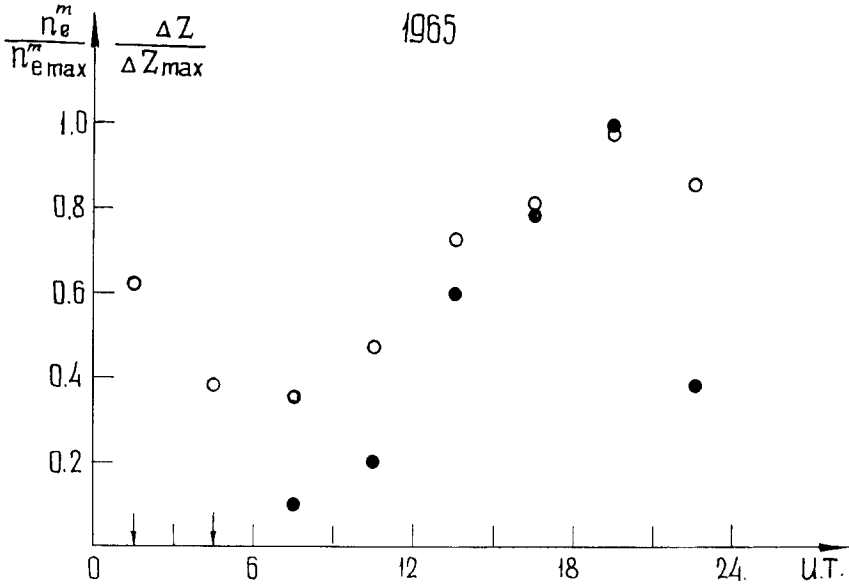


Fig. 23. Diurnal variations of the relative values of magnetic disturbances and maximum ionization in E -layer at Resolute Bay in July–August, 1965. ○: $n_e^m/n_e^m_{max}$; ●: $\Delta Z/\Delta Z_{max}$.

variations made during this interval at the stations located at $80^\circ \leq \Phi' \leq 84^\circ$ in the day sector. Unfortunately, such observations are not available from the WDCs. However, the observations at Heiss station ($\Phi' = 74.5^\circ$) may be used to some limited extent for this purpose, since DPC (Y_{SE}) affects the Z -component variations at such latitudes during the day-time (see Baker Lake station in Table VI).

The correlation factors and the response of Z -variations to Y_{SE} intensity at these stations near noon are presented for comparison in Table IX. At Heiss the Z intensity varies together with Y_{SE} at 3^h–6^h UT at the same values of correlation factors as at Baker Lake, which is indicative of the existence of DPC (Y_{SE}) currents at these hours. The ratios of Z -response to Y_{SE} intensity in various UT intervals were 2.1 in 1965 (maximum 2.5 and minimum 1.7) and 1.9 in 1966 (maximum 2.6 and minimum 1.35); and the corresponding ratios of conductivities were 1.26 and 1.21 when the day cusp

TABLE IX

Correlation factors (r) and regression equations of the azimuthal component of the interplanetary magnetic field (Y_{SE}) and the vertical (Z) component of the geomagnetic field at Baker Lake and Heiss stations in July–August, 1965

	15 ^h –18 ^h UT 1965	18 ^h –21 ^h UT 1966
Baker Lake	0.65 ± 0.08	0.5 ± 0.09
	$(5.2 \pm 0.6) Y_{SE}$	$(5.8 \pm 1.0) Y_{SE}$
	3 ^h –6 ^h UT 1965	3 ^h –6 ^h UT 1966
Heiss	0.75 ± 0.06	0.57 ± 0.1
	$(2.5 \pm 0.2) Y_{SE}$	$(3.1 \pm 0.5) Y_{SE}$

was located at $\Phi' = 81^\circ$. Though the higher ratios of responses as compared with those of conductivity variations may be due to the lower geomagnetic latitude of Heiss station, the effect of the mechanism proposed by Svalgaard is also possible. The effect of this mechanism may also explain a more rapid decrease in magnetic disturbance intensities with the season in 1965 than that expected from conductivity variations (see Fig. 22).

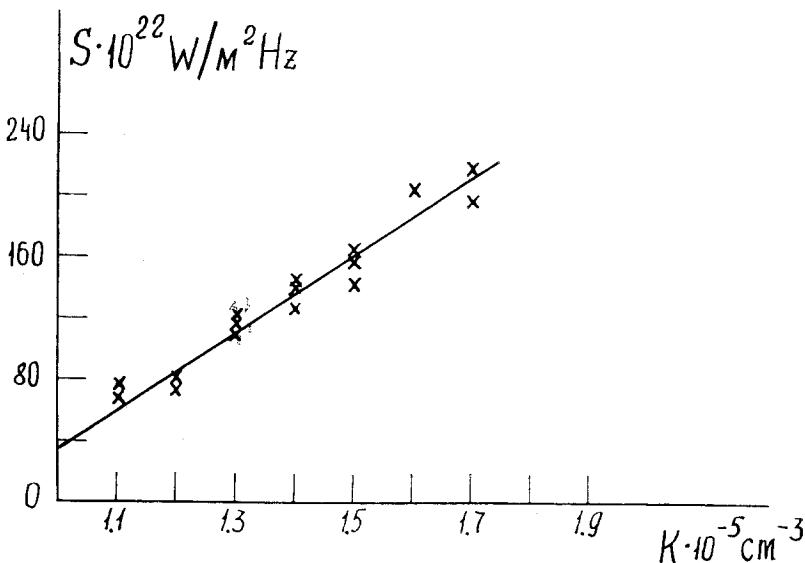


Fig. 24. Relationships between the parameter K characterizing ionization density in the ionospheric E -region in July and the solar radioemission intensity S at a frequency of 2800 MHz from 1957 to 1972. The straight line equation has been obtained by the least square method.

The values of n_e^m displayed in Figure 21 may be used to calculate the expected values of $DPC(Y_{SE})$ variations in various components as functions of universal time and month on the basis of $DPC(Y_{SE})$ data for July–August, 1965 (Tables VI–VIII). The $DPC(Y_{SE})$ intensity variations relative to the sunspot cycle are determined by n_e^m variations during the cycle. Figure 24 presents the parameter K in relation (5) as a function of solar radio-emission intensity at a 2800 MHz frequency. Use has been made of the monthly averages for July from 1957 to 1972 published in *Solar-Geophysical Data*. The linear correlation factor between S and K is $r=0.99\pm 0.01$ and the linear regression equation is

$$S = 250 K - 213,$$

where S is in units of $10^{-22} \text{ W m}^{-2} \text{ Hz}^{-1}$, and K is in units of 10^5 cm^{-3} . The relation may be used to determine n_e^m for various levels of solar radioemission and, hence, to calculate the $DPC(Y_{SE})$ intensity for any phase of a sunspot cycle.

7. The Delay of Ground Field Variations Relative to Y_{SE} -component Variations

It was noted by Friis-Christensen *et al.* (1972), Sumaruk and Feldstein (1973a) that the Z variations on the Earth's surface were delayed relative to the variations in the IMF azimuthal components. Correlation of hourly mean values of Y_{SM} and Z in Thule in 1969 near noon was found by Friis-Christensen *et al.* (1972) to be substantially better when the ground variations are shifted by 1 hour relative to IMF azimuthal component. Figure 25 shows the ΔZ variations in July–August, 1965 obtain by Sumaruk and Feldstein (1973a) using the epoch superposition method and by counting-off in each 5 minutes from the corresponding field values for July 11. Transition of Y_{SE} through zero corresponds to the moment $\Delta t=0$. The change of Y_{SE} sign results in the ΔZ sign change at near-pole stations. The moment of ΔZ transition through zero is delayed by ~ 40 min at Thule and ~ 25 min at Resolute Bay relative to the transition of Y_{SE} through zero. It was found when comparing the short-term Y_{SE} fluctuations with Z at Thule (Kawasaki *et al.*, 1973) that in the summer of 1965 the best visual correlation corresponds to a ~ 25 min shift of ground variations relative to interplanetary variations. Bearing in mind that in the summer of 1965 the ground variation delay due to IMP-3 signal transfer to the Earth was on the average ~ 10 min (maximum delay was ~ 14 min), we shall discuss possible causes of the observed substantial delay of ground variations. Such causes may be:

(1) The near-pole Z variations are controlled not by Y_{SE} component of IMF but by some effective IMF. This field in practice varies simultaneously with Z variations (including the time of satellite signal transfer to the Earth).

(2) The delay is due to a relatively slow polar electrojet displacement from the evening to the morning sector when turning from $Y_{SE} < 0$ to $Y_{SE} > 0$ and the reverse displacement at opposite variations of IMF (see location of electrojets in Figure 17). In this case the delay time is essentially a function of the Φ' of the observation station and the Y_{SE} variation mode.

(3) The delay is due to current induction inside the Earth. In this case the value of Δt is determined by the nature of the underlying surface; is different at individual stations; and is differently reflected in horizontal and vertical components.

Figure 26 presents, following Feldstein *et al.* (1973b), the values of Δt between the time

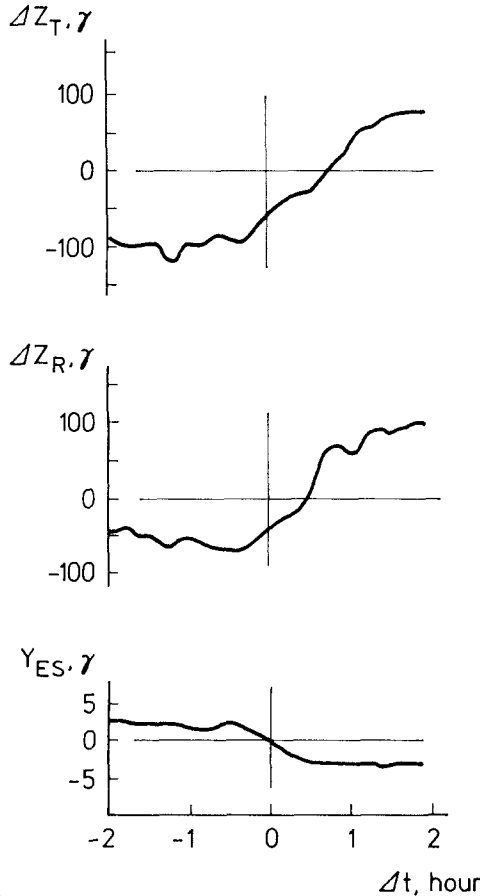


Fig. 25. Delay Δt of the moment of change in Z sign at Thule (at the top) and Resolute Bay (in the middle) in the summer months of 1965 relative to the moment of Y_{SE} transition through zero. The value ΔZ has been determined relative to the field value for 11 July 1965. The moment $\Delta t=0$ corresponds to Y_{SE} transition through zero. According to Sumaruk and Feldstein (1973c).

of abrupt change of Y_{SE} sign derived from IMP-3 5 min IMF values and the transition of ΔZ values through zero at Thule and Resolute Bay during the day-time. The dipole axis inclination to the ecliptic plane varies with universal time and, on the average, IMF will be differently orientated relative to the dipole. Therefore, if Δt on the Earth's surface is determined by the effective IMF, Δt should vary as a function of UT. The

data displayed in Figure 26 fail to show the existence of clear systematic variations in Δt with UT.

The value of Δt increases from 10–30 min at Resolute Bay to 30–50 min at Thule and is practically independent of the mode of Y_{SE} orientation change (the crosses and

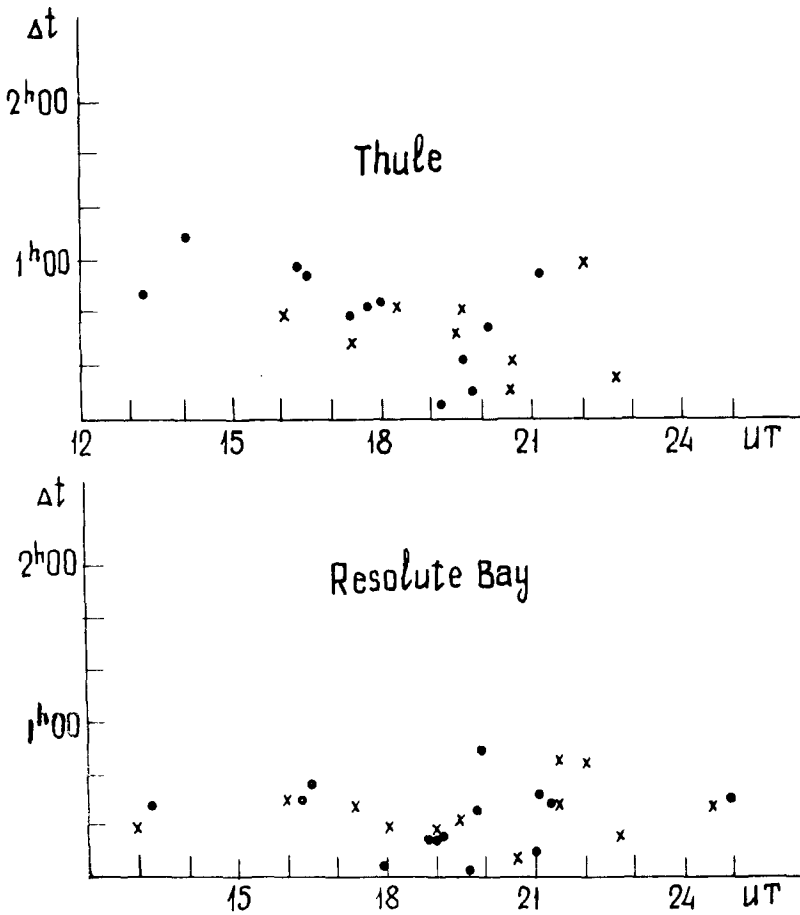


Fig. 26. Delay (Δt) of the moment of change in Y_{SE} component sign on IMP-3 and at Thule and Resolute Bay according to Feldstein *et al.* (1973b). The crosses and circles denote the moments when $Y_{SE} < 0$ becomes $Y_{SE} > 0$ and when $Y_{SE} > 0$ becomes $Y_{SE} < 0$ respectively.

dots in Figure 26). This feature of Δt makes it difficult to explain the ground variation delay by polar electrojet displacement in case of abrupt changes in Y_{SE} orientation. It should be assumed that the location of polar electrojets and the direction of currents in them are determined by Y_{SE} sign, while the Y_{SE} orientation change is accompanied by attenuation of the electrojet with the same direction, and generation of the electrojet with the opposite direction.

Consider the delay due to induction effects. The solution of the problem of electromagnetic induction in stratified media on the natural assumption of conductivity distribution with depth, results in the values of $\Delta t \sim 15$ min in the presence of a conductive layer at depths of 50–70 km and $\Delta t \sim 8$ min in the absence of such a layer (Berdichevsky *et al.*, 1972, 1973) for the Z -component relative to horizontal components. The Δt delay is essentially a function of variation period. The values presented above correspond to a 2 hr period. Approximately the same values have been obtained by Nopper and Hermance (1974). In this case the horizontal component variations are delayed by 2–11 min relative to the inducing field.

The ground variation delay due to current induction inside the Earth can probably explain the observed delay in the horizontal components which is equal to or somewhat greater than the time of satellite signal transfer to the Earth (see Figure 8), and a more durable delay in the vertical component. These differences in the delay can also be seen when calculating the correlation factors between the ground and satellite field variations. It appeared when comparing the IMF component derived from IMP-3 measurements in 1965 and 1966 with the ground variations in X and Z that a higher correlation was observed when comparing the coinciding hourly averages of the X -component; and approximately the same correlation was observed for the coinciding and 1 hr-shifted hourly averages of Z . For example, when comparing Y_{SE} with X at Resolute Bay at 21^h–24^h UT the values of r without shift in July–August were 0.92 ± 0.02 in 1965 and 0.8 ± 0.05 in 1966: with a 1 hr shift they were 0.8 ± 0.05 and 0.56 ± 0.08 respectively. When comparing Y_{SE} with Z in the same months of 1966 the values of r were -0.77 ± 0.05 at 12^h–15^h UT at Thule and -0.7 ± 0.07 at 21–24^h UT at Resolute Bay without time shift; and -0.82 ± 0.05 and -0.8 ± 0.05 respectively with 1 hr shift. It may be deduced from these data that the total delay of the ground variations in X -component was smaller than half an hour, and in Z -component it was somewhat more than half an hour. When comparing the ground field variations with the data from satellites more remote than IMP-3, the delay in Z may approach 1 hr: which explains the better correlation of the ground and satellite data at 1 hr shift according to Friis-Christensen *et al.* (1972). Probably this work used the observations from a more remote satellite (Explorer-33 or 35).

8. Diagnostics of the IMF Azimuthal Component of the Basis of Ground Data

On the basis of the relationships between the IMF sector polarity and the near-pole magnetic field variations, ground data were used by Svalgaard (1968), Friis-Christensen (1971), Friis-Christensen *et al.* (1971), and Mansurov and Mansurova (1973a, b) to determine the daily-mean sector polarity and to show a good agreement between the inferred IMF orientation in interplanetary space, and that actually observed from satellites.

Figure 27 presents the results of such a comparison according to Friis-Christensen *et al.* (1971). The IMF polarity in 1969 inferred from Explorers-33 and 35 observations is indicated on the wide bar under K_p -indices of magnetic activity. Indicated on the

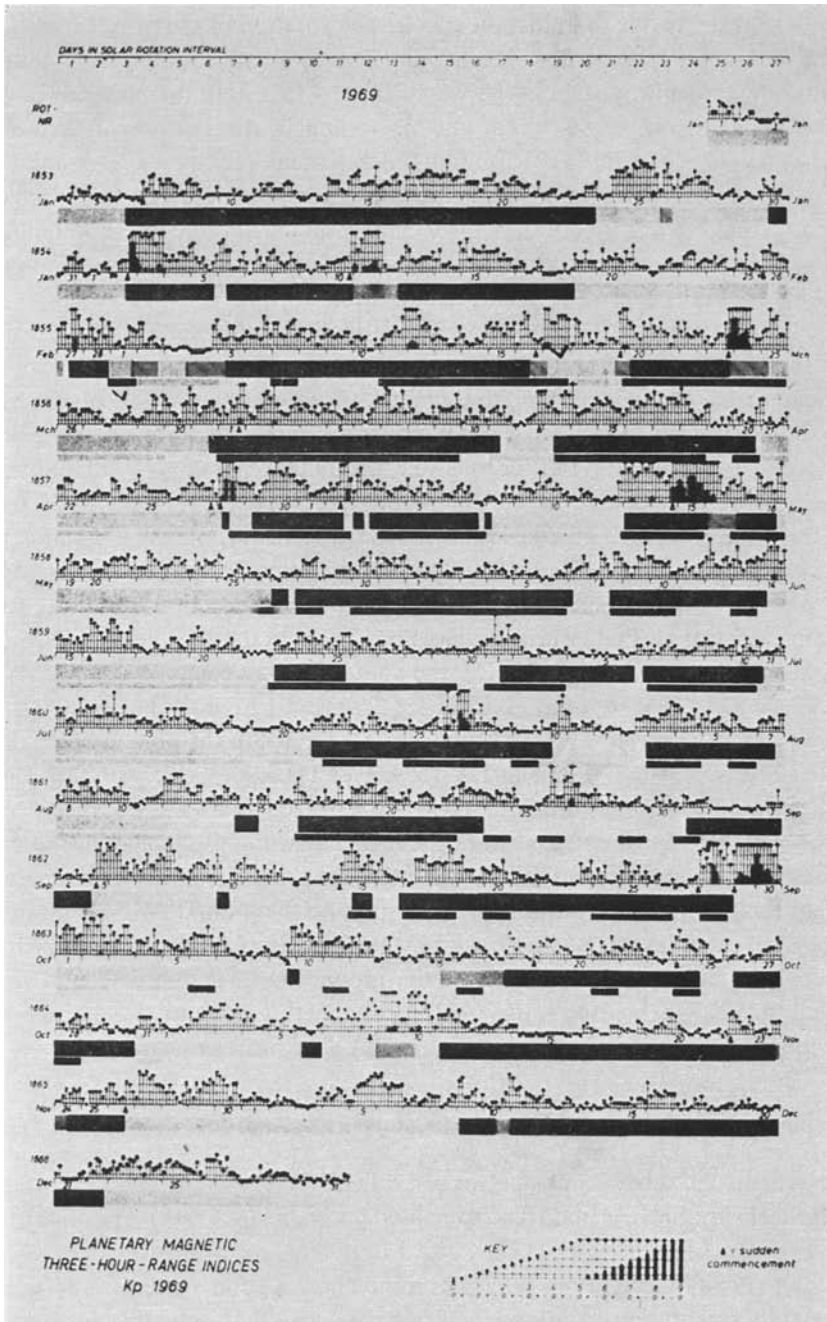


Fig. 27. Interplanetary magnetic field polarity during 1969 as observed from Explorer 33 and 35 (the wide bar) and that inferred from observations of the polar-cap magnetic field variations according to Friis-Christensen *et al.* (1971). The dark shading shows the IMF toward sector; the light shading shows the IMF away sector; the crosses denote the intervals of ambiguous field polarity.

narrow bar is the sector polarity direction inferred from near-pole ground magnetic variations. The dark shading denotes the toward sector: the light shading, the away sector; and the crosses denote the intervals of ambiguous field polarity. In the winter months when the variation amplitude decreases substantially at ground stations on the polar cap, the polarity could not be objectively determined and, is not shown therefore in Figure 27. The IMF polarity was independently determined from the ground and satellite observations in various countries (Denmark and USA). The sector polarities inferred from ground observations and those actually observed are in good agreement; they coincide for 156 days and disagree for 18 days. The sector boundary locations are usually in agreement within less than a day; in some cases the passage of the sector boundary through the Earth's orbit may be determined within a few hours. The independent determination of polarity appears to be an objective verification of the possibility of diagnosing the IMF direction on the basis of ground observations. At the same time, the good agreement between IMF directions determined by direct and indirect methods indicate that the ground observations on the polar cap may be used for a sufficiently reliable determination of IMF polarity. According to Mansurov and Mansurova (1973a) the number of days when the sector polarities, determined by direct (satellites) and indirect (ground variations of magnetic field) methods, coincide is on the average $\sim 80\%$; reaches $\sim 90\%$ in case of a simple and stable IMF structure; and decreases near the sector boundaries.

Observations at the Greenland station Godhavn have been continuously carried out during the last four solar cycles and were used by Svalgaard (1972) to determine the IMF sector polarity and to compile a catalogue covering the period from 1926 through 1971. This determination has been derived on the basis of the close relationships between the deviations of the field daily mean values from the monthly mean values for Z at Thule and H at Godhavn in July–August, 1959 assuming that such relationships are persistent throughout the year. At $\Delta H > 0$, IMF in the ecliptic plane is directed away from the Sun ($-$ sector), at $\Delta H < 0$ IMF is sunwards ($+$ sector).

During the winter season, the IMF polarity is difficult to determine from ground observations because of an abrupt decrease in the $DPC(Y_{SE})$ field variation amplitude (see Figure 13 for sunspot minimum). Meanwhile, according to Svalgaard (1972), the sector polarity is often easier to determine from variations in H at Godhavn than in Z at Thule. However, the exclusive use of Godhavn observations for determining the sector polarity restricts the reliability of data presented in the catalogue, especially for the winter season when the field variations at Godhavn latitudes from other sources become comparable to, or even more intensive than, $DPC(Y_{SE})$ variations.

The reliability of the catalogue data for the winter months was discussed by Feldstein *et al.* (1972); and it was concluded that these data should be used with a high degree of caution. In particular, the winter variations in H at Godhavn are substantially affected by the frequency and intensity of substorms and not by the IMF sector polarity.

Figure 28 presents the daily mean values of ΔZ at Thule and ΔH at Godhavn in November–December, 1965, in deviations from the monthly means on international

magnetically quiet days according to Feldstein *et al.* (1972). The dashed line shows the mean monthly field values for all days. The crosses and large circles denote the international magnetically disturbed and quiet days respectively. In practice, throughout the two months, in the deviation from the quiet field level $\Delta H < 0$, and $\Delta Z > 0$. If these variations are accounted for by sector polarity, IMF should be directed exclusively sunwards during the two months. Such polarity disagrees both with the variations recorded on IMP-3 and with the polarity presented by Svalgaard (1972). The ΔH sign in the deviations from monthly mean values can also not be relied upon to determine the sector polarity. In fact, with such a method of ΔH calculation, all 10 mag-

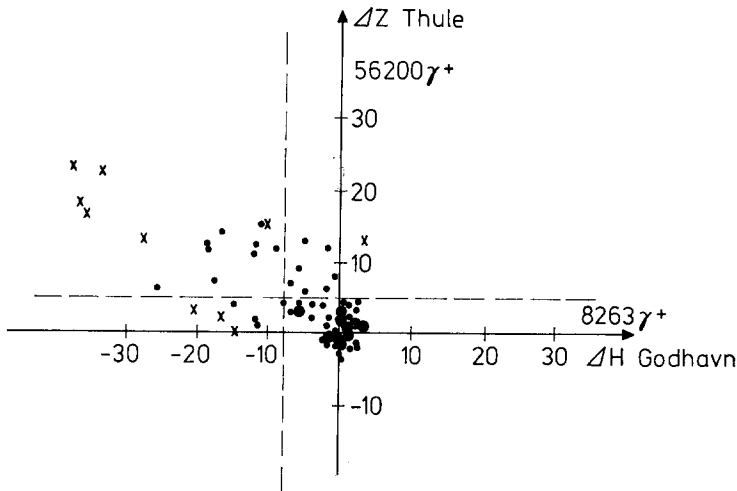


Fig. 28. The mean-daily values of ΔH at Godhavn and ΔZ at Thule in November–December, 1965 in deviations from the mean-monthly values of quiet days. The dashed line shows the mean-monthly values for all days. The crosses denote the international magnetically disturbed days; the large circles denote the international magnetically quiet days. According to Feldstein *et al.* (1972).

netically quiet days are characterized by $\Delta H > 0$; while 9 of 10 magnetically disturbed days by $\Delta H < 0$. The winter ΔH sign is probably determined not by IMF polarity in the ecliptic plane but by magnetic substorm development.

Close relationships between the sector polarity determined by Svalgaard (1972) and the geomagnetic disturbance, have been analyzed in detail by Fourgere (1974), who also cast doubt on the accuracy of the catalogue data on IMF polarity. He showed that the IMF away sector relates to low geomagnetic and solar activity, whereas the toward sector is accompanied by an appreciable increase of activity. He also called in question the possibility of using the indices from Svalgaard's (1972) catalogue as indicators of IMF sector polarity, since they are mainly 'determined' by magnetic activity and affected but little by the IMF sector polarity.

The ΔH sign in deviations from monthly means in November–December, 1965 fails to determine the IMF polarity. The IMP-3 observations were used to determine

the daily mean values of the Y_{SE} component direction which was shown to coincide (with few exceptions) with the sector polarity according to the data of Ness and Wilcox (1967) and Wilcox (1969). The polarities observed and inferred from ground data (on the basis of ΔH sign) coincide for 17 and disagree for 29 days. According to Campbell and Matsushita (1973), the sector polarity in the winter months of 1965 is difficult to determine on the basis of ground observations of magnetic field at Godhavn and Thule, whereas such determinations can be made more safely during the summer season.

Such criticism of the accuracy of the IMF polarity data presented in Svalgaard's (1972) catalogue has made him propose an objective method (1975) to infer the IMF polarity using the H -component at Godhavn. Essentially, this method is to determine the maximum (HA) and minimum (HC) deviations of H from the mean-monthly value in the 15^h–21^h UT interval. If $HA > -\frac{1}{2} HC$, the day is classified as the $-$ (away sector) type; if $HC < -\frac{1}{2} HA$, the day is classified as the $+$ (toward sector) type. The remaining cases relate to the \times (mixed) type. The objectively inferred IMF polarities are compared for individual time intervals with those presented in the catalogue and it is concluded that no significant difference exists between the data obtained using the two methods.

Figure 29 presents the diurnal variations of H at Godhavn for November–December, 1965 in the same format as recommended by Svalgaard. In the lower row, the sector polarity inferred from these data on the basis of his recipe is indicated. The upper row shows the sector polarity inferred from IMP-3 measurements of Y_{SE} component (at $Y_{SE} < 0$ toward sector, at $Y_{SE} > 0$ away sector, at $Y_{SE} \geq 0$ the polarity is mixed). Out of 61 days, the polarities determined by the two methods coincide for 16, disagree for 23 and are mixed for 22 cases. This result is an additional proof of the impossibility of objectively determining the sector polarity in the winter season on the basis of Godhavn data during sunspot minimum. A doubt arises in this connection as to the extent to which the regularities established on the basis of the analysis of the IMF polarity data presented in Svalgaard's (1972) catalogue correctly reflect the physical reality; and a further doubt arises as to the extent to which these regularities are due to the artifacts in the inferred indices. The catalogue in its present form can probably be used only to a very limited extent for studying the large-scale evolution of the sector structure throughout the sunspot cycle. For example, it follows from Figure 29 that the domination of the away polarity near sunspot minimum is a result of an inaccuracy in the inferred polarity. It is not impossible, therefore, that the conclusion of Wilcox (1972) about the almost invariable IMF direction away from the Sun for a few solar rotations near sunspot minimum fails to reflect the real regularities of solar magnetism. Near the sunspot maximum, the agreement between the catalogue data and IMF measurements are even better (Fairfield and Ness, 1974).

The observations at the corresponding near-pole ground observatories undoubtedly permit the polarity of the IMF azimuthal component to be fairly safely determined. Such determinations are most accurate if made on the basis of the Z -component data for daylight hours of the summer season at $83^\circ \leq \phi' \leq 86^\circ$. Until recently, the sector polarity published regularly in the *Journal of Geophysical Research* (Geomagnetic and

Solar Data section) had been determined on the basis of observations at Vostok station for the first half-day UT and at Thule for the second half-day UT. It is possible at present to use the relations listed in Table VI for determining not only the sign but also the value of the IMF Y_{SE} component on the basis of ground data. Figure 30 presents, according to Feldstein *et al.* (1975a), the ΔZ isolines (ΔZ values have been calculated from the reference level determined using the method set forth in Section 3)

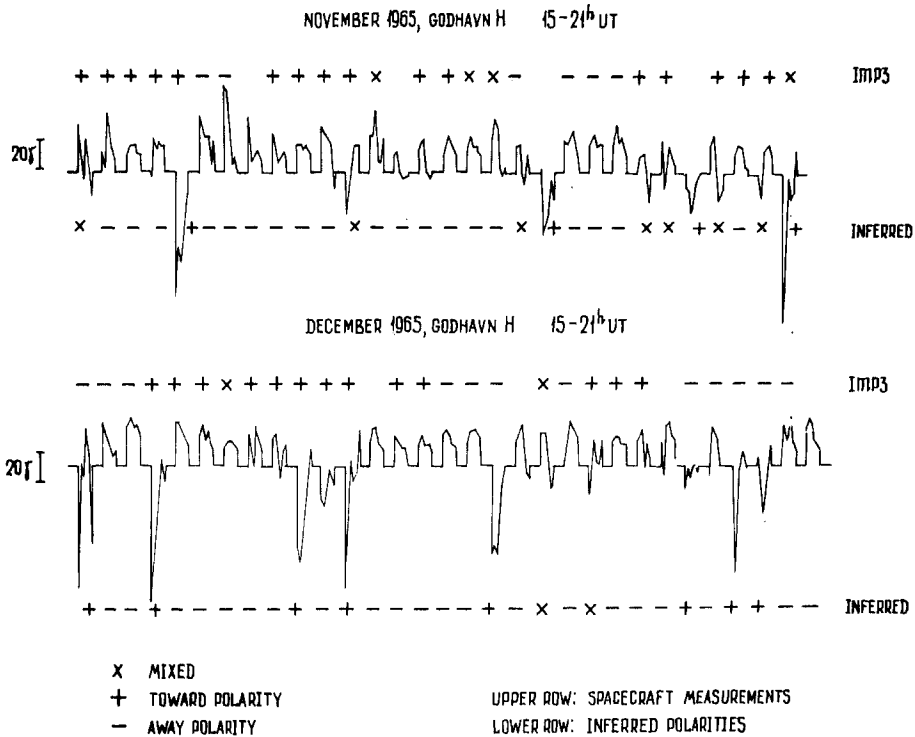


Fig. 29. The data for November and December, 1965 plotted in such a way that during the 15^h-21^h UT interval the actual variations in the horizontal component at Godhavn are shown for each day, while the straight line segments denote the mean-monthly values for all other intervals. The upper row shows the polarity of interplanetary magnetic field (+ is for toward polarity, - is for away polarity, × is for mixed polarity) as measured from IMP-3; the lower row shows the polarity inferred using the recipe described in Svalgaard (1975).

for $Y_{SE} = 6 \gamma$ in July-August of 1965 and 1966. The highest intensity of ΔZ is observed near noon at $\Phi' \sim 84-85^\circ$. The increase in ΔZ from 1965 to 1966 is due to the increase in ionospheric conductivity because of solar activity increase. The mean-hourly values and direction of Y_{SE} in July-August of 1965 and 1966 may be determined by calculating ΔZ on the basis of ground observations at the western hemisphere stations and using the isolines presented in Figure 30. The knowledge of conductivity variations with sunspot cycle (see Figure 24) makes it possible to use the ground data for deter-

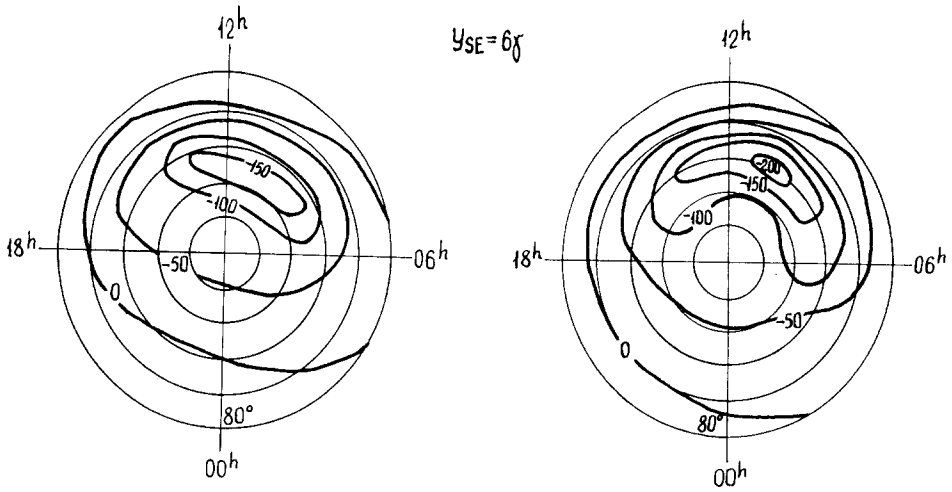


Fig. 30. Spatio-temporal distribution of ΔZ in the polar region ($\Phi' \geq 80^\circ$) in July–August, 1965 (on the left) and July–August, 1966 (on the right) at $Y_{SE} = 6 \gamma$ according to Feldstein *et al.* (1975a). Coordinates: corrected geomagnetic latitude and local time.

mining Y_{SE} in the summer months of any year. Similar diagrams may be used to diagnose Y_{SE} for other months. The variations in the reference level throughout the day, season, and sunspot cycle should be known in order to calculate ΔZ at any given hour. These variations are determined both by the main geomagnetic field (secular variations) and by external sources independent of Y_{SE} . Figure 31 presents the variations in the reference level at Thule from July to December, 1965. The diurnal variations in Z ($Y_{SE} = 0$) are $\sim 20 \gamma$ in summer months and decrease down to $\leq 5 \gamma$ toward winter. They are superposed on the systematic increase in Z_T from July to December.

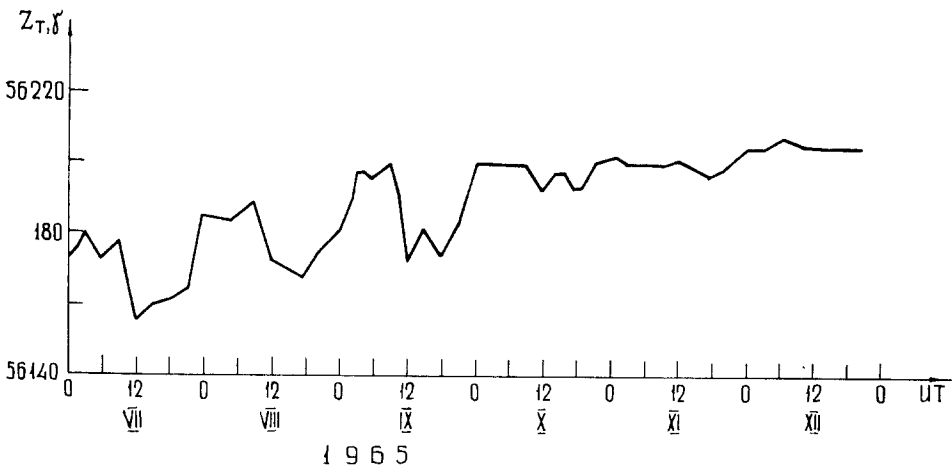


Fig. 31. Variations in the zero level of Z_T at Thule throughout a day for each month from July to December, 1965 according to Sumaruk *et al.* (1974).

This change equalling $\sim 18 \gamma$ can be naturally related to the secular variations in Z_T of the main geomagnetic field which are 30γ per year at Thule as inferred from the observation data of many years (Orlov *et al.*, 1968). An additional effect of Z_T decrease by several gammas can also be observed at night-time during summer months. The value of this decrease and the diurnal variation amplitude are closely associated with season and sunspot cycle and can be predicted in advance, which makes it possible to diagnose the values of the reference level for any given moment. Thus, the possibility arises of using the ground observations of the vertical component at near-pole stations for determining not only the polarity but also the value of the IMF Y_{SE} component for a long time interval.

9. The Structure of the Near-pole Geomagnetic Variation Field

The observed magnetic disturbance pattern in the polar cap may stem from:

- (1) the distant effect of auroral electrojets including the field-aligned currents penetrating the auroral oval;
- (2) The high-latitude S_q^o currents which are the extension of middle-latitude S_q on magnetically quiet days to the polar region;
- (3) ionospheric currents associated with magnetospheric convection;
- (4) ring currents (especially in Z -component);
- (5) the DPC (Y_{SE}) current system discussed in detail above and
- (6) other possible field sources, in particular the one-vortex DPC current system with its focus in the evening sector at $\Phi' \sim 80^\circ$ with counterclockwise current.

As the activity level varies, dramatically different mixtures of all these effects are produced and, therefore, it is difficult to isolate the variations of different types. A separation procedure which is not based on physical concepts of possible variation sources can hardly result in a correct representation of physical reality. The use of intervals with $AE \leq 150 \gamma$ and $D_{st} > -10 \gamma$ can considerably weaken the effects of auroral electrojets and ring currents. The contribution from the DPC (Y_{SE}) current system to the near-pole variations may be excluded by finding a reference level in all three components of the geomagnetic field. In this case the variations in the reference level throughout the day should be due mainly to the effects of S_q^o , quasistationary magnetospheric convection, and other possible hypothetical sources.

Figure 32 presents the variations in the reference level of three geomagnetic field components (X – toward geographic north, Y – eastwards, Z – vertically downwards) for the summer season of 1965. The horizontal line indicates the field level interpolated from the winter months of 1965 including the secular variations, which represents the mean value between the near-midnight and mean-daily field values for the international quiet days of January and December, 1965. The difference between the night and mean-daily values did not exceed, as a rule, $\sim 5 \gamma$. Since the polar ionospheric conductivity decreases by an order during the season, it is natural to suppose a simultaneous abrupt decrease of the near-pole variation intensity in winter and, in connection with this, to accept the winter field values as the absolute reference

level for determining the resulting near-pole field variation. This method for finding the absolute reference level is similar to that proposed by Friis-Christensen (1971).

Examination of the field variations shown in Figure 32 suggests that at least three sources of variations exist:

(1) S_q^o currents which are the extension of S_q variations of middle latitudes on magnetically quiet days to the near-pole region. At the altitudes of the E -region in

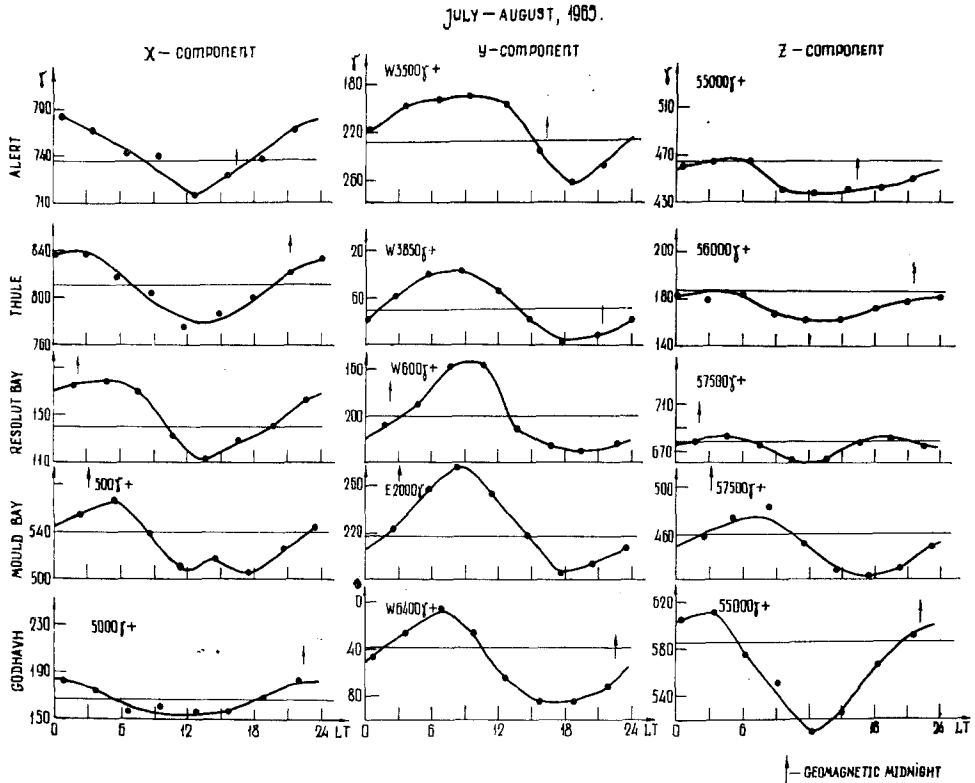


Fig. 32. Diurnal variations in the zero level at high-latitude stations in July–August, 1965 according to Feldstein *et al.* (1975a). The north, east, and vertical components are shown on the left, in the center, and on the right respectively. Local time. The arrow shows the moment of geomagnetic midnight. The horizontal line shows the field values on the international magnetically quiet days of January and December interpolated for 1 August 1965 (the night and mean-diurnal values).

July–August, the ionosphere is sunlit throughout the day; and, therefore, S_q^o currents may flow as an almost uniform layer from the evening to the morning side for nearly 24 hrs a day. The S_q^o field intensity was $\sim 20 \gamma$ in July–August, 1965 in the horizontal components, if S_q for this interval at Agincourt, Victoria, and Meanook stations located in the western hemisphere from 43° NL to 54.5° NL is extrapolated to the polar region. The positive values of $X \sim 20 \gamma$ at night and the negative values of X during the day-time at Alert, Thule, Resolute Bay, and Mould Bay are due to S_q^o . The 6^{h}

increase and 18^h decrease in the Y -component field is also due to S_q^o . The nature of S_q is an object for frequent discussion nowadays. Commonly adopted up to now, the dynamotheory of S_q origin was contested by Krylov (1973), and Lyatsky and Maltzev (1975). According to Krylov, S_q current systems occur automatically with the generation of the electric field in the magnetosphere, as a consequence of the geomagnetic field character and of the existence of global conductivity distribution in the E -layer of the ionosphere. Lyatsky and Maltzev assume that the S_q current system in middle and low latitudes is closely connected with the magnetosphere convection electric field and is therefore determined by the interplanetary magnetic field direction and intensity.

(2) The S_q^p quasistationary convection currents flowing as a uniform layer through the polar region from the night to the day side and closing through the evening and morning sectors at lower latitudes. The field of these currents, in addition to S_q^o , increases the X -component soon after midnight and decreases this component somewhat before midnight at the near-pole stations, thereby shifting the maximum decreases in X from noon to the evening. The S_q^p currents most clearly affect the Y -component variations: the time of Y sign change is shifted from 0^h and 12^h (if only S_q^o currents exist) to 3^h and 15^h; and the values of Y decrease by 30–40 γ near midnight relative to the values near noon.

(3) The counterclockwise current vortex on the day side with its focus in the early afternoon at $\Phi' \sim 78^\circ$ – 80° . The existence of such a vortex follows from the intensive decrease in Z at Godhavn and Mould Bay during the day; from the appreciable increase in the diurnal amplitude of Y -component from Thule (58 γ) to Mould Bay (90 γ) with subsequent decrease at Baker Lake (48 γ); and from the unstable diurnal dependence of X at Mould Bay. The mode of diurnal variations in X at Mould Bay is similar to the variation at the stations located near the focus of the middle-latitude S_q current system. The increase in X at 15^h LT is not casual, for it recurred in the summer of 1966 with an even larger amplitude; a similar unstable dependence in 1966 was also observed at Godhavn.

Figure 33a presents the distributions of the vectors characterizing the variations in the accepted zero reference level for $DPC(Y_{SE})$ in terms of deviations from the quiet-day field values for the winter season. The S_q^o variations (the uniform surface current from the evening to the morning side determining a 20 γ change of the field in the horizontal plane on the Earth's surface) have been excluded. The current system which approximately describes the field variations is represented in the form of the distribution of the polar-cap current from the night to the day side which is, nevertheless, deflected towards the morning and forms a current vortex in the day-evening sector with its focus at $\Phi' \sim 78^\circ$. This current system may exclude the field of S_q^p stationary convection, which can be described by the uniform current band in the polar cap yielding $\Delta T \sim 20$ – 30 γ in the horizontal plane, when the field is directed along the 6^h–18^h meridian and the current flows symmetrically from this band through the morning and evening sides to lower latitudes. Figure 33b presents the equivalent current system of the asymmetric part of the current system shown in Figure 33a, on

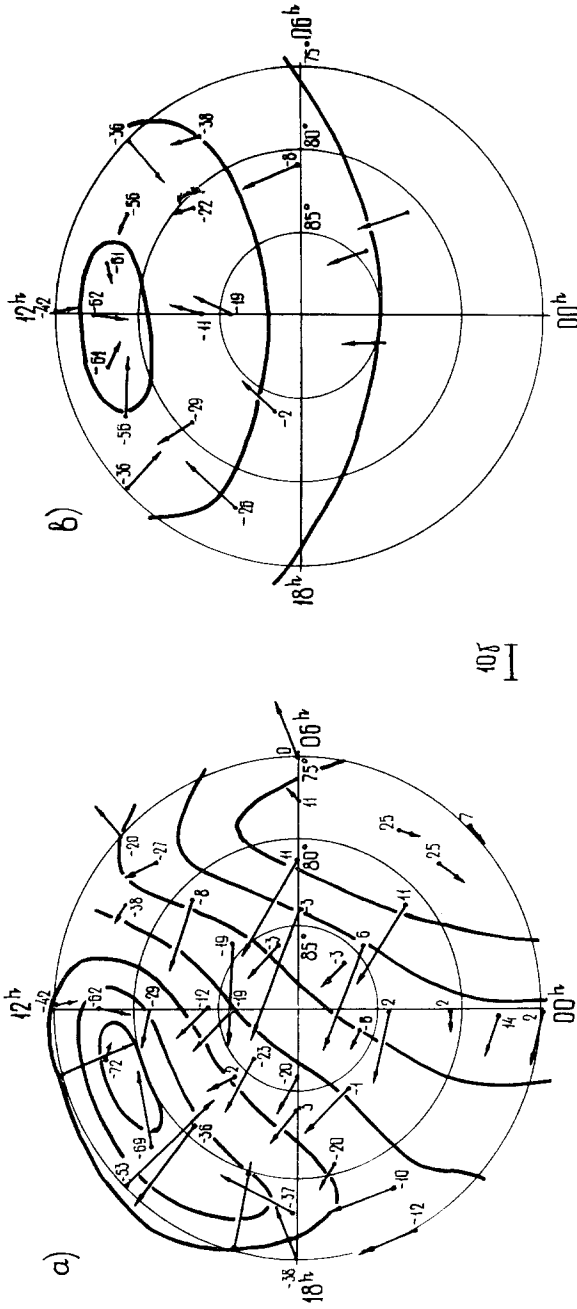


Fig. 33a-b. Spatio-temporal distribution of magnetic variation vectors in July-August, 1965 characterizing the changes of the zero level in terms of deviations from the field values for the winter season. The arrows and numerals show the horizontal and vertical planes respectively. The solid lines with arrows show the equivalent overhead current system in the northern polar region with a contour interval of 1.5×10^4 A. Coordinates: corrected geomagnetic latitude and local geomagnetic time. (a) S_{e^o} variations are excluded; (b) S_{e^o} and S_{e^p} variations are excluded.

the assumption that S_q^p is symmetric relative to the noon-midnight meridian and that the asymmetric part is due to the effect of an additional source. This current vortex is similar to that described earlier in the literature. When separated on the basis of ground observations, it is called DPC (Feldstein and Zaitsev, 1968a) and on the basis of satellite observation, PCD (Langel, 1973b) or HLS (Langel, 1974). Shabansky (1968) suggested that this current vortex was due to the projection of the magnetospheric plasma motion around the neutral point. It should be noted that according to magnetic data the polar-cap S_q^p field is $\sim 30 \gamma$. At a ~ 7 mhos integral ionospheric conductivity the field intensity $E \sim 5 \text{ mV m}^{-1}$.

The most characteristic sign of the DPC current vortex in the ground variations is the day-time decrease in Z -component at Godhavn (Z_G). According to the data listed in Table VI, the values of Z_G at $18^{\text{h}}\text{--}21^{\text{h}}$ UT are not related to the IMF azimuthal

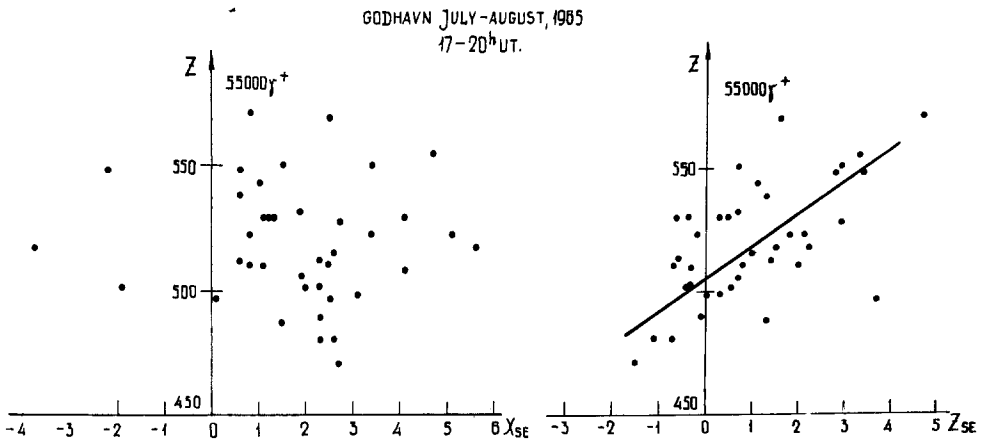


Fig. 34. Mean-hourly values of Z at Godhavn in July–August, 1965 during magnetically quiet intervals of $18^{\text{h}}\text{--}21^{\text{h}}$ UT as functions of IMF X_{SE} and Z_{SE} components at the preceding hour. The straight line shows the regression equation obtained by the method of least squares.

component. Figure 34 presents the values of Z_G at $18^{\text{h}}\text{--}21^{\text{h}}$ UT in the summer of 1965 as functions of the intensity of the IMF X_{SE} and Y_{SE} components during magnetically quiet intervals which were used to determine the zero reference level for DPC (Y_{SE}). To include a possible delay of ground variations relative to IMF, the correlation functions of the mean-hourly values were plotted for both coinciding and 1 hr shifted intervals. In any case, the values of Z_G fail to reveal a relation to the IMF X_{SE} component (the correlation factor in Figure 34a is 0.23), whereas Z_G is more closely associated with Z_{SE} intensity. When comparing the coinciding and time-shifted values, the correlation factor increases from 0.47 ± 0.1 to 0.56 ± 0.1 . Z_G takes the value of the absolute reference level at $Z_{SE} = +5\text{--}6 \gamma$ (one value is for the winter mean-diurnal absolute level of $Z_G = 55585 \gamma$ and the other value is for $Z_G = 55575 \gamma$ at $18^{\text{h}}\text{--}21^{\text{h}}$ UT). If the day-time Z_G decreases in summer relative to the absolute level are assumed to be

due to the DPC current system, this system disappears at $Z_{SE} \sim 5.5 \gamma$. Such high positive values of Z_{SE} are very infrequent; and, hence, the DPC current system exists permanently on high latitudes. Its intensity increases with decreasing Z_{SE} . At $Z_{SE} < -1 \gamma$ the substorm effects count, and the dependence of Z_G on Z_{SE} cannot be revealed in such an explicit form. Thus, the intensity of the DPC current system is controlled by the IMF Z_{SE} component and, therefore, we shall further denote this system as $DPC(Z_{SE})$. This current system is likely to be not closely associated with magnetospheric convection whose intensity is controlled by the value and direction of Z_{SE} . In particular, in case of abrupt negative bursts of Z_{SE} , characteristic variations of DP2 field are generated which, in high latitudes, are due to enhanced magnetospheric convection. Langel (1975) has concluded that no correlation between the DP2 fluctuation and $DPC(Z_{SE})$ was found and that $DPC(Z_{SE})$ was not a portion of the DP2 current system.

10. Discussion

The high-latitude magnetic field variations are the result of field superposition from several sources. The increased ionospheric conductivity in summer makes it possible to separate several variation sources during magnetically quiet periods which cause tens-of-gammas changes in magnetic field on the Earth's surface.

The fields originating from these sources also exist during magnetically disturbed periods when the field variations are more complex and variable because of field superposition from additional sources. At present, the types of high-latitude field variations covering both quiet and disturbed periods may probably be classified as follows. Table X lists the types of variations, the IMF components determining these types, the characteristic features of the equivalent current system describing the corresponding variations, and the proposed unified denominations for the variations. The first character D denotes disturbances and is used for all variations, except for S_q^o , even if the variations have a permanent basis: the variability of the interplanetary magnetic field can be seen as intensity variations in the corresponding current systems and can be observed on the Earth's surface in the form of rapid variations even if the current system is permanent. PC, MC, R and P denote respectively the polar cap, the magnetospheric convection, the ring (for ring current), and the polar (for magnetospheric substorm). This classification will be used below to examine the spatio-temporal distributions of magnetic variation vectors proposed in the literature, or the equivalent current systems based on them, with special attention to near-pole variations.

10.1. $DPC(B_Y)$ VARIATION

It is surprising that the $DPC(B_Y)$ variations, whose intensity may reach hundreds of gammas in summer, had not been detected and described before 1968 (Svalgaard, 1968). This may probably be explained by the fact that the variation nature (eastward or westward electrojets) is determined by the direction of the IMF azimuthal component; and that when averaging the data for a fairly long time interval covering B_Y

TABLE X
Nomenclature of geomagnetic field variations in high latitudes

Variation	IMF component controlling the variation	Proposed, denomination	Characteristic features of current system
S_q^o	–	S_q^o	Homogeneous current sheet. Current flow from the evening to morning side
DPC	B_Y	DPC(B_Y)	Single-vortex current system with polar electrojet in the day-side cusp latitudes. The current direction is determined by the B_Y sign
S_q^p or DP2	B_Z	DMC(B_Z)	Two-vortex current system of magnetospheric convection in the form of a homogeneous current sheet in the polar cap with sunward direction closed through lower latitudes
DPC	B_Z	DPC(B_Z)	Single-vortex counterclock-wise current system with focus in the day-side cusp region
D _p or DP1	B_Z	DP(B_Z)	Westward electrojet along the auroral oval and eastward electrojet in the evening sector of the auroral zone
DR	B_Z	DR(B_Z)	Increase in the Z-component modulus during intense magnetic storms
DCF or SC	Solar plasma pressure B_Z	DCF	The sum of current systems analogous to DP(B_Z) and DPC(B_Z) but in different combinations

of various directions, the variations of this type are mutually compensating. The DPC(B_Y) features can hardly therefore be apparent in the medium field variations on international quiet or disturbed days. The case is different when considering specific variations. In fact there is some research dating from before 1968 where the vector distribution of the ground magnetic field fluctuations is so similar to that displayed in Figure 14 that its connection with the B_Y fluctuation is indubitable.

The horizontal arrows in Figure 35 show the value and direction of the high-latitude magnetic field fluctuation started at 01^h 06^h UT on 12 December 1958 (Mansurov and Mansurova, 1965). The vectors are superposed on the S_q variation current system for the summer of that year in order to illustrate the diverse mode of the field variation in this fluctuation on international magnetically quiet days.

The zonal nature of the currents with polar electrojet in the day-side sector, the electrojet location at $\Phi' \sim 80^\circ$, and the pronounced decrease in the disturbance activity at $\Phi' < 70^\circ$, suggest that the field fluctuation examined is due to the enhancement of the IMF component directed from the evening to the morning side. The specific distribution of the vectors shown in Figure 35 can hardly be explained by the high-

latitude geomagnetic effect of solar chromospheric flares as was proposed by Mansurov and Mansurova (1965). The time coincidence between the solar flare and IMF fluctuation on the Earth's orbit is probably only occasional, though some increase in ionospheric conductivity caused by the flare may contribute to the $DPC(B_Y)$ current system intensification.

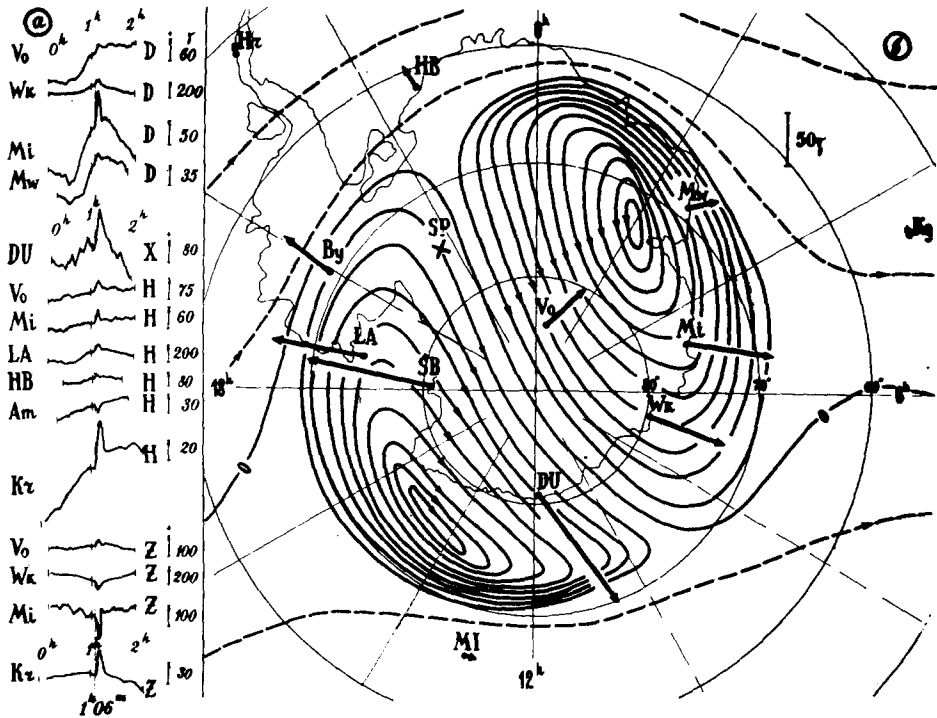


Fig. 35. Equivalent S_α current system for five international quiet days of the summer season in 1958 in Antarctica. 10^4 A flows between the stream lines. The vectors show the value and direction of the short-term magnetic field fluctuations at 01^h06^m UT on 12 December 1958. Shown to the left are the magnetograms from some stations according to Mansurov and Mansurova (1965). The coordinates are the corrected geomagnetic latitude and the local geomagnetic time.

The diurnal variations in the horizontal and vertical components were analyzed by Berthelier (1972), and, at greater length, by Berthelier *et al.* (1974), for four stations in the northern hemisphere and five stations in the southern hemisphere in 1967–1968 at $|B_Y| \leq 1 \gamma$ (taken as the reference level), $B_Y \leq -3 \gamma$ and $B_Y \geq 3 \gamma$. The $DPC(B_Y)$ current systems shown in Figure 36 are very similar to those displayed in Figure 16. The characteristic vector asymmetry at $\Phi' < 80^\circ$ relative to the noon meridian can be traced; and also some difference in the details of the pattern of equivalent currents at $\Phi' \sim 84^\circ$ (the current for $B_Y > 0$ is not exactly symmetrical to that for $B_Y < 0$). The latter is probably due to the incomplete exclusion of the substorm effects from the

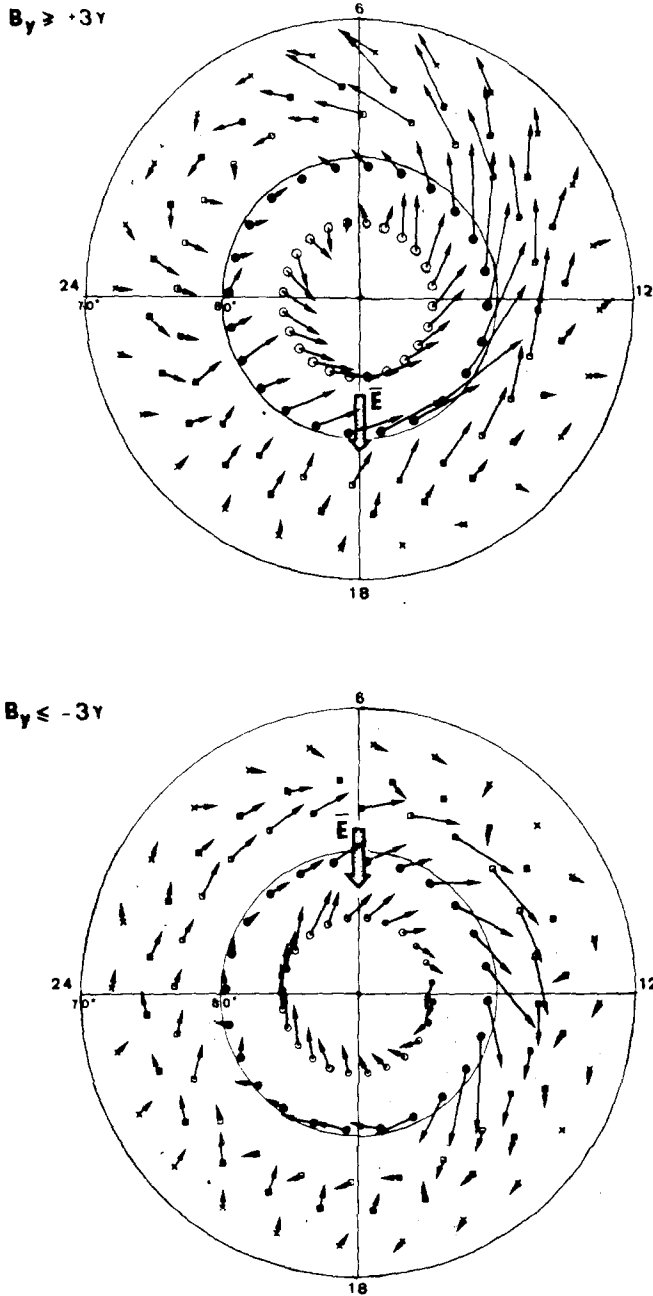


Fig. 36. The pattern of the equivalent currents on the southern hemisphere high latitudes at $B_Y \geq +3\gamma$ and $B_Y \leq -3\gamma$ in 1967–1968 according to Berthelier *et al.* (1974). The coordinates are the corrected geomagnetic latitude and the local geomagnetic time.

sector structure effect on the intensity of the positive and negative bays, as described by Langel (1973) and (Burch (1973). The reference level for Z at $\Phi' \sim 84^\circ$ remains practically the same throughout the day (diurnal amplitude in $\leq 30 \gamma$ with minimum field values at day-time), while large diurnal variations appear at $75^\circ < \Phi' < 82^\circ$ (cf. Figure 32). No effect has been found of the IMF B_x component on high-latitude

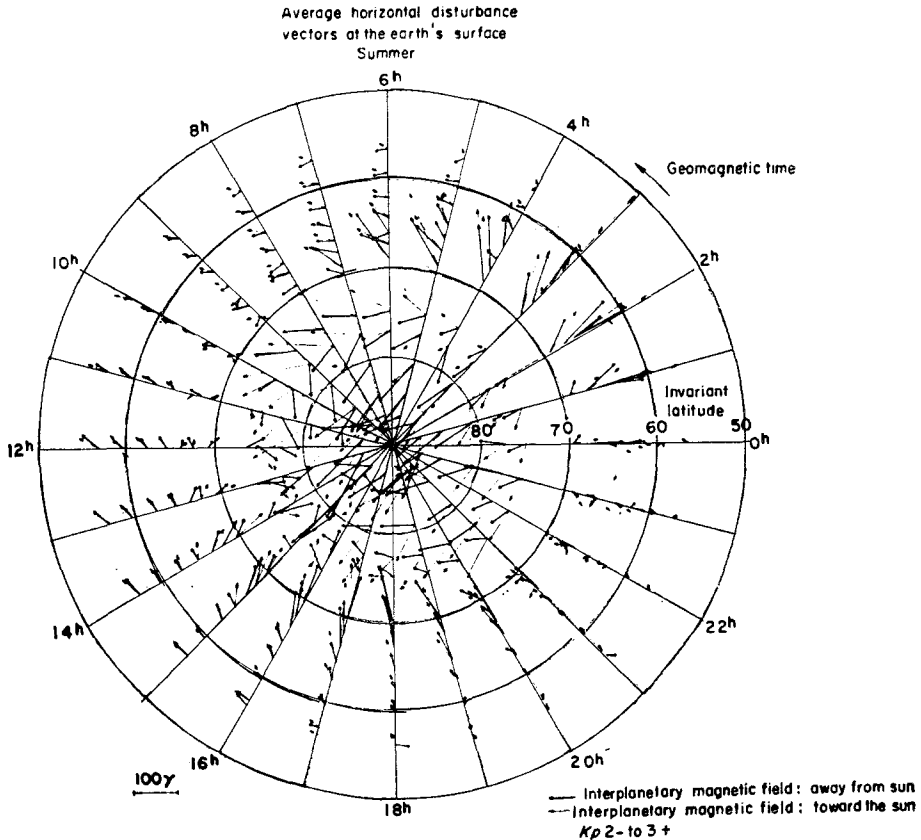


Fig. 37. The pattern of disturbed vectors in the horizontal plane on the Earth's surface during the summer season at $2^- \leq K_p \leq 3^+$ according to Langel (1973). The coordinates are the corrected geomagnetic latitude and the local geomagnetic time.

magnetic variations. It is assumed that at least the day-side field variations of the DPC (B_y) type are due to the ionospheric currents flowing around the invariant pole from $\sim 6^h$ to $\sim 18^h$ LGT at $\Phi' > 75^\circ$ with a peak near $\Phi' \sim 80^\circ$.

Langel (1973) studied the distribution of disturbed vectors in the horizontal and vertical planes from June 1965 to July 1968 for different seasons, in terms of deviations from the mean daily values of quiet days, including secular variations, at $2^- < K_p < 3^+$. Figure 37 presents the corresponding data for the summer season, the

characteristic features of which are similar to those displayed in Figure 17 at the same reference level. The higher level of magnetic disturbance is indicated by the greater field vector in the morning sector at $60^\circ < \Phi' < 70^\circ$. The equatorward direction of the vectors at $\Phi' \sim 80^\circ$ during the noon-evening irrespectively of Y_{SE} sign, which is a characteristic feature of the vector distribution, can be seen in the patterns shown in Figures 17 and 37. This feature is associated with the superposition of S_q^o and $DPC(B_Z)$ on $DPC(B_Y)$ at these times, which results in a decrease of the poleward $DPC(B_Y)$ vector at $B_Y > 0$ and, hence, in the eastward electrojet limitation by the morning sector. Subsequent analysis for more quiet ($1^- < K_p < 1^+$) and disturbed ($K_p > 4^+$) conditions has shown a similarity of the variations between the seasons and IMF polarity for all the studied disturbance levels (Langel and Brown, 1974).

Svalgaard (1973) examined the IMF polarity effect on the geomagnetic disturbance mode in 1965. The permanent ionospheric current system embraces the magnetic pole and is located at $\Phi' > 75^\circ$ with the maximum current intensity at $\Phi' \sim 80^\circ$ – 82° . Figure 38 presents the distribution of the magnetic disturbances and the 18^h UT circulating current flowing eastwards around the magnetic pole during the away IMF polarity. The location of the current system, its relation to B_Y , and the seasonal variations, are similar to the regularities of the $DPC(B_Y)$ variation whose current system is shown in Figure 14. One difference is the more rapid $DPC(B_Y)$ intensity decrease when turning from the day to the night values shown in Figure 14 whereas there is an almost constant current intensity in all the time sectors shown in Figure 38. The $DPC(B_Y)$ intensity is undoubtedly at maximum when the magnetic pole intersects the day meridian ($\sim 18^h$ UT) and decreases as the magnetic pole approaches the night side. The $DPC(B_Y)$ current intensity, however, is hardly constant at $\Phi' \sim 80$ – 82° in all the time sectors. The seasonal variation of magnetic elements in the polar cap is assumed to be due to a greater number of days with one polarity than with the other during any given season. As a result, the mean value of the field components would be contaminated by the IMF polarity effect. Besides that, the summer-to-winter variations in the intensities of other components of the disturbed field and S_q^o also contribute to the seasonal variation.

Matsushita *et al.* (1973) and Mishin *et al.* (1973) have analyzed in detail the IMF sector structure effects on magnetic field variations not only in the polar region but also at lower latitudes respectively, for international quiet days in 1965 and 1958. Use was made of the series expansions of the variations observed at a great number of stations of the spherical and harmonic functions. The high-latitude current systems for which values were obtained are not different from those described above, the only new element being the detection of the middle-latitude $DPC(B_Y)$ effect. Figure 39 presents, following Mishin *et al.* (1973), the equivalent current system of the summer season at $\Phi > 45^\circ$ during May–August, 1958 in the northern hemisphere. The day-time variation intensity is below 10γ at $\Phi < 60^\circ$. Matsushita *et al.* (1973) showed that the daily mean values of the field in the toward or away IMF sectors on quiet days differ from the daily mean values of all quiet days by $\sim 5 \gamma$ in the X -component at $\Phi < 60^\circ$. The middle-latitude $DPC(B_Y)$ intensity is, thus, only several gammas, and the separation of such

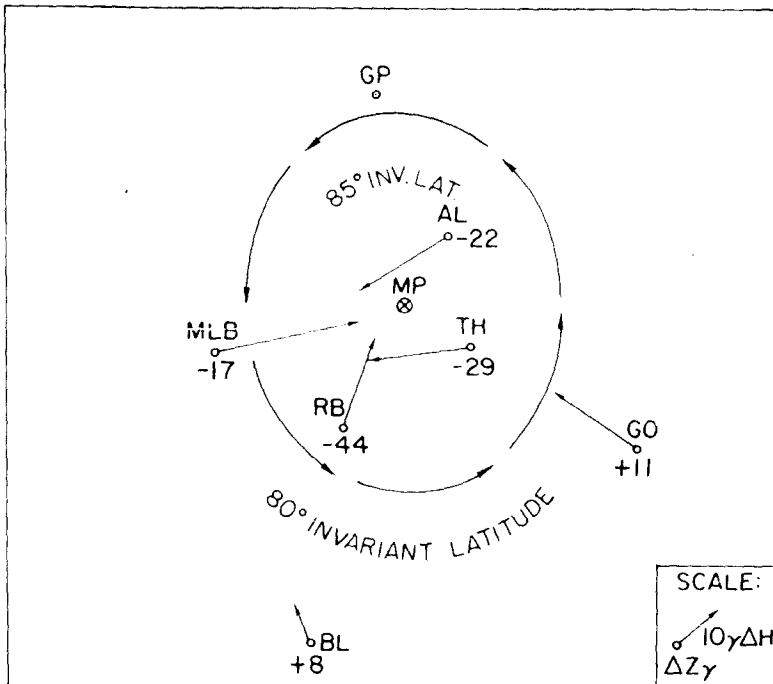


Fig. 38. Synoptic map of the polar cap magnetic disturbances at 18^h UT during IMF away polarity. Horizontal and vertical disturbances are shown as vectors and numerals respectively. The circulating current which may produce the displayed magnetic disturbances is also shown according to Svalgaard (1973).

weak effects requires an extremely thorough analysis of the observation material. The effects of magnetospheric disturbances which undoubtedly affected the quiet-day variations in 1958 must be carefully excluded. Establishment of the relation between the effect found in middle latitudes and the B_y intensity permits these variations to be included in the DPC(B_y) current system. It also remains obscure whether the middle-latitude variations are the result of ionospheric or magnetospheric currents. Rostoker *et al.* (1974) again showed convincingly that the form of the equivalent current flow pattern is extremely sensitive to the reference level and that the substorms can occur even on so-called quiet days. However, during both quiet and disturbed periods there are cell currents associated with the IMF azimuthal component in the polar cap (Rostoker *et al.*, 1974; Chen and Rostoker, 1974).

Friis-Christensen and Wilhelm (1975) analyzed the polar-cap geomagnetic variations as functions of the IMF direction in the Y - Z plane of the geocentric solar magnetospheric coordinate system for 1966–1968 on the basis of the data from six

stations in the northern hemisphere. The equivalent current pattern in magnetically quiet periods ($B_Z > 1 \gamma$) for $B_Y > 0$, $B_Y < 0$, in deviations from the field values at $B_Y \sim 0$, is very similar to that shown in Figures 16 and 36. Some differences from the current system of Svalgaard (1973) are to be noted: the spiral shape of the currents which results in a lower latitude of the current maximum in the afternoon sector for $B_Y > 0$ and in the pre-noon sector for $B_Y < 0$; and the pronounced reduction of the magnitude of currents at the local magnetic midnight. Predominant at $B_Z < -1 \gamma$ is the

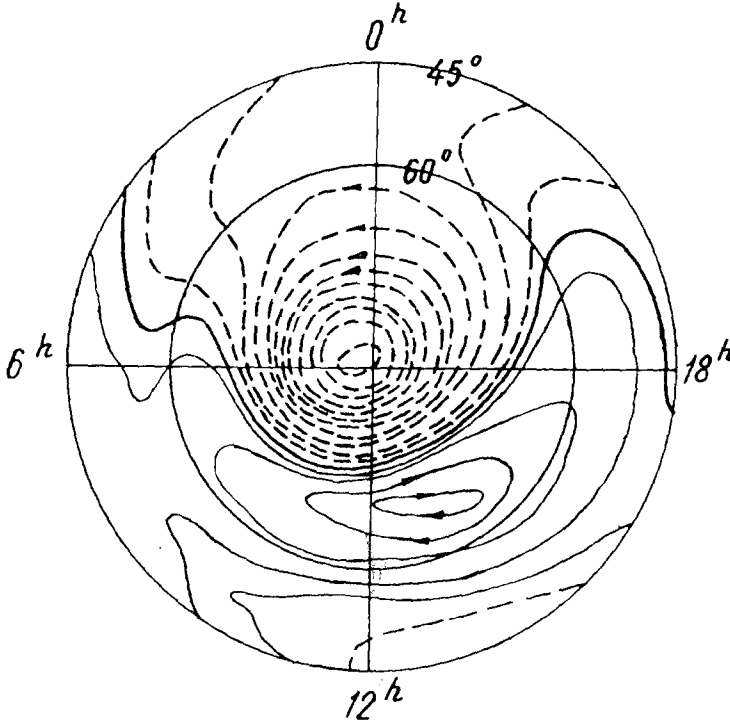


Fig. 39. Equivalent current system in May-August, 1958 in the northern hemisphere for the IMF away sector (half-difference of variations for the IMF away and toward polarities) according to Mishin *et al.* (1973).

two-cell current system with auroral electrojets upon which is superimposed the single-cell DPC(B_Y) current system. Thus, the high-latitude magnetic disturbances may be described as a simple superposition of the single-cell current controlled by B_Y and the two-cell current system related to B_Z . The main contribution to the two-cell system is from the DP1 and DP2 variations. It is assumed that the well known two-cell current system which is generally considered to be related to the convection across the polar cap vanishes completely at $B_Z > 1 \gamma$. In fact, such convection is substantially weakened at positive B_Z but is conserved, as it was noted above, up to $B_Z \sim 5-6 \gamma$. The conclusion about disappearance of the two-cell current system at

$B_z > 1 \gamma$ may be changed if the absolute value of the main geomagnetic field is taken as the reference level of geomagnetic variations, instead of the seasonal mean value. The equatorward shift of the polar electrojet with decreasing B_z but with no considerable increase in the current intensity of this electrojet, has been convincingly demonstrated. The shift amounts to 3.5° (from 81° to 77.5°) with B_z changing from $+3 \gamma$ to -3γ . The ground variation responses to B_y for each hour of the day in summer, winter and equinox have been calculated on the assumption of a linear relationship between the intensities of ground variations. The values of the response for magnetically quiet periods ($B_z > 1 \gamma$) somewhat exceed the values listed in Tables II, VI, VII and VIII, which is natural if the higher ionospheric conductivity near the sunspot maximum is borne in mind. The response decrease from summer to winter during the day-time for $B_z > 1 \gamma$ is by a factor of 5 and somewhat smaller than the values of ~ 10 presented above. This is natural since the difference between the solstice periods should exceed that for the mean seasonal values. In other respects the modes of the diurnal and seasonal variations of the responses from Friis-Christensen and Wilhjeln (1975) and those presented in Sections 2, 3 and 5 are similar, sometimes even in fine details.

The polar-cap geomagnetic disturbances observed during weak magnetic disturbances at auroral oval latitudes were described by Iwasaki (1971) and classified as a particular type of disturbance (DP-pole). The characteristic features of the DP-pole are the limitation to the $\Phi' > 75^\circ$ region; the maximum intensity on the dayside $\Phi' \sim 83^\circ$; the most frequent occurrence near the noon of local or corrected geomagnetic time and near 17^h UT in the northern polar cap; and the dominance in local summer and in the years of high solar activity. The DP-pole intensity sometimes exceeds 500γ during sunspot maximum, but seldom exceeds 300γ during sunspot minimum.

All the above mentioned features of the DP-pole are also characteristic of the DPC (B_y) variation. It follows from the comparison between the IMF B_z component and the horizontal component variations at Vostok station for 23 December 1963 (Iwasaki, 1971) that the northward turn of B_z is not always accompanied by the appearance of the DP-pole-type disturbances. Additional study would probably be needed to confirm the necessity for distinguishing the DP-pole as a special type of near-pole geomagnetic field variation. Such a research has been carried out in Maezawa's (1976) paper, which has shown the existence of a two-cell current system of DP-pole, when the present review was already written.

10.2. DMC (B_z) VARIATION

The two-cell current system of near-pole magnetospheric convection was first isolated by Nagata and Kokubun (1962) for the IGY international magnetically-quiet days (Figure 40a) and was called S_q^p . A similar form of the polar-latitude current system, but covering the latitudes from pole to equator, was described by Nishida (1968) and proved to be closely associated with the IMF B_z component fluctuations to the south (Figure 40b). According to Troshichev *et al.* (1974), during magnetically-quiet

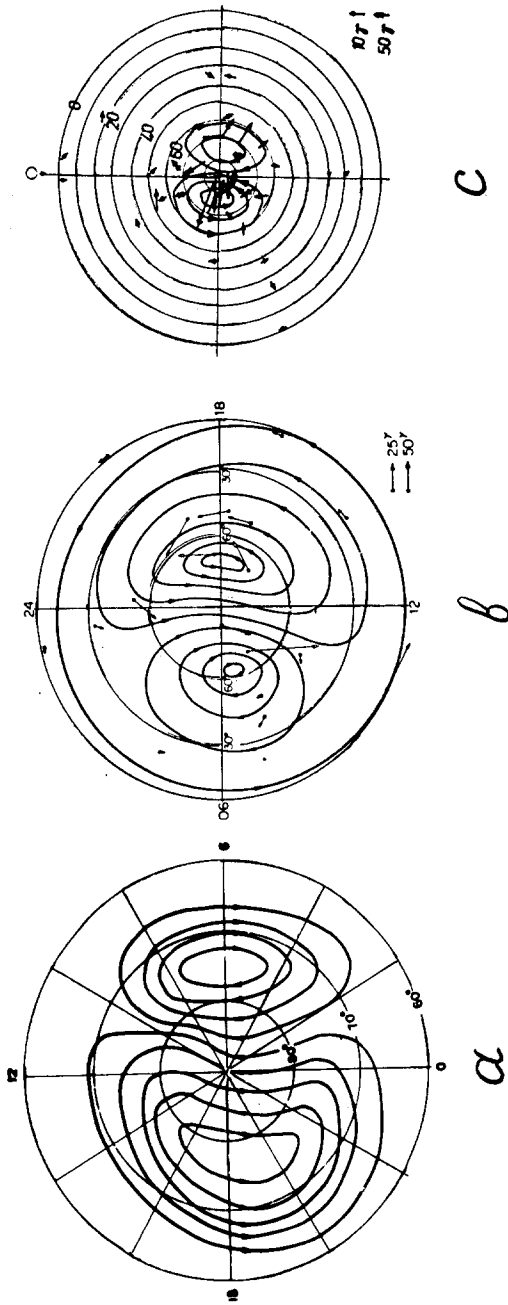


Fig. 40a-c. Equivalent DMC (B_z) current systems in the northern hemisphere: (a) on the international magnetically quiet days of the summer in 1958 according to Nagata and Kokubun (1962), $\Delta I = 2 \times 10^4$ A; (b) during the IMF B_z fluctuations on 2 December 1963 at 15^h30^m–16^h30^m UT according to Nishida (1968), $\Delta I = 5 \times 10^4$ A; (c) at 11^h and 12^h UT on 29 August 1967 according to Troshichev *et al.* (1974).

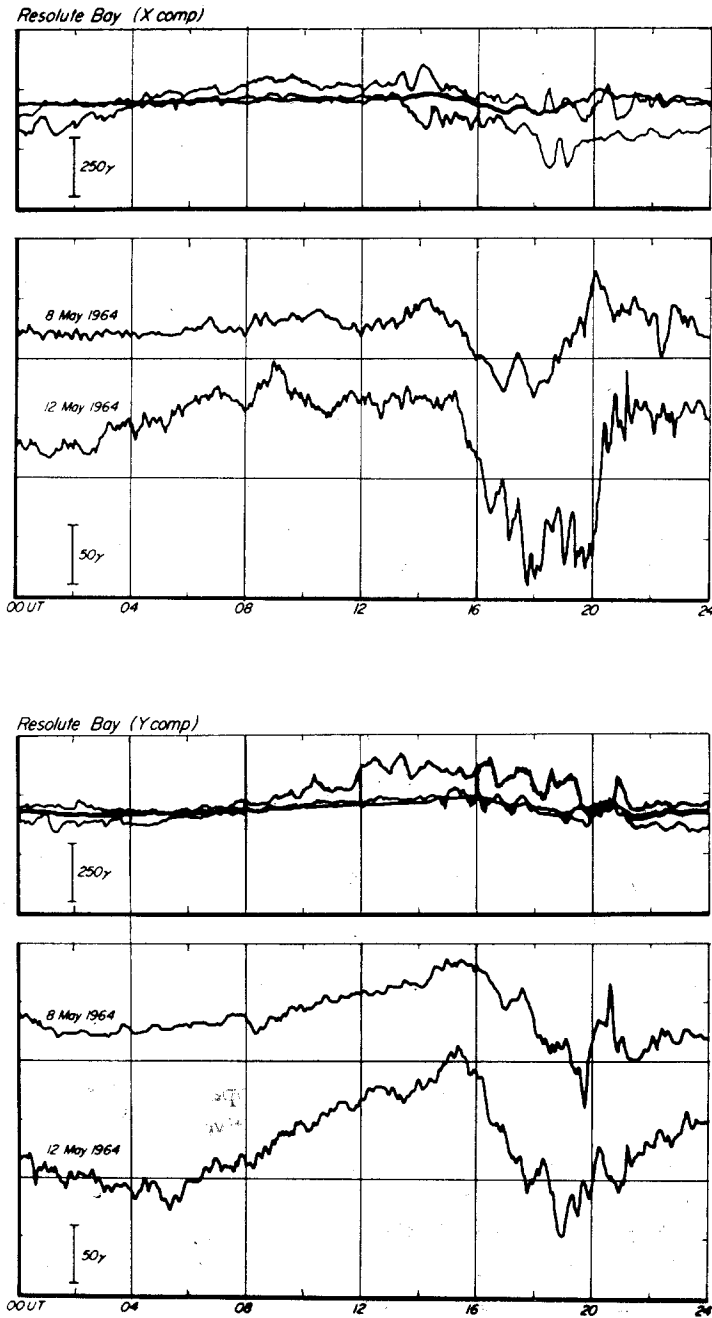


Fig. 41. Comparison between the daily record (the solid line) of the X and Y components at Resolute Bay for very quiet days of IQSY (8 and 12 May 1964) and the upper and lower envelopes of the daily records on several moderately disturbed days at the same station according to Kawasaki and Akasofu (1972).

periods the two-cell current system embraces the high-latitude region ($\Phi' > 50^\circ$); while the zonal currents which flow in the middle and low latitudes are due to the extra ionospheric ring current and the magnetospheric surface current (Figure 40c). However, the precise parameters of the $DMC(B_z)$ current system (locations of focuses, current intensity and directions), can be determined only in the future: since, apart from $DMC(B_z)$, other sources (for example, $DP(B_z)$, DR) undoubtedly contribute to the field distribution shown in Figures 40a, b; and a $DPC(B_y)$ variation contribution, which may be very considerable in the day-side polar region, is not excluded in Figures 40b, c. The $DMC(B_z)$ variation will undoubtedly retain the main features of the S_q^p or DP2 current systems (distributed current flowing through the polar region from the night to the day side and closing through lower latitudes); however, the separation of the pure form of this variation will make it possible to obtain quantitative relations between $DMC(B_z)$ intensity and IMF parameters.

The $DMC(B_z)$ variations are present on very quiet days and are enhanced during moderate disturbances. Figure 41 shows, following Kawasaki and Akasofu (1972), the variations in X and Y components at Resolute Bay on the very quiet days of 8 and 12 May 1964, and the envelopes of diurnal variations for moderately disturbed days. When the variation modes are conserved, the variation amplitudes increase by several times from quiet to disturbed conditions. Such enhancement in diurnal variations can be naturally related to an increase in the polar cap electric field directed from the morning to the evening side during disturbed periods (Mozer *et al.*, 1974). The X -component decrease at 14^h–20^h UT on 8 May shown in Figure 41 may be assumed to be due to variation in the IMF azimuthal component. The distribution of field variation vectors obtained for that day by Kawasaki and Akasofu (1967) is in fact very similar to that presented in Figure 17 for the intervals with $Y_{SE} < 0$. The current direction proposed by Afonina and Feldstein (1971) which generalizes the variation vector distribution for 8 May 1964 proved to be very similar to that shown in Figure 17. The three-dimensional current system (Kawasaki and Akasofu, 1973) adequately describing the variation vector distribution on that particular day consists of an inward field-aligned current from the morning-side magnetopause to the pre-noon sector of the auroral oval and an outward field-aligned current from the afternoon sector of the auroral oval to the evening-side magnetopause together with ionospheric (Pederson and Hall) currents. The positive and negative charges in the morning and evening sectors respectively of the auroral oval are likely to be responsible for the morning-to-evening electric field across the polar cap. Such a current system, however, can hardly be used to explain the $DPC(B_y)$ variations, since the B_y polarity change should be accompanied by the change of the field-aligned current direction and the electric field through the polar cap. However, it follows from the observations of the high-latitude electric field that such a field exists at any disturbance intensity and is always directed from the morning to the evening side irrespective of IMF orientation (Caufman and Gurnett, 1971; Heppner, 1972). The magnetic effects of the three-dimensional current system consisting of longitudinal currents flowing to and from the auroral oval latitudes in the morning and evening sectors, and ionospheric

currents, have been examined by Leontiev *et al.* (1974) on various assumptions about ionospheric conductivity. For a uniformly conducting ionosphere or when the day-time conductivity exceeds that at night by a factor of 2 (the Hall and Pedersen conductivities are assumed to be equal) the equivalent current systems consist of two cells resembling the $DMC(B_z)$ current systems displayed in Figure 40. In connection with the permanent presence of the morning-to-evening electric field across the polar cap, the magnetic field variation varies with the night-to-day current in this region. The enhancement of field-aligned currents flowing into and from the auroral oval latitudes causes the ground magnetic field fluctuations described by equivalent current systems similar to those shown in Figure 40b. Since the field-aligned current intensity is controlled by the IMF B_z component, it is natural to assume that DP2 is a display of intensification of the permanently existing $DMC(B_z)$ current system. This conclusion also agrees with the model calculations (Volland, 1973) of three-dimensional current systems explaining the existence of the $DMC(B_z)$ variation and its enhancement during disturbed periods as well as the appearance of DP2 as a result of the short periodic enhancement of $DMC(B_z)$.

Shabansky has made a quantitative analysis of the appearance of the $DMC(B_z)$ current system as a result of the interactions of the solar wind and its magnetic field with the magnetosphere and the processes in the magnetospheric tail (see Afonina *et al.*, 1975).

10.3. DPC (B_z) VARIATION

The single-cell equivalent counterclockwise current system with focus at $\Phi' \sim 80^\circ$ on the 15th meridian in the day sector was first proposed by Feldstein and Zaitsev (1967) to explain the field variations on the international magnetically quiet days of the IGY summer season. Figure 42a presents the vector distribution and Figure 42b shows the equivalent current vortex in the day sector with an intensity of 13×10^4 A which caused the observed variations at day-evening hours. Though the $DPC(B_y)$ variations are largely excluded when averaging the data, their traces for $B_y < 0$ may be found if the vector distribution in Figure 42a is thoroughly studied. During magnetically extremely quiet periods the vortex focus is displaced to the noon meridian and the vortex intensity decreases markedly (Feldstein and Zaitsev, 1968). The denomination DPC was proposed for this current system, and it can probably not be explained by the system of convective motions in the magnetosphere proposed by Axford and Hines. A mechanism based on the properties of the boundary layer between the plasma and the magnetic field in the day-cusp region was proposed by Shabansky (1968) to explain the DPC current cell. The medium with its magnetic field at the boundary of the magnetosheath must move, relative to the fieldless plasma, toward $\mathbf{n} \times \mathbf{B}$, where \mathbf{n} is a normal to the boundary directed toward the plasma, and \mathbf{B} is the geomagnetic field. This motion arises due to the difference in mass between the electrons and the ions reflected from the magnetic wall and penetrating the magnetosphere up to various distances. As a result, the magnetospheric plasma rotates westwards (clockwise) relative to the interplanetary plasma, filling the day-side cusp.

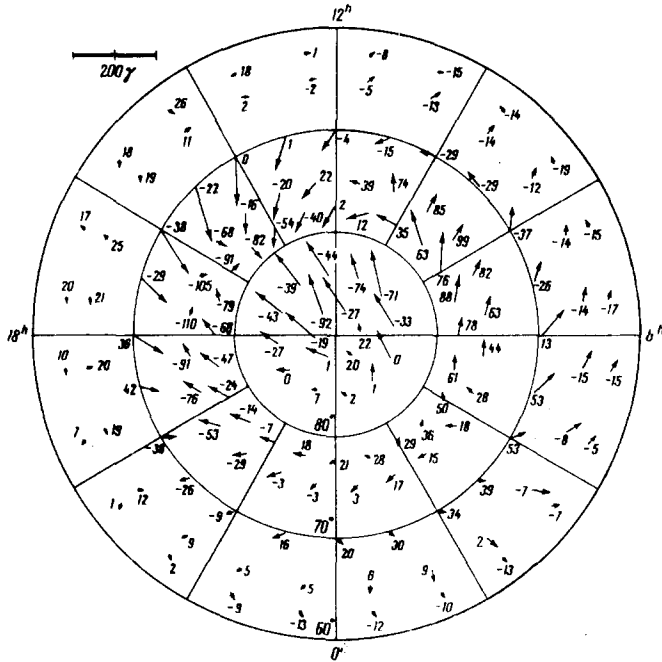


Fig. 42a. Spatio-temporal distribution of the variation vector for five international quiet days of the summer season of IGY at the stations of the western hemisphere according to Feldstein and Zaitsev (1967).

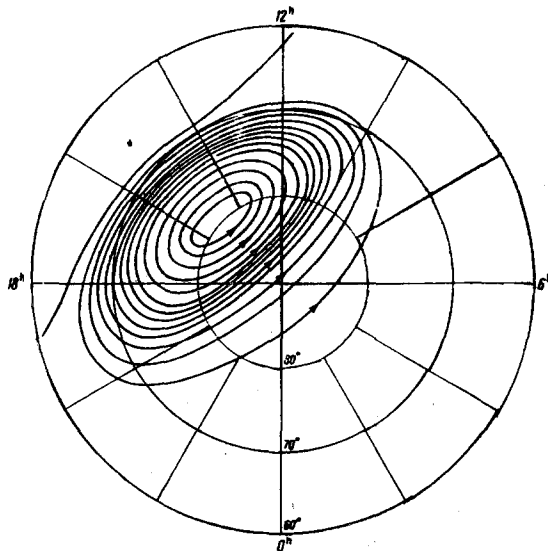


Fig. 42b. Equivalent current cell on magnetically quiet days of the summer season of IGY. 10^4 A flows between stream lines. The coordinates are the corrected geomagnetic latitude and the geomagnetic time.

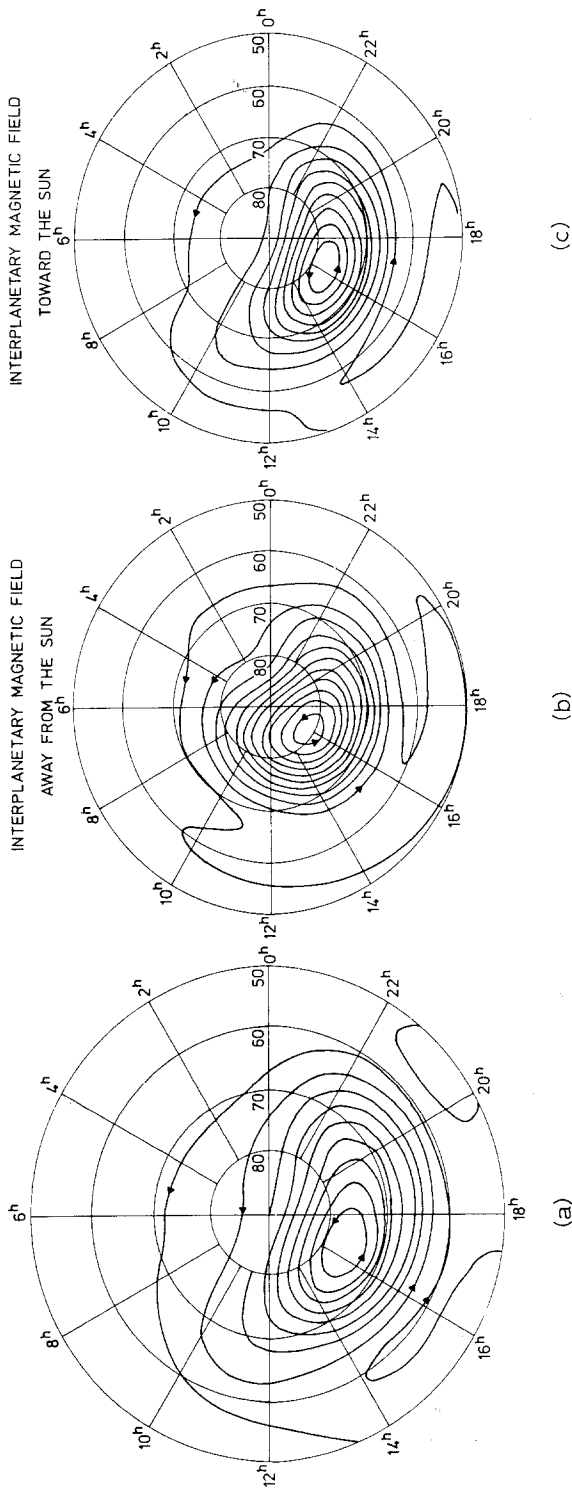


Fig. 43a-c. Equivalent current cell in the region of negative magnetic field modulus during the summer season at $2 - < K_p < 3^+$ according to Langel (1973, 1974a). 10^4 A flows between the stream lines. The coordinates are the corrected geomagnetic latitude and the geomagnetic time. (a) all days; (b) IMF away sector; (c) IMF toward sector.

A rotating moment permanently affects the magnetosphere because of the continuous 'renewal' of the interplanetary plasma at the boundary with the day-side cusp. This effect is enhanced in the presence of the southward IMF B_z component as a result of the greater intensity of the plasma streams in the day-side cusp. Projection of the westward vortex motion of magnetospheric plasma along geomagnetic force lines onto ionospheric altitudes will give rise to an eastward (counterclockwise) ionospheric Hall current with its focus in the region of the day-side cusp.

Additional convincing confirmations of the existence of the $DPC(B_z)$ current cell in the ionosphere were obtained by Langel (1973, 1974a) who examined the OGO-2, 4, 6 observations of the total magnetic field at different heights above the ionosphere. Figure 43 presents the equivalent current system calculated by Langel for the region of decreased values of the field modulus ($\Delta B < 0$) from 10^h to 22^h of local geomagnetic time. The abrupt decrease of Z in the region of the focus, which is the most characteristic feature of the variation, is practically the same in Figures 42 and 43. The intensity of negative ΔB decreases substantially from summer to winter and with an increase in the altitude, which indicates that the current system is located at ionospheric altitudes. The current system exists permanently and fails to disappear even during magnetically extremely quiet periods; its intensity, however, increases with any increase in the disturbance. The vortex intensity is 9×10^4 A for moderate disturbances during the summer season. The current cell exists at any B_Y polarity, which indicates that its origin is independent of B_Y . The only effect of sector structure polarity is the equatorward shift of the focus for the IMF toward sector. Thus, the current cell in Figure 43 varies but slightly with changes in the IMF polarity. This result is in surprisingly good agreement with the several degrees of latitude displacement of the focus of the evening current cell (see Figure 17) of the resultant current system during the summer season at different B_Y polarity, as was noted in Section 3 above. The $DPC(B_z)$ current cell location in the day-evening sector at ionospheric altitudes was further confirmed by Langel (1974). The simultaneous OGO-6 measurements of the intensities of the electric and magnetic fields in the summer polar cap at altitudes below 600 km have shown that the changes in the patterns are highly correlated. This correlation extends to the pattern shapes, the boundary locations, and the amplitudes of the correlated quantities. Apart from proving the ionospheric origin of the field variations at 11^h–18^h LGT, the data obtained are in good agreement with the form of the current system as a vortex with counterclockwise current covering a wide latitude range.

The $DPC(B_z)$ current system is probably responsible for the unusual field variations at Godhavn near noon for $B_z > 0$ described by Friis-Christensen and Wilhjelm (1974). In the author's opinion these variations can be explained by the return currents, while the primary current was located 3–4 degrees to the north. In connection with the fact that during magnetically quiet periods the $DPC(B_z)$ current cell focus is displaced toward noon, it is the above mentioned primary and return currents that form a current system similar to that shown in Figure 33b.

10.4. DP (B_z), DCF, AND DR (B_z) VARIATIONS

The aim of the present review is to examine the near-pole magnetic field variations during magnetically quiet periods. The DP(B_z), DCF and DR(B_z) variations are among the known types of the near-pole magnetic field variations systematized in Table X. Refraining from describing these variations in detail, we refer the reader to sufficiently comprehensive reviews (Rostoker, 1972, 1974; Fukushima and Kamide, 1973; Ivanov and Mikerina 1974; Feldstein *et al.*, 1974b). The near-pole variations in the Z -component during magnetic storms were examined by Maisuradze (1967).

10.5. ELECTRIC FIELD MEASUREMENTS IN POLAR CAPS

The large-scale convection pattern in the polar cap, based on electric field measurements from satellites and balloons, consists of a two-cell system with antisunward convection across the polar cap, and sunward return flow along the auroral oval (Cauffman and Gurnett, 1971; Heppner, 1972c, 1973). The balloon measurements at three points (Mozer *et al.*, 1974) showed that the average direction of the flow across the polar cap deviated from the antisolar direction by 15° clockwise. The resultant current direction in the polar-cap DMC(B_z)+DPC(B_z) current system shown in Figure 33a differs by $\sim 180^\circ$ from the convection direction, which suggests that the ground field variations are due to the ionospheric Hall currents.

Observations have shown that both B_z and B_y substantially affect the polar cap convection pattern. According to Heppner (1972b), the IMF sector polarity – it is possible that the B_y sign is more significant than the sector polarity – is in close correlation with the asymmetry in the polar cap electric field pattern on the 6^{h} – 18^{h} meridians. At $B_y > 0$ and $B_y < 0$ the electric field is at maximum on the polar cap morning and evening side respectively. This agrees with the polar electrojet locations shown in Figure 17 (electric field measurements give the total field at ionospheric altitudes and, therefore, comparison should be made with the current systems representing the total variations of the magnetic field). The form of asymmetry in the location of the convection maximum changes simultaneously with variations in the relative size of the antisolar convection cells. In this case the polar cap–auroral belt boundary is shifted. The boundary shifts proposed by Heppner (1972b) to explain the observed IMF polarity effect on the polar cap magnetic field fail to reproduce the more detailed pattern of magnetic disturbances of the DPC(B_y) variation reported in the present review.

The position of the convection maximum on the morning (evening) meridian at $B_y > 0$ ($B_y < 0$) is due to the superposition of the convective motions along the day-side cusp (DPC(B_y) current system) on the day-night convection (DMC(B_z) current system), which results in electric field enhancement in the morning or evening sectors. Such superposition may be interpreted in terms of electric fields as apparent shifts of the two-cell convection pattern related to the B_y sign.

The existence of convective motions along the cusp follows from the observations. Very few electric field measurements near magnetic local noon at cusp latitudes have

been made. The Injun-5 measurement results published by Cauffman and Gurnett (1971, 1972), Gurnett (1971, 1972), and Gurnett and Frank (1973) showed an abrupt change of the convective motion direction along longitude in the day-side cusp region. Comparison of convection with the direction of polar electrojet in the DPC(B_Y) current system (Wilhelm and Friis-Christensen, 1972) has revealed an agreement with the assumption that the polar electrojet is a Hall current. The current is also poleward of the average location of the electric field reversals in the noon meridian. According to the observations of Galperin *et al.* (1974), the day-side cusp convection of the summer hemisphere is along the auroral oval; in the morning and afternoon sectors the convection becomes an antisunward motion through the polar cap. These measurements are also in agreement with the existence of the polar electrojet of the DPC(B_Y) current system at day-side cusp latitudes. Apart from the convective motions along the longitude, a noticeable antisunward convection exists at day-side cusp latitudes. The latter was observed both from rocket observations (Maynard and Johnstone, 1974) and when studying the aurora drift (Vorobyev *et al.*, 1974).

According to Mozer *et al.* (1974) the ionospheric morning-evening electric field tends to be larger when the IMF is large and directed southwards. The experimental data can be described by the regression equation $E \text{ mV m}^{-1} = 22 - 3 B_Z$ (in gammas), i.e. the electric field vanishes at $B_Z \sim 7 \gamma$. The correlation factor between the ionospheric electric field and the IMF B_Z component is ~ 0.4 , i.e. it is sufficiently high to suggest that the observed relationship is real. Thus, the data on the characteristic features of the DMC(B_Z) and DPC(B_Z) variations do not contradict the available results from near-pole electric field measurements.

11. Concluding Remarks

The relationships between IMF components and the various types of ground magnetic variations found in recent years make it possible to use the observations in the vicinity of the Earth to forecast the magnetic field variations on the Earth's surface. This must lead eventually to a procedure whereby an estimate of the magnetic field value at any point of the Earth's surface can be deduced from the measurements made in space. The inverse procedure of IMF diagnostics on the basis of ground observations of magnetic variations is also possible. Both methods are used in practice at present. The ground observations of the polar cap geomagnetic field have become a fairly reliable means of determining large-scale solar magnetic fields, which makes it possible to obtain information on the solar magnetism for several decades, and may prove to be essential for understanding solar magnetism regularities and the IMF-geomagnetic field interaction. It seems necessary in this connection to search for such a system of IMF component representation that the value and direction of azimuthal component variations would be most closely related to a certain type of near-pole geomagnetic variations.

The high-latitude geomagnetic variations on the Earth's surface are often used to substantiate theoretical considerations about the magnetospheric dynamics and proces-

ses. It is topical, in this connection, to select a proper field reference level. The high-latitude field variations are very complicated in connection with the superposition of the fields from various sources. Division of the total field variations into individual components characterizing the various sources seems to be the most topical problem of geomagnetism at present. Only after completely solving this problem may the experimental equivalent current systems be compared to the real ionospheric and magnetospheric currents, and the conclusion drawn about the validity of one or other theoretical concept. Separation of the fields of various sources will also make it possible to determine whether the polar latitudes cover the field variations controlled by the IMF radial component.

There is every reason at present to believe that the IMF state indirectly affects the processes in the lower atmosphere and, correspondingly, the weather formation. Studies in this direction are being carried out in connection with the explicit necessity to include the solar activity effects when compiling weather forecasts. However, we are now far from approaching the end of the long road to awareness of the effects of the corpuscular and electromagnetic solar radiations on the Earth, and to the exposition of the total diversity of solar-terrestrial relationships.

Acknowledgements

The present review makes extensive use of results obtained by the author in cooperation with A. M. Lyatskaya, P. V. Sumaruk, and N. F. Shevnina, to whom the author expresses his gratitude. The valuable and informative discussions with S. V. Leontiev, V. B. Lyatsky, Yu. P. Maltsev, and V. P. Shabansky are also greatly appreciated. R. G. Afonina and A. E. Levitin read the manuscript and made helpful remarks. The author acknowledges the use of Dr N. F. Ness's data from the IMP-3 magnetometer experiment supplied to us from World Data Center A for Rockets and Satellites.

A table listing the corrected geomagnetic latitudes, local time, and local geomagnetic time of midnight UT at magnetic stations used in the analysis is presented as an Appendix on p. 861.

References

- Afonina, R. G. and Feldstein, Ya. I.: 1971, *Geomag. Aeron.* **11**, 567.
 Afonina, R. G., Feldstein, Ya. I., and Shabansky, V. P.: 1975, coll. papers, *Aurora and Airglow*, No. 22, Nauka, Moscow.
 Akasofu, S. I.: 1974, *Planet. Space Sci.* **22**, 885.
 Akasofu, S. I. and Chapman, S.: 1972, *Solar-Terrestrial Physics*, Clarendon Press, Oxford.
 Akasofu, S. I., Yasuhara, F., and Kawasaki, K.: 1973, *Planet. Space Sci.* **21**, 2232.
 Banks, P. M., Chappell, C. R., and Nagy, A. F.: 1974, *J. Geophys. Res.* **79**, 1459.
 Bassolo, V. S., Mansurov, S. M., and Shabansky, V. P.: 1972, *Studies Geomagnet., Aeronomy, Solar Physics*, No. 23, 125.
 Berdichevsky, M. N., Dmitriev, V. I., Mescherikova, N. A., and Rotanova, N. M.: 1972, Moscow State Univ., Computer Center.
 Berdichevsky, M. N., Obuhov, G. G., and Fainberg, E. B.: 1973, *Geomagn. Aeron.* **13**, 143.
 Berthelier, A.: 1972, *C.R. Acad. Sci. URSS* **275(B)**, 841.
 Berthelier, A., Berthelier, J. J., and Guerin, C.: 1974, *J. Geophys. Res.* **79**, 3187.
 Bobrov, M. S.: 1961, *Solar Activity*, No. 1, 36.

- Burch, J. L.: 1972, *J. Geophys. Res.* **77**, 6696.
- Burgh, J. L.: 1973, *J. Geophys. Res.* **78**, 1047.
- Campbell, W. H. and Matsushita, S.: 1973, *J. Geophys. Res.* **78**, 2079.
- Cauffman, D. P. and Gurnett, D. A.: 1971, *J. Geophys. Res.* **76**, 6014.
- Cauffman, D. P. and Gurnett, D. A.: 1972, *Space Sci. Rev.* **13**, 369.
- Chen, A. J. and Rostoker, G.: 1974, *Planet. Space Sci.* **22**, 1101.
- Fairfield, D. H. and Ness, N. F.: 1974, *J. Geophys. Res.* **79**, 5089.
- Feldstein, Ya. I. and Zaitzev, A. N.: 1967, *Geomagn. Aeron.* **7**, 204.
- Feldstein, Ya. I. and Zaitzev, A. N.: 1968a, *Kosm. Issled.* **6**, 155.
- Feldstein, Ya. I. and Zaitzev, A. N.: 1968b, *Tellus* **20**, 338.
- Feldstein, Ya. I. and Zaitzev, A. N.: 1968c, *Ann. Geophys.* **24**, No. 2.
- Feldstein, Ya. I.: 1969, *Rev. Geophys.* **7**, 179.
- Feldstein, Ya. I. and Starkov, G. V.: 1970, *Plan. Space Sci.* **18**, 501.
- Feldstein, Ya. I., Starkov, G. V., Sumaruk, P. V., and Shevina, N. F.: 1972, 'Interplanetary Magnetic Field in Ecliptic Plane and Aurora Activity', *Proc. Conf.*, Ashkhabad, October, 1972.
- Feldstein, Ya. I.: 1973, *Vestn. Akad. Nauk SSSR* **8**, 532.
- Feldstein, Ya. I., Sumaruk, P. V., and Afonina, R. G.: 1973, 'Interplanetary Magnetic Field Orientation and Types of Surface Geomagnetic Disturbances', *AGA Bulletin*, No. 34, 435.
- Feldstein, Ya. I.: 1974, in *High-Latitude Geophysical Phenomena*, Nauka, Moscow, p. 22.
- Feldstein, Ya. I., Shevnina, N. F., and Sumaruk, P. V.: 1974a, *Geomagn. Aeron.* **14**, 863.
- Feldstein, Ya. I., Goncharova, E. E., Shashunkina, V. M., and Yudovich, L. A.: 1974b, in M. N. Fatkullin and L. A. Yudovich (eds.), *Investigations of F Layer and Outer Ionosphere*, Moscow, p. 318.
- Feldstein, Ya. I., Sumaruk, P. V., and Shevnina, N. F.: 1975a, *C. R. Acad. Sci. URSS* **222**, 833.
- Feldstein, Ya. I., Lyatskaya, A. M., Sumaruk, P. V., and Shevnina, N. F.: 1975b, *Geomagn. Aeron.* **15**, 1021.
- Forbes, T. G. and Speiser, T. W.: 1971, *J. Geophys. Res.* **76**, 7542.
- Foster, J. C., Fairfield, D. H., Ogilvie, K. W., and Rosenberg, T. J.: 1971, *J. Geophys. Res.* **76**, 6971.
- Fougere, P. F.: 1974, *Planet. Space Sci.* **22**, 1173.
- Friis-Christensen, E.: 1971, *Geophys. Papers R-27*, Danish Meteorol. Inst.
- Friis-Christensen, E., Lassen, K., Wilcox, J. M., Gonzalez, W., and Colburn, D. S.: 1971, *Nature Phys. Science* **233**, 48.
- Friis-Christensen, E., Lassen, K., Wilhjelm, J., Wilcox, J. M., Gonzalez, W., and Colburn, D. S.: 1972, *J. Geophys. Res.* **77**, 337.
- Friis-Christensen, E. and Wilhjelm, J.: 1975, *J. Geophys. Res.* **80**, 1248.
- Fukushima, N.: 1962, *J. Phys. Soc. Japan* **17**, 70.
- Fukushima, N. and Kamide, Y.: 1973, *Rev. Geophys. Space Phys.* **11**, 795.
- Galperin, Y. I., Ponomarev, V. N., and Zosomova, A. G.: 1974, *Ann. Geophys.* **30**, 1.
- Gosling, J. T., Asbridge, J. R., Bame, S. J., Hundhausen, A. J., and Strong, I. B.: 1967, *J. Geophys. Res.* **72**, 1813.
- Gurnett, D. A. and Frank, L. A.: 1973, *J. Geophys. Res.* **78**, 145.
- Gustafsson, G.: 1970, *Ark. Geofys.* **5**, 595.
- Heikkila, W. J.: 1974, private communication.
- Heikkila, W. J. and Winningham, J. D.: 1971, *J. Geophys. Res.* **76**, 883.
- Heikkila, W. J. and Winningham, D.: 1974, *J. Geophys. Res.* **79**, 949.
- Heppner, J. P.: 1972a, *J. Geophys. Res.* **77**, 4877.
- Heppner, J. P.: 1972b, *Planet. Space Sci.* **20**, 1475.
- Heppner, J. P.: 1972c, in *Critical Problems of Magnetospheric Physics*, IUCSTP, Washington, p. 107.
- Heppner, J. P.: 1973, *Radio Sci.* **8**, 933.
- Iijima, T.: 1973, *Rep. Ionos. Space Res. Jap.* **27**, 199.
- Iijima, T. and Kokubun, S.: 1973, *Rep. Ionos. Space Res. Jap.* **27**, 195.
- Ivanov, K. G.: 1973, *Geomagn. Aeron.* **13**, 1127.
- Ivanov, K. G.: 1974, 'The Electric Field of the Outer Magnetosphere and the Magnetopause', lecture delivered at the School on *Electric Fields in the Ionosphere and the Magnetosphere*, Leningrad, May, 1974.
- Ivanov, K. G. and Mikerina, N. V.: 1974, in K. G. Ivanov (ed.), *Solar Wind and the Magnetosphere* Moscow, 3.

- Iwasaki, N.: 1971, *Rep. Ionos. Space Res. Jap.* **25**, 163.
- Jørgensen, T. S., Friis-Christensen, E., and Wilhelm, J.: 1972, *J. Geophys. Res.* **77**, 1976.
- Kawasaki, K. and Akasofu, S.-I.: 1967, *J. Geophys. Res.* **72**, 5367.
- Kawasaki, K. and Akasofu, S.-I.: 1972, *WDCA for Solar-Terrest. Physics*, Report UAG-18.
- Kawasaki, K. and Akasofu, S.-I.: 1973a, *Planet. Space Sci.* **21**, 329.
- Kawasaki, K. and Akasofu, S.-I.: 1973b, *Planet. Space Sci.* **21**, 692.
- Kawasaki, K., Yasuhara, F., and Akasofu, S.-I.: 1973c, *Planet. Space Sci.* **21**, 1743
- Kennel, C. F. and Rees, M. H.: 1972, *J. Geophys. Res.* **77**, 2294.
- Kokubun, S.: 1971, *Planet. Space Sci.* **19**, 691.
- Krilov, A. L.: 1973, *Geomagn. Aeron.* **13**, 1037.
- Langel, R.: 1973a, *Planet. Space Sci.* **21**, 839.
- Langel, R. A.: 1973b. 'A Study of High Latitude Magnetic Disturbance', Tech. Note BN-767, Univ. Maryland.
- Langel, R. A.: 1974a, *Planet. Space Sci.* **22**, 1413.
- Langel, R. A.: 1974b, 'A Comparison of Electric and Magnetic Field Data from the OGO-6 Spacecraft', preprint X-922-74-235, GSFC.
- Langel, R. A.: 1975, *J. Geophys. Res.* **80**, 1261.
- Langel, R. A. and Svalgaard, L.: 1974, *J. Geophys. Res.* **79**, 2493.
- Langel, R. A. and Brown, N.: 1974, *Planet. Space Sci.* **22**, 1611.
- Leontyev, S. V.: 1974, private communication.
- Leontyev, S. V. and Lyatsky, V. B.: 1974, *Planet. Space Sci.* **22**, 811.
- Leontyev, S. V., Lyatsky, V. B., and Maltzev, Yu. P.: 1974, *Geomagn. Aeron.* **14**, 112.
- Lyatsky, V. B. and Maltzev, Yu. P.: 1975, *Geomagn. Aeron.* **15**, 118.
- Loginov, G. A. and Starkov, G. V.: 1972, in S. I. Isaev (ed.), *Geophysical Investigation in the Auroral Zone*, Apatity, p. 87.
- Maewawa, K.: 1976, *J. Geophys. Res.* **81**, in press.
- Maisuradze, P. A.: 1967, *Geomagn. Aeron.* **7**, 369.
- Mansurov, S. M. and Mansurova, L. G.: 1965, *Geomagn. Aeron.* **5**, 740.
- Mansurov, S. M.: 1969, *Geomagn. Aeron.* **9**, 768.
- Mansurov, S. M. and Mansurova, L. G.: 1970a, *Ann. Geophys.* **26**, 397.
- Mansurov, S. M. and Mansurova, L. G.: 1970b, Program and Abstracts, *STP Symp.* Leningrad.
- Mansurov, S. M. and Mansurova, L. G.: 1973a, *Geomagn. Aeron.* **13**, 794.
- Mansurov, S. M. and Mansurova, L. G.: 1973b, *Geomagn. Aeron.* **13**, 1020.
- Mansurov, S. M. and Mansurova, L. G.: 1973c, Program and Abstracts, IAGA Assembly, Kyoto, 156.
- Mansurov, S. M., Mansurova, L. G., Heckman, G. R., Wilcox, J. M., Svalgaard, L., Troitskaya V. A., and Howard, R.: 1973d, Program and Abstracts, IAGA Assembly, Kyoto.
- Matsushita, S. and Balsley, B. B.: 1972, *Planet. Space Sci.* **20**, 1259.
- Matsushita, S. and Balsley, B. B.: 1973, *Planet. Space Sci.* **21**, 1260.
- Matsushita, S., Tarpley, J. D., and Campbell, W. H.: 1973, *Radio Sci.* **8**, 963.
- Matveev, M. I.: 1974, *Issled. Geomagn. Aeron. Solar Phys.*, No. 30, 71.
- Mayaud, P. N.: 1955, *Result Sci. Exped. Antarct., Terre Adelie, 1951-1952*, fasc. II, Paris.
- Maynard, N. C. and Johnstone, A. D.: 1974, *J. Geophys. Res.* **79**, 3111.
- Mishin, V. M., Bazarzhapov, A. D., and Nemtsova, E. I.: 1972, 'The Effect of the B_x Component of the Interplanetary Magnetic Field on Magnetospheric Convection and Hall Currents in the Polar Ionosphere', preprint SibIZMIRAN, 10-72, Irkutsk.
- Mishin, V. M., Bazarzhapov, A. D., Nemtsova, E. I., Popov, G. V., and Shelomentsev, V. V.: 1973, 'The Effect of the Interplanetary Magnetic Field on Magnetospheric Convection and Magnetospheric Electric Currents', preprint SibIZMIRAN, 5-73, Irkutsk.
- Montbriand, L. E.: 1970, *J. Geophys. Res.* **75**, 5634.
- Mozer, F. S., Gonzalez, W. D., Bogot, F., Kelley, M. C., and Achutz, S.: 1974, *J. Geophys. Res.* **79**, 56.
- Nagata, T. and Kokubun, S.: 1962, *Rep. Ionos. Space Res. Jap.* **16**, 256.
- Ness, N. F., Scarce, C. S., Seek, J. B., and Wilcox, J. M.: 1966, *Space Res.* **6**, 581.
- Ness, N. F. and Wilcox, J. M.: 1967: *Solar Phys.* **2**, 351.
- Nikolsky, A. P.: 1956, *Proc. Arct. and Ant. Inst.* **83**, 5.
- Nishida, A.: 1968a, *J. Geophys. Res.* **73**, 1795.

- Nishida, A.: 1968b, *J. Geophys. Res.* **73**, 5549.
- Nishida, A.: 1971a, *Planet. Space Sci.* **19**, 205.
- Nishida, A.: 1971b, *Cosm. Electrodyn* **2**, 350.
- Nishida, A.: 1973a, *Planet. Space Sci.* **21**, 691.
- Nishida, A.: 1973b, *Planet. Space Sci.* **21**, 1255.
- Nishida, A. and Kokubun, S.: 1971, *Rev. Geophys. Space Phys.* **9**, 417.
- Nishida, A., Iwasaki, N., and Nagata, T.: 1966, *Ann. Geophys.* **22**, 478.
- Nopper, R. W. and Hermance, J. F.: 1974, *J. Geophys. Res.* **79**, 4799.
- Onwumechilli, A., Kawasaki, K., and Akasofu, S.-I.: 1973, *Planet. Space Sci.* **21**, 1.
- Orlov, V. P., Ivchenko, M. P., Bazarzhapov, A. D., and Kolomiytseva, G. I.: 1968, *Secular Variation of Geomagnetic Field for 1960–1965*, IZMIRAN, 1968.
- Osipova, I. L.: 1973, Ph.D. Thesis, IZMIRAN.
- Ponomarev, V. N. and Galperin, Yu. I.: 1973, *Kosm. Issled.* **11**, 88.
- Rostoker, G.: 1972, *Rev. Geophys. Space Phys.* **10**, 157.
- Rostoker, G.: 1974 *Trans. AGU* **55**, 593.
- Rostoker, G., Chen, A. J., Yasuhara, F., Kawasaki, K., and Akasofu, S.-I.: 1974, *Planet. Space Sci.* **22**, 427.
- Russell, C. T.: 1972, 'The Configuration of the Magnetosphere', preprint, Inst. Geophys. Plan. Phys., Univ. Calif.
- Shabansky, V. P.: 1968, *Space Sci. Rev.* **8**, 366.
- Shabansky, V. P.: 1971, *Space Sci. Rev.* **12**, 299.
- Shelomentsev, V. V.: 1974, *Issled. Geomagn. Aeron. Solar Phys.* No. **30**, 85.
- Stern, D. P.: 1973, *J. Geophys. Res.* **78**, 7292.
- Sumaruk, P. V. and Feldstein, Ya. I.: 1973a, *Kosm. Issled.* **11**, 155.
- Sumaruk, P. V. and Feldstein, Ya. I.: 1973b, 'Summer Season Current Systems in the Polar Region', preprint, IZMIRAN, No. 13.
- Sumaruk, P. V. and Feldstein, Ya. I.: 1973c, *Geomagn. Aeron.* **13**, 545.
- Sumuruk, P. V. and Feldstein, Ya. I.: 1973d, 'Magnetic Field Variation in the Polar Cap', preprint, IZMIRAN, No. 24.
- Sumaruk, P. V. and Feldstein, Ya. I.: 1973e, 'High-Latitude Magnetic Disturbances Connected with the Y-Component of the Interplanetary Magnetic Field', *Symp. on the Physics of the Disturbed Magnetosphere*, Murmansk, April, 1973.
- Sumaruk, P. V., Feldstein, Ya. I., and Shevnina, N. F.: 1974, *Geomagn. Aeron.* **14**, 1069.
- Sumaruk, P. V. and Feldstein, Ya. I.: 1975, *Usp. Fiz. Nauk* **116**, 344.
- Svalgaard, L.: 1968, Geophys. Papers R-6, Danish Meteorol. Inst.
- Svalgaard, L.: 1972, Geophys. Papers R-29, Danish Meteorol. Inst.
- Svalgaard, L.: 1973, *J. Geophys. Res.* **78**, 2064.
- Svalgaard, L.: 1974, in D. E. Page (ed.), *Correlated Interplanetary and Magnetospheric Observations*, D. Reidel, Dordrecht-Holland, p. 61.
- Svalgaard, L.: 1975, *J. Geophys. Res.* **80**, 2717.
- Svalgaard, L. and Wilcox, J. M.: 1974, *The Spiral Interplanetary Magnetic Field: a Polarity and Sunspot Cycle Variation*, preprint, SUIPR, No. 573.
- Troshichev, O. A., Pudovkin, M. I., Pegov, L. A., and Grafe, A.: 1974, *Gerlands Beitr. Geophys.* **83**, 275.
- Volland, H.: 1973, *J. Geophys. Res.* **78**, 171.
- Vorobjev, V. G., Gustafsson, G., Starkov, G. V., Feldstein, Y. I., and Shevnina, N. F.: 1974, KGO preprint, No. 74, 301.
- WDCA, AE data for 1965, version 27 May, 1969.
- Wilcox, J. M.: 1968, *Space Sci. Rev.* **8**, 258.
- Wilcox, J. M.: 1969, 'Magnetic Field Variations in Interplanetary Space', Univ. Calif., Berkeley, ser. 10, issue 39.
- Wilcox, J. M.: 1972, *Rev. Geophys. Space Sci.* **10**, 1003.
- Wilhjelm, J. and Friis-Christensen, E.: 1972, Geophys. Papers R-31, Danish Meteorol. Inst.

APPENDIX

Corrected geomagnetic latitudes and geomagnetic midnight at the stations used in the analysis

Station	Corrected geomagnetic latitude ^a	Geomagnetic local midnight time, UT ^b	Local midnight time, UT
Alert	86.6	20 ^h 24 ^m	4 ^h 10 ^m
Thule	86.1	2 48	4 35
Resolute Bay	84.2	8 08	6 20
Mould Bay	80.5	10 42	7 58
Godhavn	77.5	2 20	3 34
Baker Lake	75.2	6 56	6 24
Heiss	74.5	19 00	20 08
Fort Churchill	70.3	6 36	6 17

^a Calculated according to Gustafsson (1970).

^b Local geomagnetic midnight for the summer season according to Montbriand (1970).